

The Northern Bay of Safaga (Red Sea, Egypt): An Actuopalaeontological Approach. IV. Thin Section Analysis

Die Nördliche Bucht von Safaga (Rotes Meer, Ägypten): ein aktuopaläontologisches Beispiel. IV. Dünnschliffanalyse

by

Werner E. PILLER*

PILLER, W. E., 1994. The Northern Bay of Safaga (Red Sea, Egypt): an actuopalaeontological approach. IV Thin section analysis. — Beitr. Paläont. 18:1–73, 19 Figures, 5 Tables, 18 Plates, 1 Appendix, Wien.

Contents

Abstract	1
Zusammenfassung	2
1. Introduction	2
2. Material and methods	2
3. Sediment constituents	3
3. 1. Foraminifera	3
3. 2. Sponges	5
3. 3. Corals	5
3. 4. Bryozoa	6
3. 5. Molluscs	6
3. 6. Worm tubes	6
3. 7. Crustaceans	6
3. 8. Ostracods	6
3. 9. Echinoderms	7
3.10. Vertebrates	7
3.11. Red algae	7
3.12. Green algae	7
3.13. Plants	8
3.14. Pellets	8
3.15. Compound grains	9
3.16. Cryptocrystalline grains	9
3.17. Ooids	10
3.18. Non-carbonate grains	10
3.19. Unidentified grains	11
3.20. Matrix	11
4. Relationships between constituents	11
5. Microfacies	13
5. 1. Coralgal facies	13
5. 2. Coralgal-molluscan facies	15
5. 3. Compound grain facies	15
5. 4. Cryptocrystalline grain facies	17
5. 5. Soritid - compound grain facies	17
5. 6. <i>Heterostegina</i> facies	17
5. 7. Scaphopod facies	17
5. 8. Peloolitic molluscan facies	17
5. 9. <i>Halimeda</i> facies	19
5.10. Soritid facies	19
5.11. <i>Operculina</i> - soritid facies	19
5.12. Foraminiferan sand facies	19
5.13. Coralgal mud facies	19
5.14. <i>Operculina</i> facies	21
5.15. Mud facies	21
5.16. Mixed mud facies	21
5.17. Terrigenous facies	21
6. Microfacies interpretation and relations to bottom facies	21
7. Microfacies versus sedimentary facies	25
8. Discussion	31
9. Conclusion	32
10. Acknowledgements	33
11. References	33

Abstract

Thin section analysis was performed on 120 bulk samples of resin impregnated sediments by point counting (961 points) from the Northern Bay of Safaga. No grain size exclusion in the form of sieving out the fine fraction was performed prior to impregnation. The most abundant category out of 20 sediment constituents, averaging all samples, is that of unidentified grains, which, together with "matrix", reflects the amount of fine fraction (silt and mud). The most frequent carbonate particles to occur are foraminifera, molluscs, corals, and compound grains. Other non-skeletal particles besides compound grains, are cryptocrystalline grains, pellets and ooids; the two latter remaining below 1 %. The mixed carbonate/siliciclastic environment to which the Northern Bay of Safaga belongs is reflected by >10 % of non-carbonate content.

Using the frequencies of these 20 categories as well as multivariate statistical methods (correlation- and cluster analyses) 17 microfacies can be distinguished. Out of these, the Coralgal facies, Compound grain f., *Heterostegina* f., Soritid f., Foraminiferan sand f., *Operculina* f., Mud f., and Terrigenous facies cover large areas. The Coralgal-molluscan f., Soritid – compound

* Institut für Paläontologie der Universität Wien, Universitätsstraße 7/II, A-1010 Wien

grain f., *Operculina* – soritid f., Coralgal mud f., and Mixed mud facies represent transitional microfacies, which, however, are clearly distinguishable. Three microfacies (Cryptocrystalline f., Scaphopod f., and *Halimeda* f.) are represented by only a single sample each. The Peloolitic molluscan facies is restricted to deeper water sites in the "East area" and is interpreted as representing relicts of an earlier sea level lowstand.

The microfacial distributional pattern coincides well with that of the Bottom facies (PILLER & PERVESLER, 1989) and Sedimentary Facies (PILLER & MANSOUR, 1990), showing, however, a higher resolution as far as details are concerned.

Zusammenfassung

An 120 Proben aus der Nördlichen Bucht von Safaga wurde eine Dünnenschliffanalyse durchgeführt. Die Proben wurden, ohne die Feinfraktion durch Siebung zu entfernen, in Kunstharz eingebettet und der Modalbestand mittels Punktzählung (961 Punkte/Schliff) erfaßt. Dabei konnten 20 Kategorien unterschieden werden. Unter Verwendung der Mittelwerte aller Proben stellen „unbestimmbare Sedimentanteile“ die häufigste Kategorie dar. Diese spiegelt zusammen mit der „Matrix“ den Anteil von Feinfraktion (Silt und Ton) wider. Unter den Karbonatkörpern dominieren Foraminiferen, gefolgt von Mollusken, Korallen und Aggregatkörnern. Unter den sogenannten nicht-biogenen Karbonatkörpern sind neben den Aggregatkörnern noch kryptokristalline Partikel, Pellets und Ooide vorhanden, wobei die beiden letzteren nur einen Gesamtmittelwert von < 1 % erreichen. Der Anteil von > 10 % an „Nicht-Karbonat“ manifestiert die Zugehörigkeit der Nördlichen Bucht von Safaga zu einem gemischt karbonatisch/siliziklastischen Sedimentationsregime.

Aufgrund der Häufigkeitsverteilung dieser 20 Kategorien wurden, unterstützt von Korrelations- und Clusteranalysen, 17 Mikrofaziestypen unterschieden. Davon sind die Korallen/Kalkalgen Fazies, die Aggregatkorn F., die *Heterostegina* F., die Soritiden F., die Foraminiferen Sand F., die *Operculinen* F., die Schlamm F. und die Terrigene Fazies flächenmäßig am bedeutendsten. Die Korallen/Kalkalgen-Mollusken F., die Soritiden-Aggregatkorn F., die *Operculina*-Soritiden F., die Korallen/Kalkalgen Schlamm F. und die Gemischte Schlamm Fazies stellen Übergangsbereiche dar, die nur in schmalen Streifen vorkommen, trotzdem aber deutlich abgrenzbar sind. Von den restlichen 4 Mikrofaziesbereichen, sind die Kryptokristallinkorn F., die *Halimeda* F. und die Scaphopoden F. nur jeweils durch eine Probe vertreten. Die Peloolitische Mollusken F. ist auf tiefere Bereiche im „Osten“ der Bucht beschränkt und wird teilweise von Reliktsedimenten gebildet, die während eines früheren

Meeresspiegeltiefstandes im Flachwasser gebildet wurden. Das Mikrofazies-Verteilungsmuster stimmt relativ gut mit jenem der Bodenfazies-Bereiche (PILLER & PERVESLER, 1989) und dem der Sedimentfazies-Bereiche (PILLER & MANSOUR, 1990) überein, ist aber wesentlich genauer.

1. Introduction

The sediments of the Northern Bay of Safaga (west coast of the northern Red Sea, Egypt; Fig. 1) were studied by grain size and coarse grain analyses as well as by some mineral and trace element analyses (PILLER & MANSOUR, 1990). The resulting data and deduced sedimentary facies correspond well with bottom facies types as established by PILLER & PERVESLER (1989) which are based on field observations. In addition, the results of these investigations served as a sedimentological base for actopalaeontological investigations of the echinoids (NEBELSICK, 1992 a, b) as well as corals and boring bivalves (KLEEMANN, 1992) of the bay and will also be used for future investigations of other organism groups (e.g., foraminifera, molluscs, bryozoa, coralline algae).

The coarse grain analyses used in the deduction of sedimentary facies only covered the fractions > 250 µm (PILLER & MANSOUR, 1990). In order to gain more information, especially on the composition of the fine grained sediment as well as on the internal composition of particles, a thin section analysis of the samples was carried out. In addition, following the actualistic concept of the investigation used in this study of the Northern Bay of Safaga, thin section analysis (microfacies analysis) is thought to be a more adequate method for comparisons with ancient carbonates than coarse grain analysis.

2. Material and methods

120 samples (Fig. 2) were selected for this analysis from the bulk samples (500 cm³), which were desalinated by washing several times with distilled water and subsequently oven dried (PILLER & MANSOUR, 1990). A subsample from each sample was produced by splitting the dry samples (preventing grain size selection). These subsamples were strewn into small boxes (4 x 4 x 1 cm) filled with epoxy resin. Gravidity separation of grain size was prevented due to the high viscosity of the resin. The hardened sediment-resin blocks were removed from the boxes and ground on one 4 x 4 cm surface, mounted on a glass plate and thin sectioned. The thin sections were studied with a polarizing microscope by point counting on a 3 x 3 cm area which included 961 points (31 x 31). Due to interparticle pore volume the number of actually counted points ranges between 493 and 885.

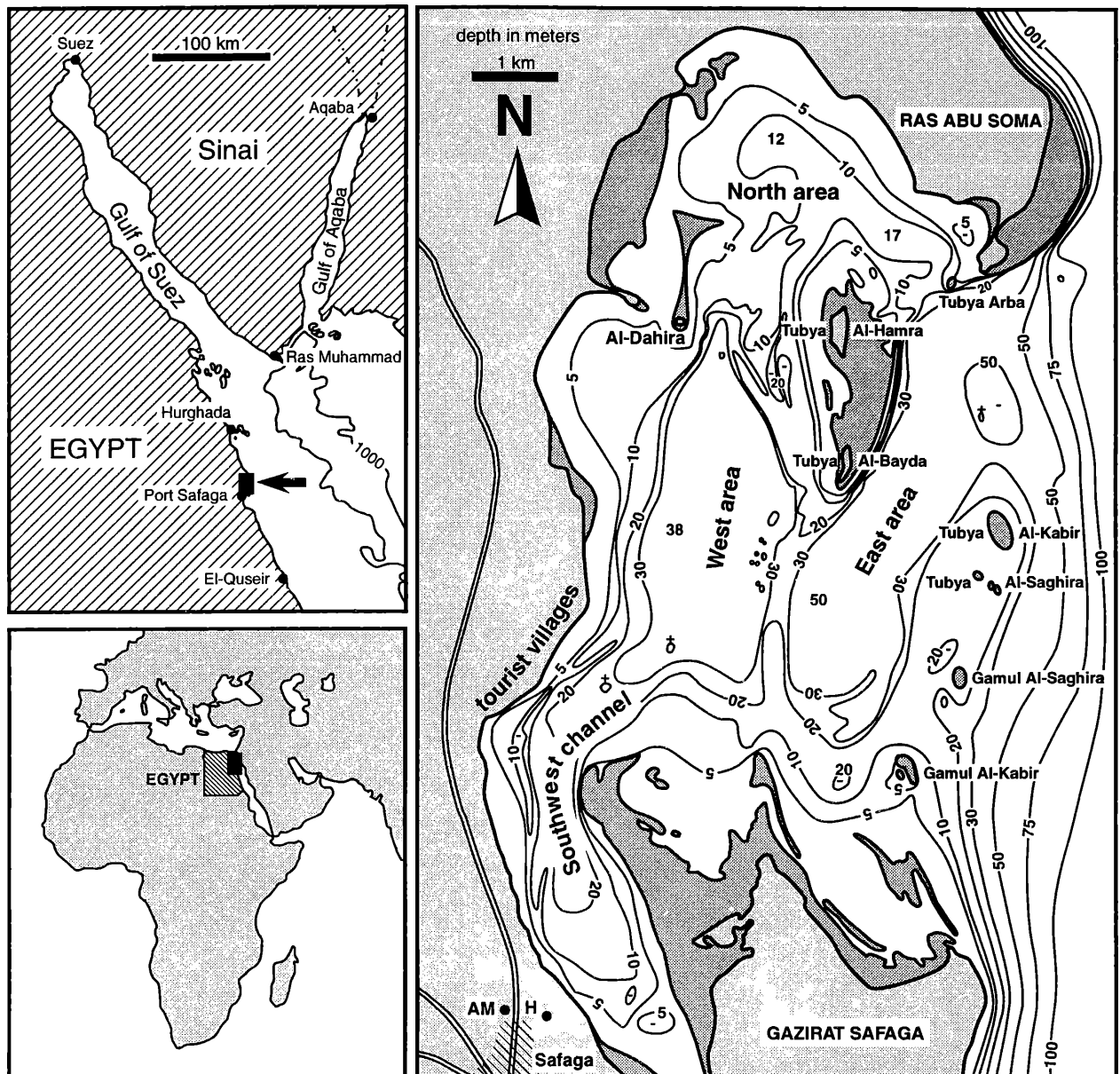


Figure 1: Location map and general topography of study area (after PILLER & MANSOUR, 1990). (Dark stippled fields in the right map represent intertidal areas).

The desalinated and dried sediments were not treated by hydrogen peroxide as suggested by several authors (in varying concentrations; e.g., GINSBURG, 1956; PUSEY, 1975) to destroy loosely bound aggregates, because these loosely bound aggregates are easily distinguishable in thin sections from true aggregate grains. The frequency of loosely bound aggregates, however, can be used as an (informal) measure for the mud content in the sediments. This information is useful as the mud content in these artificially produced "rocks" is difficult to detect, especially as it is obscured by its diffused distribution in the "resin matrix".

Most statistical analyses were performed with the SPSS software package on the main frame at the Computer center of the University of Vienna.

3. Sediment constituents

The sediment constituents were categorized as far as possible in the manner used for the coarse grain analysis (PILLER & MANSOUR, 1990). Additional categories have been introduced (e.g., ooids, cryptocrystalline grains) due to the higher degree of information which can be gained by thin section analysis. All frequency data about sediment constituents are presented in Appendix 1, some statistical data in Tab. 1.

3.1. Foraminifera (Pl. 1, Figs. 1–16; Pl. 2, Figs. 1–16; Pl. 3, Figs. 1–15)

Foraminifera are the most abundant sediment constituents except for unidentified particles using the mean value of all 120 samples ($\bar{x} = 14.83\%$, $s = 11.67\%$). Only one

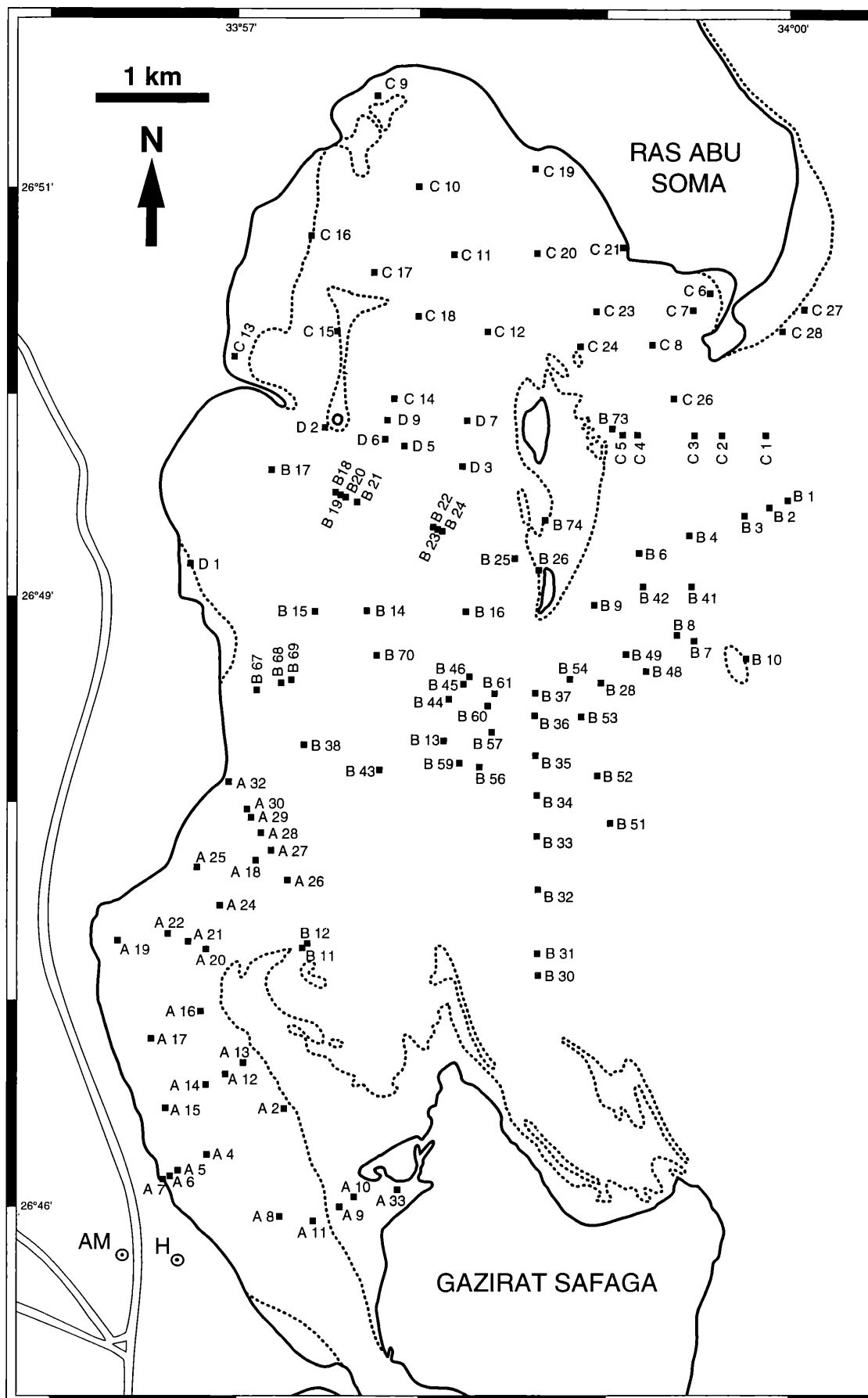


Figure 2: Sample map (AM = Aerial mast, H = "Safaga Hotel"). (A, B, C, D: prefix of sample numbers; A: samples of the "Southwest channel", B: samples of transects starting at Tubya al-Bayda, C: samples of transects starting at Tubya al-Hamra, D: samples of transects starting at Al-Dahira).

	mean	st. dev.	range
foraminifera	14.38	11.67	0–55.34
agglutinated f.	1.39	1.74	0– 9.43
miliolid f.	6.70	7.76	0–35.59
hyaline f.	6.74	7.60	0–34.18
sponges	0.01	0.05	0– 0.27
corals	9.71	12.03	0–44.81
bryozoa	0.08	0.18	0– 1.17
molluscs	11.80	8.34	0.25–42.26
worm tubes	0.58	0.82	0– 5.81
crustaceans	0.29	0.42	0– 2.71
ostracods	0.09	0.14	0– 0.71
echinoderms	0.88	0.87	0– 4.40
vertebrates	0.01	0.03	0– 0.31
red algae	3.73	5.33	0–30.99
green algae	0.53	5.40	0–59.38
plants	0.13	0.84	0– 9.06
pellets	0.33	0.93	0– 7.46
compound grains	8.81	9.77	0–66.36
cryptocrystalline g.	3.81	5.77	0–52.12
ooloids	0.41	1.44	0–12.97
non-carbonate g.	11.26	22.62	0–95.25
unidentified grains	27.14	20.86	0–76.42
matrix	5.66	11.13	0–57.18

Table 1. Mean values, standard deviations and ranges (%) of all sediment constituents (120 samples).

sample is free of foraminifera (A 33, highly terrigenous Mangrove sample), two samples are composed of more than 50 %. The distributional pattern (Fig. 3) shows three areas with generally high abundances: the “East area”, particularly the two basins, but also the slope outside the bay continuing to the deep ocean; the shallow water areas of the “North” and the northwestern part of the “West area”; the “Southwest channel”, in more marginal locations as well as in the central depression of the channel. The highest percentages are reached in the southern part of the channel (A 4, A 12). Lowest percentages occur in the basin of the “West area”. Although the number of smaller foraminifera may be very high in some samples, larger foraminifera dominate by far volumetrically. According to test wall structure, foraminifera were separated in three groups: agglutinated, miliolid, and hyaline; no further distinctions were made during counting. The agglutinated foraminiferal group (Pl. 1, Figs. 1–7) is the least abundant, not exceeding 10 % in any sample, with only 7 samples reaching more than 5 %. Larger areas with more than 1 % agglutinated foraminifers cover the main part of the “East” (mainly in deeper water), the middle part of the “Southwest channel” and a smaller patch in the northwest of the “West area”. The agglutinated foraminiferan fauna in the samples with highest abundances is characterized by large (up to 4 mm) paraperforate forms (Pl. 1, Fig. 2), like *Textularia foliacea* HERON-ALLEN & EARLAND.

The average abundance of miliolid ($x = 6.70 \%$, $s = 7.76 \%$) and hyaline foraminifera ($x = 6.74 \%$, $s = 7.60 \%$) is nearly identical, their distributional pattern, however, differs widely. The miliolid group (Fig. 4; Pl. 1, Figs. 8–16, Pl. 2, Figs. 1–3) is more frequently represented in the shallow water area of the “North” and “West areas”, parallels the NW coast in the northern part of the “Southwest channel”, and reaches its highest abundances in the southern part of the “Channel” ($> 30 \%$). Besides high numbers of smaller forms of *Quinqueloculina-Triloculina*-type (Pl. 1, Figs. 8, 10, 11), samples with highest percentages of porcellaneous forms are characterized by soritids (Pl. 2, Figs. 1–3) and *Borelis* (Pl. 1, Figs. 15, 16), being in some samples accompanied by *Peneroplis* (Pl. 1, Figs. 13, 14). Not only the average, but also the highest percentages (around 35 %) of hyaline and miliolid foraminifera are similar. The main distribution of hyaline forms (Pl. 2, Figs. 4–16; Pl. 3, Figs. 1–15) is in the “East area”, in particular in the southern basin and on the outer slope of the bay, and along the central axes of the “Southwest channel” (Fig. 5). High abundances of hyaline foraminifera usually exclude frequent occurrence of miliolids. An exception are some samples in the southern part of the “Channel”. The sample with the highest percentage of hyaline foraminifers (C 1: 34.18 %) is dominated by *Heterostegina* (Pl. 2, Figs. 4, 8–12), whereas most of the samples with high percentages are characterized by *Operculina* (e.g., B 34, A 4) (Pl. 2, Figs. 13–16). [Although this foraminifer is currently grouped into the genus *Assilina* (LOEBLICH & TAPPAN, 1988), the old but widely used generic name *Operculina* is applied herein]. *Amphistegina* (Pl. 2, Figs. 5–7) and sessile hyaline forms, such as homotrematid (Pl. 3, Figs. 6–8), acervulinid (Pl. 3, Fig. 13, 14) and planorbulinid (Pl. 3, Figs. 9–12) species, are volumetrically of greater importance only in a few samples. Acervulinid foraminifers form the main part of the macrooids on the outer slope of the bay (B 2, C 1) (PILLER & PERVESLER, 1989). A detailed study on foraminifera, washed as well as in thin section, is in preparation.

3.2. Sponges (Pl. 1, Fig. 11; Pl. 3, Fig. 16)

Sponges are volumetrically unimportant sediment constituents and occur mainly as spicules in fine grained sediments. They never exceed 1 % (Tab. 1). In some cases the soft tissue of sponges is present as encrustations on other skeletal grains.

3.3. Corals (Pl. 4, Figs. 1–16)

Corals range fifth in average abundance ($x = 9.71 \%$) with a high variance ($s = 12.03 \%$) reflecting their patchy distribution. A relatively large area is covered by $> 10 \%$ corals (Fig. 6): the shallow water area north of Gazirat

Safaga and around the Tubya island group, the southern part of the “North area”, the slope along the western margin of the basin of the “West area”, and the submarine ridge between the Tubya islands and parts of the ridge along the eastern margin of the bay. Highest percentages ($>40\%$) occur in reef samples (e.g., C 27: from the fringing reef off Ras Abu Soma; A 28: base of a densely coral covered submarine elevation, A 17: patch reef). The majority of the corals present in the samples originates from scleractinians; octocorallian spicules (Pl. 4, Figs. 12–16) make up a higher proportion only along the submarine ridges (e.g., B 2, B 61) or in some samples with higher content of fine fraction (e.g., B 8, B 15, D 3, A 16). Two types of these spicules occur: one type is clear and show well developed spheroidal structures in polarized light, the other type shows a pronounced internal zonation of clear, amber or pinkish zones with brown to dark brown zones. Additional cnidarian particles (e.g., *Tubipora*) are extremely rare.

3.4. Bryozoa (Pl. 5, Figs. 1–8)

Bryozoans are a volumetrically unimportant group exceeding 1 % only in one sample (D 7). Although rare, a variety of growth forms could be detected: crustose types of different species (Pl. 5, Figs. 5–8) as well as ramosiform with subparallel zoocia (Pl. 5, Figs. 1–4) as well as bifoliate forms (Pl. 5, Fig. 5).

3.5. Molluscs (Pl. 5, Figs. 9–16; Pl. 6, Figs. 1–3)

Molluscs range third among all sediment constituents with an average frequency of 11.8 %. The relatively low variance ($s = 8.34\%$) indicates the persistent occurrence of this particle category across the whole study area. They are the only category represented in every thin section. Although composed of several groups (as in foraminifera), a distinction between these main groups is not consistently possible in thin section. Gastropods are usually relatively easy identifiable when more or less completely preserved (Pl. 5, Figs. 9, 10), but fragments are often indistinguishable from those of bivalves. Scaphopods are the only molluscs relatively easy to identify, due to their circular or elliptical cross sections or longitudinal sections of the tubular shell in combination with the very pronounced wall structure. The latter is composed of a thinner inner layer of dark brown color and bended lamellae in longitudinal section and a thicker, bright transparent outer layer (Pl. 6, Figs. 1–3). Highest abundances are reached on the submarine ridges along the eastern margin of the bay and between the “West” and “East area” (Fig. 7). However, only one sample exceeds 40 % and three reach values between 30 and 40 %. The basinal sediments and that of a large area in the “North” contain $< 10\%$ molluscs.



Figure 3: Distribution of foraminifera.

3.6. Worm tubes (Pl. 6, Figs. 4–7)

This category comprises exclusively worm tubes of serpulid type and exceeds 1 % only in a few samples which are located on the submarine ridges or in isolated locations in shallow water. The typical circular and ellipsoidal cross and tubular longitudinal sections are characterized by a dark laminated microstructure. In cross sections the lamellae show a concentric internal arrangement, in longitudinal section an orientation oblique to the surface (Pl. 6, Figs. 4–7). The tubes are frequently intergrown with corals, coralline algae and molluscs.

3.7. Crustaceans (Pl. 6, Figs. 8–10)

Only decapod crustaceans and – extremely rare – balanid fragments are combined in this category ($x = 0.29$, $s = 0.42$), ostracods are treated separately (see chap. 3.8.). Sections through decapod carapaces are characterized by a brownish to greyish color and a radial perforate microstructure (Pl. 6, Fig. 8–10).

3.8. Ostracods (Pl. 6, Figs. 11, 12)

Because of their higher fossilisation potential ostracods were counted separately from other crustaceans. Most individuals occur as double-valved carapaces often with



Figure 4: Distribution of miliolid foraminifera.

typical inner lamella, but sections parallel to the hinge line are also usually easy to identify (Pl. 6, Fig. 12). Their abundance, however, never reached 1 % in a single sample. Individual numbers are relatively higher in fine grained sediments, but they remain volumetrically unimportant.

3.9. Echinoderms (Pl. 6, Figs. 13–16)

Echinoderms are represented mainly as echinoid fragments. The dominating particles are spines of different genera (Pl. 6, Fig. 13–15); corona fragments also occur, but are less abundant. A detailed differentiation was not performed, especially as the echinoid fragments of the bay are studied in detail by NEBELSICK (1992a,b). Although ophiurids (Pl. 6, Fig. 16), holothurians as well as crinoids were also observed in the field, they are nearly absent in the studied thin sections. The average abundance does not reach 1 %, the maximum remains below 5 % (Tab. 1).

3.10. Vertebrates

Vertebrate remains are extremely rare with only fish teeth being recognized.

3.11. Red algae (Pl. 7, Figs. 1–4)

Red algae are present in the sediments as coralline algae or as squamariaceans. Coralline algae are dominated by



Figure 5: Distribution of hyaline foraminifera.

crustose forms, articulated species are rare, and preserved exclusively as isolated genicula (Pl. 7, Fig. 4). Squamariaceans (Pl. 7, Fig. 3) are rare and present mainly in samples of deeper water (e.g., B 60, C 1) (Pl. 7, Fig. 2). Crustose coralline algae occur as crusts (Pl. 7, Fig. 1), for example on corals or molluscs, or as crustose or branched rhodoliths; they are also involved in the formations of the macroids present on the outer slope of the bay (PILLER & PERVESLER, 1989). Squamariaceans also form part of these macroids, which are usually dominated by acervulinid foraminifers. The macroids will be documented in a separate study.

The distribution of red algae is generally patchy, a larger area with higher red algal contents is present in the shallow water area west of the Tubya islands and its southern continuation to the submarine ridge (5–20 %) which connects these islands with Safaga island (Fig. 8). The highest percentage (> 30 %) of all samples occurs at the northwestern tip of Gazirat Safaga (B 11).

A detailed study on red algae will be published in the next future.

3.12. Green algae (Pl. 7, Figs. 5–8)

In the studied thin sections green algae belong exclusively to udoteaceans and are dominated by *Halimeda*. Another



Figure 6: Distribution of corals.



Figure 7: Distribution of molluscs.

form, *?Tydemania* (Pl. 7, Figs. 7, 8), is extremely rare and recognized (but not counted) only in a few thin sections (e.g., B 11, B 67) in transverse as well as in longitudinal sections. *Halimeda*, as also observed in the field (PILLER & PERVESLER, 1989) and in the coarse grain analyses (PILLER & MANSOUR, 1990), is rare and exceeds 1 % only in 2 samples (C 3, B 51). However, in sample B 51 it constitutes nearly 60 % of the point countings (Appendix 1).

3.13. Plants (Pl. 7, Figs. 9, 10)

Although fragments of higher plants (seagrass) have nearly no fossilisation potential they were counted for this study, in particular to test correlations to other particle categories. Due to their cellular composition and their reddish or brownish color they are easily recognized in thin sections (Pl. 7, Figs. 9, 10). Their frequency usually remains <1 % but in one sample it reaches >9 % (C 15) (Tab. 1).

3.14. Pellets (Pl. 7, Figs. 11–16)

Three different kinds of particles are classified within this category (Tab. 2, Fig. 9):

a) Relatively large ellipsoidal or cylindrical particles

(Tab. 2) with a sharp outline, which often is pronounced by a thin coating at the surface (Pl. 7, Figs. 12, 14). These particles are composed of larger particles of different origin (small skeletal fragments, pellets of the small type c, non-carbonate particles, but mainly unidentifiable grains) in a very dense micritic matrix (Pl. 7, Figs. 13, 14). The color of the micrite is dark brown, frequently the marginal part is obviously darker than the center. In some of these pellets thin straight channels, circular in cross section, are observable, which may be empty (Pl. 7, Fig. 11) or filled with dark material (Pl. 7, Fig. 12). Due to the channels these pellets can be attributed to anomuran crustaceans (e.g., BROMLEY, 1990), which are also well documented in the fossil record.

b) Relatively large ellipsoidal grains (Tab. 2) with a pronounced zonal structure made up of two layers (Pl. 7, Figs. 15–16): an outer amber to dark brown rim of relatively homogenous material with only rare and small embedded particles; an inner core composed of silt to sand size particles of different origin with a subordinate amount of matrix. The outer cortex seems to be composed of a high portion of organic material. Sometimes these pellets seem to be flattened by



Figure 8: Distribution of red algae.

compression (Pl. 7, Fig. 16). They show the greatest variation in length/diameter ratio of the 3 categories (Fig. 9) and occur in muddy sediments (e.g., B 14, B 21, B 43).

c) Small, ellipsoidal or spheroidal but also angular, dark brown or nearly black, structureless grains (Pl. 7, Figs. 15, 16). They may represent fecal pellets or small micritized particles, probably also of skeletal origin. A distinction from the latter is difficult and if there was even a small hint as to a skeletal origin they were counted as unidentifiable particles. This volumetrically unimportant type of pellet occurs predominantly in fine grained sediments (e.g., B 14, B 16, B 22, B 44).

Pellets are not very important volumetrically, reaching more than 5 % in only two samples (B 28, B 49). Out of the samples with more than 1 % pellets those with small pellets are nearly restricted to the basin of the "West", whereas those with crustacean pellets occur exclusively in the deeper part of the "East".

3.15. Compound grains (Pl. 8, Figs. 1-8)

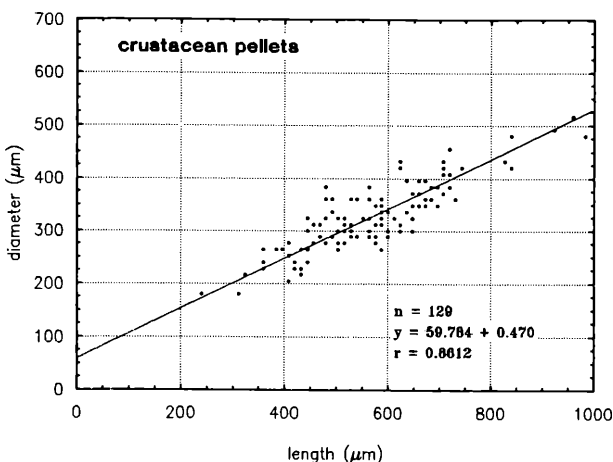
Particles which are composed of several grains are summarized in this group. The grains mainly belong to

molluscs, foraminifera, corals, coralline algae, and non-carbonate grains. They are bound together by micrite which is highly variable in density. Due to this variation the compound grains sometimes contain a substantial amount of open pore space (Pl. 8, Figs. 1, 2), sometimes, however, there is no interparticle space (Pl. 8, Figs. 3, 7, 8). The outline of these particles is also variable ranging from rounded or angular, clearly bordered to those with irregular outlines with pronounced projecting single grains. There is a continuous transition between different densities and outlines. The compound grains with irregular outer surfaces and relatively high interparticle pore space (Pl. 8, Fig. 2) correspond with grapestones (sensu PURDY, 1963a). The denser compound grains may be comparable to PURDY's mud aggregates (Pl. 8, Figs. 4, 5), in some cases perhaps representing transported – and sometimes rounded – rock fragments (Pl. 8, Fig. 6). An additional origin results in the fragmentation of skeletal encrustations (e.g., around corals by calcareous algae, foraminifera, worm tubes, etc.). A consistent distinction between these different modes of origin was not possible.

The average abundance of compound grains comes close to 9 %, with a wide range between 0 and > 66 %. A continuous area with more than 10 % is in the "North" continuing south in two stripes. The one paralleling the west coast of the "West", the other running along the west coast of the Tubya islands continuing southward on the submarine ridge. Another small stripe runs from Ras Abu Soma southward on the submarine ridge which represents the eastern margin of the bay. Grapestone type compound grains occur predominantly in the "North". The other occurrences are mainly of the dense type or sometimes of (?) rock fragments.

3.16. Cryptocrystalline grains (Pl. 8, Figs. 9-11)

This category comprises grains composed of cryptocrystalline material lacking structures recognizable in thin sections and coincide with those described by several authors, e.g., ILLING (1954) and PURDY (1963a). The density of this micrite is highly variable and particle shape ranges from angular to well rounded, with, however, a dominance of the latter. Dimensions are variable with the majority of particles ranging between 150–200 µm rarely exceeding 400 µm. Their production may be explained diagenetically, originating from different kinds of skeletal and non-skeletal grains. The density of the cryptocrystalline materials is frequently highest around the periphery of the grains and decreases towards the center pointing to a micritization process (Pl. 8, Figs. 9, 10). Small cryptocrystalline grains may be confused with pellets of the small category c (chapt. 3.14.). Independently of the density of micritization, if there was any hint as to the origin of a grain, it was counted as such and not categorized



	mean	st.dev.	min.	max.
crustacean pellets				
$n = 129$ length (μm)	563.1	143.1	240	984
diameter (μm)	324.2	78.0	132	516
zonal pellets				
$n = 30$ length (μm)	656.8	104.4	456	828
diameter (μm)	374.0	120.6	216	660
non-zonal pellets				
$n = 77$ length (μm)	206.5	56.8	102	528
diameter (μm)	117.8	18.6	72	168

Table 2: Some statistical parameters of the three types of pellets.

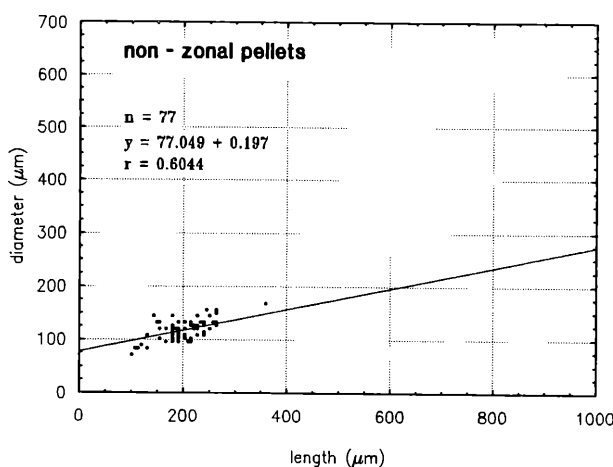
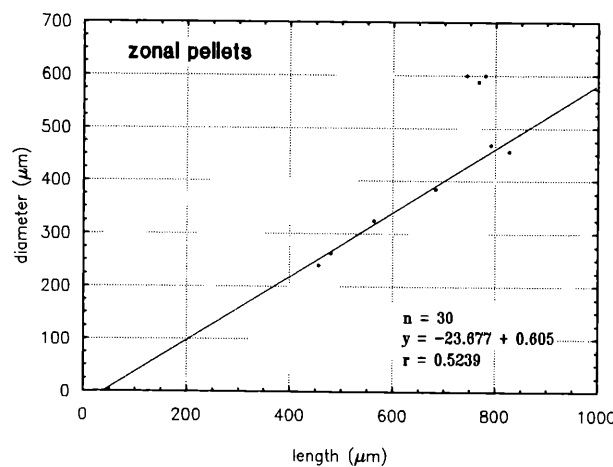


Figure 9: Length/diameter ratios as well as linear regressions and correlation coefficients of the 3 pellet types.

as cryptocrystalline. This practice was used by several authors (e.g., ILLING, 1954, PURDY, 1963). Due to this usage no separate category for particles with micritic envelope was tabulated.

The average abundance of cryptocrystalline grains is <4 % (Tab. 1); they only dominate in a single sample (B 74: 52.12 %) with an additional (D 2) in which more than 20 % were counted. The largest area with an amount >10 % is around the Tubya islands (Fig. 11).

3.17. Ooids (Pl. 8, Figs. 12–16)

Ooids are developed either as superficial (Pl. 8, Fig. 15) or as those with multilamellar coatings (Pl. 8, Figs. 12–14). Skeletal, non skeletal as well as non-carbonate particles act as nuclei. Pellets of the larger type frequently occur as non-skeletal particles (Pl. 8, Fig. 14). The superficial coating is sometimes discontinuous. In some samples a few ooids are again coated by ooid layers. In this case they were also counted as ooids; if a few ooids were cemented by interparticle cement they were counted as compound grains (Pl. 8, Fig. 8).

Ooids are of subordinate importance, exceeding 10 % in a single sample (C 13) and 5 % only in an additional one (B 26). In general, there are two areas of occurrence:

a) intertidal to very shallow subtidal: these samples are characterized either by a high percentage of non-carbonate particles (along the main coast) or by compound and cryptocrystalline grains (west coast of Tubya al-Bayda).

b) deeper subtidal: samples with >1 % ooids occur in the basins of the “East area” between 34 and 42 m water depth. The amount of multilamellar coatings is relatively higher than in the shallow water group and the ooids sometimes occur together with compound grains which could be interpreted as fragments of oolitic rocks (Pl. 8, Fig. 6). In these samples, black impregnations of particles (including ooids) frequently occur (Pl. 8, Fig. 13)(comp. Fig. 19).

3.18. Non-carbonate grains

This category comprises all non-carbonate monomineralic grains (quartz and feldspar) as well as rock fragments of non-carbonate composition. The latter are relatively rare with quartz grains dominating by far.

The average abundance with >11 % is high, but the high variance ($s = 22.6 \%$) reflects the discontinuous distribution ranging between 0 and >95 %. The samples with high percentages are concentrated along the main coast and the west coast of Gazirat Safaga (Fig. 12). Higher abundances also occur in the central axis of the northern “Southwest

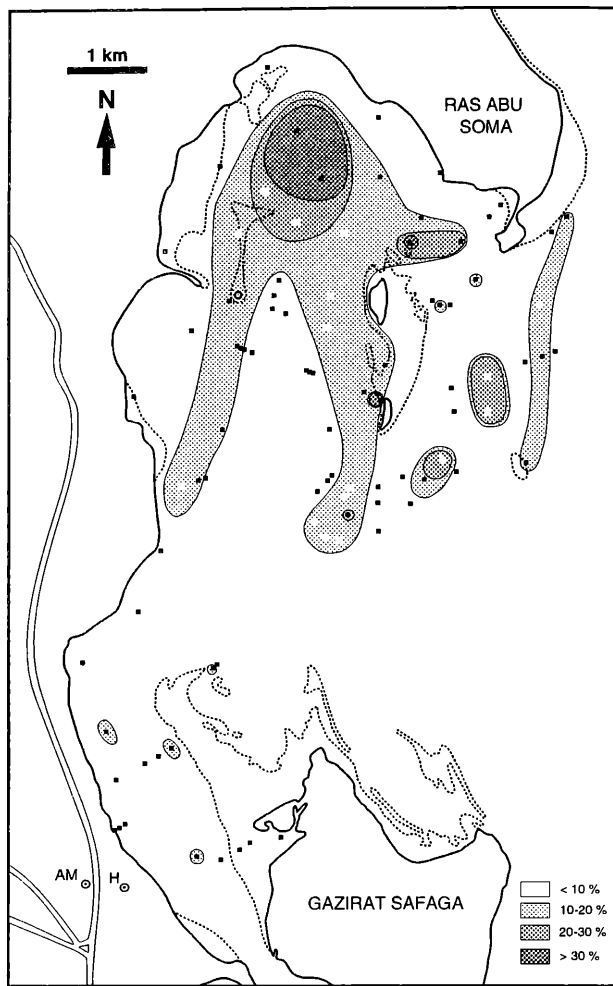


Figure 10: Distribution of compound grains.

channel". The origin and transportation mode of these particles are discussed in PILLER & MANSOUR (1994).

3.19. Unidentified grains

All particles for which a clear classification within one of the above listed particle-categories (chapt. 3.1.–3.18.) was not possible are counted herein. These particles are predominantly of fine sand or silt sized or smaller than 1/8 mm respectively. Larger particles are also included, however, only in a few exceptions.

The average frequency of unidentified grains is the highest of all particle categories (> 27 %, $s = 20.9 \%$), and ranges between 0 and >76 %. The largest area with the highest percentage (> 50 %) occurs in the basin of the "West", some isolated samples in the "East" also reach > 50 % (Fig. 13). Lowest percentages (< 10 %) occur around the islands and along the main coast.

3.20. Matrix

Everything which was not recognizable as an individual particle is included into this category. Matrix is usually difficult to recognize due to its diffuse distribution in the resin; these problems arise particularly in very thin thin-sections. In thicker thin sections it has a cloudy appearance.



Figure 11: Distribution of cryptocrystalline grains.

Average abundance is 5.66 % by a high variance (11.13 %) and range between 0 and >57 %. Highest percentages (> 30 %) are reached exclusively in the basin of the "West", all the other samples are distinctively below this percentage (Fig. 14).

4. Relationships between constituents (Tab. 3)

A correlation analysis was applied in order to detect relationships between the sediment constituents. Due to their low frequency sponges and vertebrates are not considered in this chapter.

Agglutinated foraminifera are highly positively correlated to hyaline foraminifera and crustaceans. Weak positive relations exist to molluscs and ostracods, negative to corals and non-carbonate particles. Miliolid foraminifera are highly positively related to crustaceans and plants and negatively to matrix and (weak) to red algae. Hyaline foraminifera are – besides agglutinated forams – highly positively related to molluscs, positively to bryozoans, and highly negatively to non-carbonate particles.

Corals have very strong positive relations to red algae, echinoderms, worm tubes, compound grains, molluscs, and bryozoans. Strong negative correlations occur to



Figure 12: Distribution of non-carbonate grains.



Figure 13: Distribution of unidentified grains.

unidentified grains, matrix and non-carbonate grains, weak to agglutinated foraminifera.

Bryozoans are positively related to corals, echinoderms, molluscs, and red algae.

Molluscs are highly positively related to compound grains, corals, red algae, echinoderms, hyaline foraminifera, bryozoa, and worm tubes, weakly to agglutinated foraminifera. Negative correlations exist to unidentified grains, non-carbonate grains, and matrix.

Worm tubes are highly positively related to corals, red algae, echinoderms, and molluscs, positively to crustaceans. Negative correlations exist to non-carbonate particles, unidentified grains, and matrix.

Crustaceans are positively related to miliolid and agglutinated foraminifera and (weak) to worm tubes; weak negative relations occur with matrix.

Ostracods have positive relations to unidentified grains, pellets, and agglutinated foraminifera, negative to corals and red algae.

Echinoderms are highly positively correlated with red algae, corals, worm tubes, molluscs, and bryozoa, negatively with non-carbonate particles.

Red algae have a very strong positive relation to corals, echinoderms, worm tubes, compound grains, and molluscs,

strong negative relations to unidentified grains, non-carbonate particles and matrix.

Green algae are not significantly correlated to any other category. Plants are only highly positively related to miliolid foraminifera. Pellets have weak correlations to ooids and ostracods.

Compound grains are highly positively related to molluscs, corals and red algae, weaker relations exist to cryptocrystalline grains. Negative relations are present to unidentified grains, matrix and non-carbonate particles. Cryptocrystalline grains show only weak correlations, positively to compound grains, negatively to matrix and unidentified grains.

The only strong positive correlation of ooids exists to non-carbonate particles, weak positive correlations to pellets. Weak negative relations occur to unidentified grains.

Non-carbonate particles are mainly characterized by negative correlations. Those exist to unidentified grains, molluscs, echinoderms, corals, hyaline foraminifera, red algae, worm tubes, compound grains, and (weak) to matrix and agglutinated foraminifera. The only positive correlation was detected with ooids.

Unidentified grains have high positive relations to matrix and ostracods, high negative one to corals, compound grains, red algae, molluscs, and non-carbonate compo-

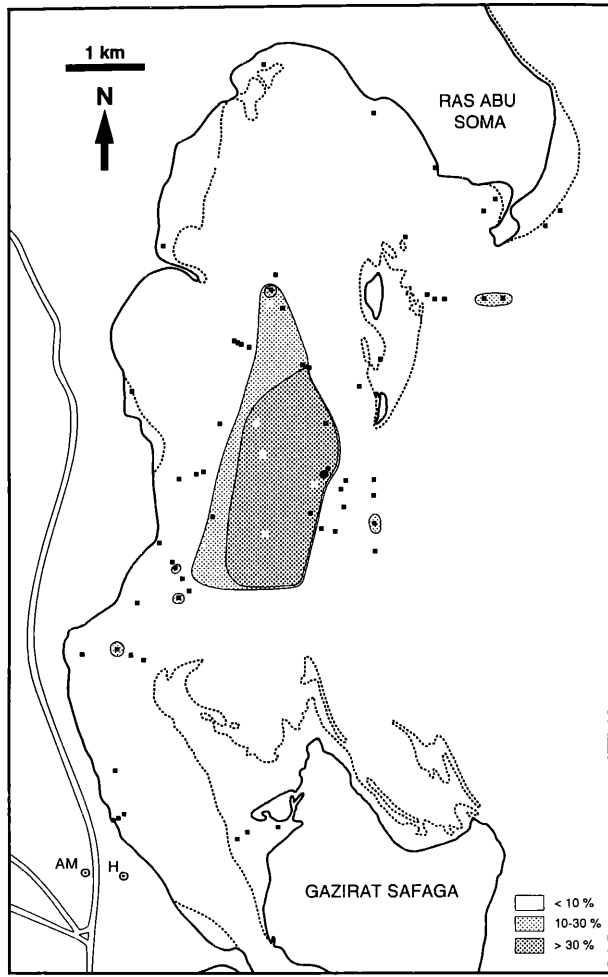


Figure 14: Distribution of matrix.

nents. Matrix is positively related only to unidentified grains, negative relations exist to compound grains, molluscs, corals, miliolid foraminifera and (weak) to cryptocrystalline grains, crustaceans, non-carbonate components, and worm tubes.

5. Microfacies

Besides subjective visual grouping of the thin sections, several statistical methods were performed in order to obtain a more objective result. No single applied statistical method (cluster analyses, factor analyses), however, produced a satisfactory result relative to the visual classification. Out of several cluster analyses those using Ward's method (SCHUBÖ & UEHLINGER, 1986) with squared Euclidian distances as similarity index brought the best results (Fig. 15). Only those clusters which were determined by one or only a few variables, however, coincide well with groups separated by visual assignment. The reason for this lack of agreement may be complex. One of the main reasons seems to originate in the absence of sharp delimitations between sample groups. All variables are highly gradational to one another without any distinct thresholds. This results in a more or less arbitrary grouping

by the clustering algorithm. Another reason may be that, in addition to the tabulated variables, the visual inspection of the thin section detects some more – partly qualitative or semiquantitative – information which were not available for the statistical analyses. The results of the cluster analysis, however, support the establishment of sample groups and encourage critical examination of visual groupings.

Basically, a distinct separation of 3 groups is possible. The separating character for one group is the amount of terrigenous material, the two other groups represent coarse grained and fine grained samples respectively. The variables "unidentified grains" and "matrix" act as an indirect measure for grain size. A further differentiation into microfacies is possible when using characters distinguished by visual identification supported by the cluster analysis. On this basis, the grain size determined groups can be subdivided in more detail on the basis of the main or characteristic constituents. The coarse grained group comprises the following: Coralgan facies, *Heterostegina* facies, Compound grain facies, Cryptocrystalline grain facies, Soritid–compound grain facies, Coralgan molluscan facies, Scaphopod facies, and Peloolitic molluscan facies. The fine grained group can be subdivided into the Mud facies, Mixed mud facies, *Operculina* facies, Foraminiferan sand facies, Soritid facies, *Operculina*–soritid facies, *Halimeda* facies, and Coralgan mud facies. Frequency data of sediment constituents of microfacies are listed in Tab. 4, their graphic representation is documented in Fig. 16, their distribution in Fig. 17.

5.1. Coralgan facies (Pl. 9, Figs. 1, 2)

The Coralgan facies (14 samples) is characterized by a high percentage of corals and red algae, representing together nearly 50 %. Both categories reach by far the highest values of all facies, however, variance of red algae is relatively high ($s = 6.6\%$). Molluscs as well as compound grains exceed 10 %, but molluscs show a high variance ($s = 7.05\%$). Foraminifera reach 8.6 % with the hyaline group dominating (4.9 %). No matrix is present in any thin section of this facies, unidentified grains are represented with only 4.5 %. This is the second lowest value of all facies. The amount of cryptocrystalline grains is low in most samples and exceeds 10 % only in sample B 25. Hyaline foraminifera are clearly dominated by *Amphistegina* with planorbulinids, acervulinids and homotrematids occurring relatively frequently. In some of the deeper samples *Heterostegina* is also present (e.g., B 56, B 59, B 60, B 61). The proportion of octocorallian spicules with respect to scleractinian fragments is also obviously higher in deeper water samples. Part of the compound grains are composed of fragments of different encrusting

	agglut. f.	hyaline f.	milliolid f.	corals	bryozoa	molluscs	crustaceans	echinoderms	green algae	red algae	plants	pellets	compound g.	cryptocr. g.	oids	non-carb.	unidentif. g.	matrix			
agglut. f.	1.000	0.144	0.347	-0.208	-0.035	0.190	-0.043	0.251	0.202	0.012	-0.159	-0.054	-0.035	0.040	-0.072	-0.105	0.055	-0.180	0.170	-0.175	
milliolid f.	0.144	1.000	0.018	-0.153	-0.055	0.009	0.114	0.408	0.072	-0.096	-0.211	-0.066	0.240	-0.166	-0.001	0.093	-0.124	-0.027	-0.091	-0.271	
hyaline f.	0.347	0.018	1.000	-0.156	0.192	0.282	-0.010	0.069	0.029	0.135	-0.095	-0.066	-0.082	0.076	-0.106	-0.159	-0.114	-0.252	0.049	-0.126	
corals	-0.208	-0.153	-0.156	1.000	0.264	0.323	0.412	-0.033	-0.245	0.473	0.790	-0.072	-0.011	-0.154	0.360	0.000	-0.124	-0.277	-0.499	-0.280	
bryozoa	-0.035	-0.055	0.192	0.264	1.000	0.244	0.134	-0.009	0.063	0.257	0.197	-0.040	-0.040	-0.058	0.032	-0.061	-0.093	-0.170	-0.145	-0.040	
molluscs	0.190	0.009	0.282	0.323	0.244	1.000	0.244	0.141	0.027	0.266	0.288	-0.123	-0.047	0.178	0.370	0.006	-0.045	-0.348	-0.404	-0.334	
worm t.	-0.043	0.114	-0.010	0.412	0.134	0.244	1.000	0.195	-0.149	0.280	0.356	-0.063	-0.021	-0.112	0.178	-0.046	-0.156	-0.243	-0.191	-0.185	
crustaceans	0.251	0.408	0.069	-0.033	-0.009	0.141	0.195	1.000	-0.038	0.052	0.030	-0.061	0.040	-0.139	-0.024	-0.030	-0.122	-0.056	-0.057	-0.205	
ostracods	0.202	0.072	0.029	-0.245	0.063	0.027	-0.149	-0.038	1.000	0.025	-0.208	0.043	-0.070	0.216	-0.169	-0.096	-0.048	-0.160	0.359	0.071	
echinoderms	0.012	-0.096	0.135	0.473	0.257	0.266	0.280	0.052	0.025	1.000	0.594	-0.094	-0.046	0.059	0.099	-0.009	-0.104	-0.319	-0.174	-0.178	
red algae	-0.159	-0.211	-0.095	0.790	0.197	0.288	0.356	0.030	-0.208	0.594	1.000	-0.063	0.015	-0.135	0.283	0.031	-0.050	-0.246	-0.444	-0.271	
green algae	-0.054	-0.066	-0.066	-0.072	-0.040	-0.123	-0.063	-0.061	0.043	-0.094	-0.063	1.000	-0.015	-0.004	-0.079	-0.057	-0.027	-0.046	0.026	-0.022	
plants	-0.035	0.240	-0.082	-0.011	-0.040	-0.047	-0.021	0.040	-0.070	-0.046	0.015	1.000	-0.015	1.000	-0.052	0.049	0.177	-0.019	-0.023	-0.077	-0.067
pellets	0.040	-0.166	0.076	-0.154	-0.058	0.178	-0.112	-0.139	0.216	0.059	-0.135	-0.004	-0.052	1.000	0.088	-0.005	0.225	-0.127	0.066	0.121	
compound g.	-0.072	-0.001	-0.106	0.360	0.032	0.370	0.178	-0.024	-0.169	0.099	0.283	-0.079	0.049	0.088	1.000	0.212	0.168	-0.236	-0.479	-0.346	
cryptocr. g.	-0.105	0.093	-0.159	0.000	-0.061	0.006	-0.046	-0.030	-0.096	-0.009	0.031	-0.057	0.177	-0.005	0.212	1.000	0.085	-0.033	-0.198	-0.219	
oids	0.055	-0.124	-0.114	-0.124	-0.093	-0.045	-0.156	-0.122	-0.048	-0.104	-0.080	-0.027	-0.019	0.225	0.168	0.085	1.000	0.274	1.000	-0.354	
non-carb.	-0.180	-0.027	-0.252	-0.277	-0.170	-0.348	-0.243	-0.056	-0.160	-0.319	-0.246	-0.046	-0.023	-0.127	-0.236	-0.033	0.274	1.000	-0.201		
unidentif. g.	0.170	-0.091	0.049	-0.499	-0.145	-0.404	-0.191	-0.057	0.359	-0.174	-0.444	0.026	-0.077	0.066	-0.479	-0.198	-0.199	-0.354	1.000	0.476	
matrix	-0.175	-0.271	-0.126	-0.280	-0.040	-0.334	-0.185	-0.205	0.071	-0.178	-0.271	-0.022	-0.067	0.121	-0.346	-0.219	-0.125	-0.201	0.476	1.000	

Table 3: Correlation coefficients between sediment constituents (120 samples) (bold type: 5 % sign. level, italic type: 10 % sign. level).

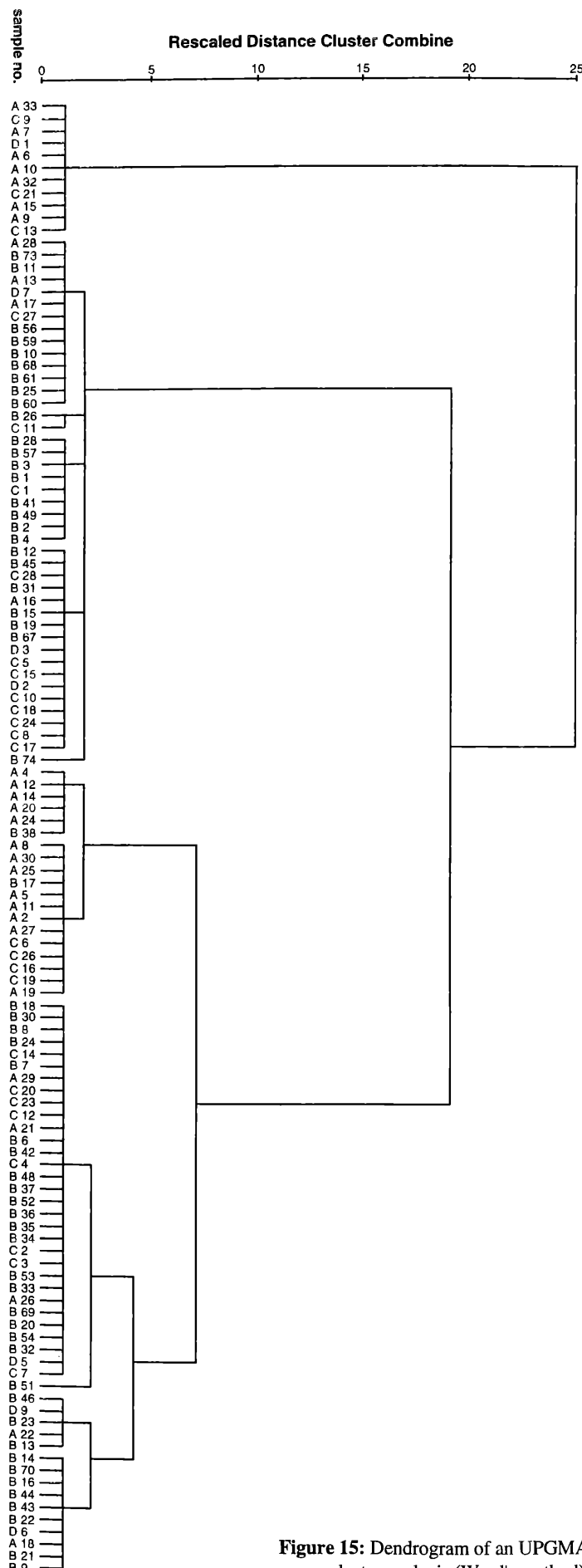


Figure 15: Dendrogram of an UPGMA cluster analysis (Ward's method).

organisms, their substrate and some fine grained material (either secreted or agglutinated).

Distribution: The main distribution area of this facies is located in the shallow water around the Tubya island group (except the immediate surrounding of its west and north coast) and in a large area north of Safaga island (Fig. 17). Additional occurrences consist of single samples off Ras Abu Soma, Tubya al-Kebir, of samples from the submarine ridge connecting Tubya al-Bayda with Safaga island, the gentle slope along the west coast of the "West area" and of some isolated samples of the "Southwest channel"

5.2. Coralgal – molluscan facies (Pl. 10, Figs. 1, 2)

This facies (8 samples) in fact represents a transition between the Coralgal and Coralgal mud facies. It is, on the one hand determined by a relatively high percentage of corals (22.9 %) and red algae (8.9 %), pointing to its affinities with the Coralgal facies. On the other hand, the relatively high percentage of unidentified grains (20.2 %) reflects the higher amount of fine grained sediment and therefore its relationship to the Coralgal mud facies. Although the mollusc content (17.4 %) is not very high, this category characterizes the coarse sediment fraction along with corals. Foraminifera are present with more than 11 % with miliolid (4.4 %) and hyaline (5.6 %) forms present in similar abundance. Hyaline foraminifera are represented by acervulinids, planorbulinids, *Heterostegina*, and *Amphistegina* as well as *Operculina* in some samples.

Distribution: The distribution of this microfacies is mainly restricted to a narrow strip along the border of the basin of the "west area" (5 samples) (Fig. 17). This position, located between the coralgal and mud facies clearly reflects its transitional character. The three additional isolated samples are also found in transitional positions (e.g., B 45: at the base of a coral covered pinnacle near the eastern margin of the "West area" basin).

5.3. Compound grain facies (Pl. 11, Fig. 1)

The characteristic components of this microfacies (7 samples) are compound grains (35.0 %) having a relatively wide frequency range (16–66 %). Corals range second (18.0 %), followed by molluscs (12.9 %) and crypto-crystalline grains (8.8 %); the latter show a high variance ($s = 7.60\%$). Unidentified grains

Coralgal facies

sample	aggl. f.	mil. f.	hyal. f.	spong.	corals	bryo	mol	worm	crust	ostr	echi	vert	red	green	plant	pellets	comp	crypto	oid	non-ca	unident	matrix
A13	0.16	8.87	2.38	0.00	35.82	0.00	22.19	0.32	0.00	0.00	0.00	3.80	0.00	0.00	0.00	12.52	7.92	0.00	3.17	2.85	0.00	
A17	0.71	1.61	2.68	0.00	41.25	0.18	18.39	0.54	0.36	0.00	0.71	0.00	10.89	0.00	0.00	18.57	0.71	0.00	0.00	3.39	0.00	
A28	1.38	3.29	6.57	0.00	44.81	0.17	10.55	0.69	0.17	0.00	2.25	0.00	13.15	0.00	0.00	7.44	2.42	0.00	0.52	6.57	0.00	
B10	0.00	1.24	4.43	0.00	34.16	0.18	22.30	0.18	0.18	0.00	1.59	0.00	18.23	0.18	0.00	12.92	0.00	0.00	0.00	4.42	0.00	
B11	0.35	1.76	7.92	0.00	27.82	0.35	5.99	1.06	0.53	0.00	4.40	0.00	30.99	0.00	0.00	11.09	0.88	0.00	0.18	6.69	0.00	
B25	0.66	1.33	2.98	0.00	25.99	0.00	24.01	0.17	0.00	0.00	0.33	0.00	12.75	0.00	0.00	14.73	11.92	0.99	0.33	3.48	0.00	
B56	0.41	1.83	7.71	0.00	29.21	0.00	16.23	1.42	0.20	0.00	0.61	0.00	17.65	0.00	0.00	17.85	3.25	0.00	0.81	2.84	0.00	
B59	2.94	3.14	4.71	0.00	29.80	0.00	15.88	1.57	0.98	0.00	0.78	0.00	18.04	0.20	0.00	15.88	0.78	0.00	0.00	5.29	0.00	
B60	0.94	0.19	2.63	0.00	22.33	0.00	34.15	1.69	0.00	0.00	1.13	0.00	15.20	0.00	0.00	16.51	3.57	0.00	0.19	1.31	0.00	
B61	1.16	0.58	3.47	0.00	29.54	0.00	24.87	1.35	0.77	0.19	0.77	0.00	11.00	0.00	0.00	18.15	0.57	0.00	0.00	6.18	0.00	
B67	1.99	7.14	1.33	0.00	25.25	0.17	21.76	1.83	0.50	0.00	1.16	0.00	8.47	0.33	0.00	14.78	3.99	0.00	1.66	9.63	0.00	
B68	0.93	6.79	3.70	0.00	30.25	0.00	21.14	1.70	0.31	0.00	0.77	0.00	13.43	0.00	0.00	12.35	2.93	0.00	0.77	4.94	0.00	
B73	0.74	4.82	4.82	0.00	41.93	0.19	9.28	0.37	0.56	0.00	3.90	0.00	20.78	0.00	0.00	6.12	2.41	0.00	0.00	4.08	0.00	
C27	0.35	1.57	10.26	0.00	41.22	0.00	14.78	1.04	0.00	0.00	4.17	0.00	9.39	0.00	0.17	0.00	10.78	2.26	0.00	0.87	3.13	0.00
C5	1.19	2.84	4.33	0.00	22.24	0.15	17.31	0.30	0.15	0.00	1.49	0.00	6.27	0.00	0.00	0.30	14.78	4.03	1.64	13.43	9.55	0.00
D7	0.19	3.31	4.87	0.00	37.04	1.17	19.49	1.56	0.00	0.00	0.97	0.00	4.87	0.00	0.00	13.65	4.48	0.00	0.00	0.78	7.60	0.00
n=16																						
mean	0.881	3.144	4.674	0.00	32.416	0.16	18.703	0.987	0.306	0.012	1.564	0.00	13.43	0.044	0.01	0.039	13.633	3.283	0.164	1.419	5.122	0.00
st. dev.	0.755	2.526	2.376	0.00	7.233	0.29	6.868	0.612	0.292	0.048	1.389	0.00	6.825	0.10	0.04	0.108	3.583	3.013	0.465	3.307	2.421	0.00
min	0.00	0.19	1.33	0.00	22.24	0.00	5.99	0.17	0.00	0.00	0.00	0.00	3.80	0.00	0.00	0.00	6.12	0.00	0.00	0.00	1.31	0.00
max	2.94	8.87	10.26	0.00	44.81	1.17	34.15	1.83	0.98	0.19	4.40	0.00	30.99	0.33	0.17	0.33	18.57	11.92	1.64	13.43	9.63	0.00

Coralgal-molluscan facies

sample	aggl. f.	mil. f.	hyal. f.	spong.	corals	bryo	mol	worm	crust	ostr	echi	vert	red	green	plant	pellets	comp	crypto	oid	non-ca	unident	matrix
A16	1.67	3.51	4.18	0.00	15.89	0.17	21.91	1.67	0.00	0.00	2.01	0.00	6.86	0.00	0.17	0.00	9.37	2.84	0.00	5.18	18.56	6.02
B12	1.95	9.40	2.43	0.00	23.34	0.16	9.08	0.65	0.32	0.16	3.89	0.00	15.07	0.16	0.49	0.00	6.81	2.92	0.00	0.16	23.01	0.00
B15	0.31	5.00	4.06	0.00	15.94	0.00	27.66	0.78	0.47	0.00	1.72	0.00	4.69	0.00	0.00	0.00	11.09	2.34	0.00	0.78	20.00	5.16
B19	1.85	2.86	8.91	0.00	12.77	0.00	29.08	1.35	0.17	0.00	2.69	0.00	6.39	0.00	0.00	0.00	12.61	2.69	0.00	3.53	12.10	3.03
B31	1.25	3.06	5.01	0.14	37.47	0.14	14.07	0.70	0.14	0.00	0.84	0.00	7.80	0.00	0.00	0.00	4.32	1.53	0.00	0.00	23.26	0.28
B45	1.21	1.56	3.64	0.00	23.05	0.17	10.40	2.77	0.00	0.00	1.39	0.00	12.13	0.00	0.00	0.00	0.52	5.37	1.21	0.00	30.50	5.72
C28	0.45	1.37	10.47	0.00	29.13	0.45	5.77	0.91	0.61	0.00	3.03	0.00	12.59	0.00	0.00	6.37	4.25	0.00	0.61	23.98	0.00	
D3	0.60	8.62	6.01	0.00	26.05	0.00	21.04	3.41	0.40	0.00	2.41	0.00	5.61	0.20	0.00	12.63	1.80	0.00	0.40	10.42	0.40	
n=8																						
mean	1.161	4.423	5.569	0.018	22.955	0.136	17.376	1.53	0.264	0.02	2.248	0.00	8.893	0.045	0.08	0.065	8.571	2.448	0.00	1.376	20.229	2.576
st. dev.	0.645	3.056	2.764	0.049	8.119	0.15	8.782	1.037	0.223	0.057	0.97	0.00	3.824	0.084	0.18	0.084	3.296	0.963	0.00	1.906	6.564	2.723
min	0.31	1.37	2.43	0.00	12.77	0.00	5.77	0.65	0.00	0.00	0.84	0.00	4.69	0.00	0.00	0.00	4.32	1.21	0.00	0.00	10.42	0.00
max	1.95	9.40	10.47	0.14	37.47	0.45	29.08	3.41	0.61	0.16	3.89	0.00	15.07	0.20	0.49	0.52	12.63	4.25	0.00	5.18	30.50	6.02

Table 4: Frequency (%) of sediment constituents and some statistical parameters of microfacies.

remain below 10 %, matrix is missing. Foraminifera reach 8.1 % and are dominated by miliolid forms (6.1 %) (Fig. 16).

Two samples differ clearly in the distinctively higher amount of compound grains (B 26: 51.7 %; C 11: 66.4 %) from the other 5 samples. This higher abundance of compound grains occurs at the expense of corals, which remain below 10 %. The compound grains are predominantly of the grapestone type, in some samples rock fragments (oolitic limestone) may be included (e.g., B 26). The miliolid foraminifers are dominated by smaller forms of the *Quinqueloculina-Triloculina* group and by peneroplids, with soritids occurring only in some thin sections.

Distribution: There are two areas – both in very shallow water – where this microfacies occurs (Fig. 17): one in the “North” mainly on and in the east of the shoal of al-Dahira; the other area is west and north of the Tubya islands, covering mainly the intertidal and very shallow subtidal.

5.4. Cryptocrystalline grain facies (Pl. 11, Fig. 2)

This facies represented by only one sample (B 74) is distinguished from all other samples by its very high proportion of cryptocrystalline grains (>52 %). Beside this dominant category, compound grains nearly reach 13 %; all other components remain below 10 %.

The relatively rare foraminifera (5.7 %) are dominated by soritids and their fragments. The sediment is dominated by finer sand fractions. Coarser grains consist mainly of molluscs, soritids, coralline algae, compound grains, and non-carbonate grains.

Distribution: The single sample representing this facies is located on the rocky tidal flat between Tubya al-Hamra and Tubya al-Bayda (Fig. 17).

5.5. Soritid – compound grain facies

Although the two samples – C 15 and C 17 – clearly represent a transition between the compound grain facies respectively cryptocrystalline grain facies and soritid facies, they are clearly differentiated from these. The transition is expressed by the high percentage of miliolid foraminifera (20.4 %) and by 20.5 % of compound grains (Fig. 16) and, in addition, by more than 8 % cryptocrystalline grains. Besides soritid foraminifera, *Borelis*, peneroplids and smaller miliolids are also frequently represented. The presence of nearly 10 % plants in sample C 15 also points to the close relationship to the soritid facies. Molluscs occur with 16 % and 8 % respectively.

Distribution: The position of the two samples belonging to this microfacies is as transitional as their microfacial content. They are located west- respectively northward of the al-Dahira shoal exactly between an area of soritid and compound grain facies (Fig. 17).

5.6. *Heterostegina* facies (Pl. 12, Fig. 1)

The most characteristic constituent of this facies (4 samples) are hyaline foraminifera (24.0 %) which are dominated by the genus *Heterostegina* (Fig. 16). Molluscs (18.9 %), compound grains (16.8 %) and corals (12.8 %) also exceed 10 %, red algae are relatively abundant with 6.4 %. Besides the characteristic *Heterostegina*, the larger hyaline forms of the genus *Amphistegina* are very abundant, fragments of acervulinid foraminifera also occur. Scaphopod shells are a characteristic component among the relatively abundant molluscs. Corals are represented by a relatively high percentage of alcyonarian spicules. Red algae comprise not only coralline algae, but also squamariacean.

Distribution: All four samples of this facies come from the “East area” Three originate from the submarine ridge which separates the Northern Safaga bay from the open sea (Fig. 17); one sample (B 4) comes from the area which separates the northern from the southern basin of the “East” (comp. PILLER & PERVESLER, 1989). All samples originate from relatively deep water (45 – 62 m).

5.7. Scaphopod facies (Pl. 12, Fig. 2)

Although cluster analysis places sample B 3 in one cluster along with the samples of the *Heterostegina* facies, it is made up of 42.3 % of molluscs which are dominated by scaphopod shells. In addition, the presence of 5.1 % matrix differentiates this sample from the matrix-free *Heterostegina* facies samples. The relatively high similarity to the latter is expressed by 19.2 % of hyaline foraminifera, which are, however, dominated by *Operculina* and *Amphistegina*. Branched bryozoans are rare but obvious.

Distribution: The sample representing this facies is located just west of the submarine ridge separating the Northern Safaga bay from the open sea and was taken in 58 m water depth (Fig. 17).

5.8. Peloolitic molluscan facies (Pl. 13, Fig. 1)

The most abundant constituents of this facies (4 samples) are molluscs (27.0 %) and compound grains (19.9 %), foraminifera are also relatively abundant (14.9 %). The most distinctive although subordinate components are, however, pellets and ooids. Pellets only occur with 4.4 % ranging between 1.4 and 7.5 %, ooids make up only 2 % and have a range between 0.9 and 4.1 %. Unidentified grains occur with 13.2 %.

Particles are frequently blackened, pellets are large and of the crustacean type (comp. chapt. 3.14.). Hyaline foraminifera, the most abundant group (9.8 %), mainly belong to *Operculina*, but *Amphistegina* and *Heterostegina* are also present; worth mentioning is the occurrence of large elphidiids. Among molluscs, the relatively frequent occurrence of scaphopods should be noted. At least some of the compound grains represent limestone clasts (oolitic

Compound grain facies

sample	aggl. f.	mil. f.	hyal. f.	spong	corals	bryo	mol	worm	crust	ostr	echi	vert	red	green	plant	pellets	comp	crypto	ooid	non-ca	unident	matrix
B26	0.33	1.81	0.49	0.00	8.07	0.00	7.25	0.00	0.00	0.66	0.00	5.93	0.00	0.00	51.73	14.83	5.60	2.14	1.15	0.00		
C8	1.11	9.34	3.07	0.00	18.13	0.00	13.39	1.12	0.00	0.14	0.42	0.14	2.93	0.00	0.00	20.08	3.49	0.00	1.95	24.69	0.00	
C10	0.17	5.41	2.20	0.00	30.24	0.00	14.02	1.18	0.00	0.00	0.85	0.00	2.87	0.00	0.00	30.24	4.05	0.00	0.34	8.45	0.00	
C11	0.00	3.47	0.73	0.00	7.31	0.00	17.73	0.18	0.00	0.00	0.18	0.00	2.19	0.00	0.00	66.36	0.00	0.00	0.18	1.65	0.00	
C18	0.30	8.71	1.50	0.00	27.48	0.15	14.71	0.00	0.00	0.15	0.75	0.00	5.25	0.00	0.15	0.00	27.03	3.60	0.00	0.90	9.16	0.00
C24	0.00	5.30	2.06	0.00	20.18	0.00	7.81	0.15	0.00	0.15	0.00	0.00	5.30	0.00	0.00	33.58	12.52	0.00	0.29	11.93	0.00	
D2	1.11	8.43	0.95	0.00	15.10	0.00	15.42	0.16	0.64	0.00	0.95	0.00	8.90	0.00	1.27	0.00	16.06	22.89	0.32	1.27	6.52	0.00

n=7

sample	aggl. f.	mil. f.	hyal. f.	spong	corals	bryo	mol	worm	crust	ostr	echi	vert	red	green	plant	pellets	comp	crypto	ooid	non-ca	unident	matrix
B74	0.00	5.55	0.15	0.00	3.50	0.00	9.63	0.00	0.00	0.88	0.00	3.50	0.00	0.00	0.00	12.99	52.12	0.00	7.15	4.53	0.00	

Cryptocrystalline grain facies

sample	aggl. f.	mil. f.	hyal. f.	spong	corals	bryo	mol	worm	crust	ostr	echi	vert	red	green	plant	pellets	comp	crypto	ooid	non-ca	unident	matrix
B74	0.00	5.55	0.15	0.00	3.50	0.00	9.63	0.00	0.00	0.88	0.00	3.50	0.00	0.00	0.00	12.99	52.12	0.00	7.15	4.53	0.00	

Soritid-compound grain facies

sample	aggl. f.	mil. f.	hyal. f.	spong	corals	bryo	mol	worm	crust	ostr	echi	vert	red	green	plant	pellets	comp	crypto	ooid	non-ca	unident	matrix
C15	0.82	21.75	1.65	0.00	8.90	0.00	7.91	0.33	0.33	0.00	0.33	0.00	4.45	0.00	9.06	0.00	13.84	13.01	0.33	2.80	14.00	0.49
C17	2.00	19.08	2.00	0.00	10.92	0.15	16.31	1.69	0.61	0.00	0.31	0.00	1.39	0.00	0.00	0.00	27.08	3.39	0.00	2.92	12.15	0.00
n=2																						
mean	1.41	20.415	1.825	0.00	9.91	0.075	12.11	1.01	0.47	0.00	0.32	0.00	2.92	0.00	4.53	0.00	20.46	8.20	0.165	2.86	13.075	0.245
st. dev.	0.834	1.888	0.247	0.00	1.428	0.106	5.94	0.962	0.198	0.00	0.014	0.00	2.164	0.00	6.406	0.00	9.362	6.802	0.233	0.085	13.08	0.346

Heterostegina facies

sample	aggl. f.	mil. f.	hyal. f.	spong	corals	bryo	mol	worm	crust	ostr	echi	vert	red	green	plant	pellets	comp	crypto	ooid	non-ca	unident	matrix
B1	1.50	4.84	28.55	0.00	10.68	0.67	16.53	0.00	0.00	0.00	2.17	0.00	5.68	0.00	0.00	0.00	9.85	6.85	0.00	0.00	12.69	0.00
B2	0.83	2.66	15.95	0.00	22.59	0.17	14.62	5.81	0.50	0.00	1.99	0.00	8.14	0.00	0.00	0.00	15.95	3.65	0.00	0.17	6.65	0.00
B4	1.24	5.75	17.39	0.00	10.87	0.00	18.48	0.47	0.00	0.00	1.40	0.00	7.14	0.00	0.00	0.00	26.09	2.64	0.00	0.78	7.61	0.00
C1	1.59	4.77	34.18	0.00	7.15	0.48	25.75	0.95	0.00	0.00	0.32	0.00	4.77	0.00	0.00	0.00	15.42	1.91	0.00	0.32	2.07	0.00
n=4																						
mean	1.29	4.505	24.018	0.00	12.823	0.33	18.845	1.808	0.125	0.00	1.47	0.00	6.433	0.00	0.00	0.20	16.828	3.763	0.00	0.318	7.255	0.00
st. dev.	0.341	1.308	8.81	0.00	6.733	0.301	4.866	2.696	0.25	0.00	0.834	0.00	1.50	0.00	0.00	0.157	6.763	2.178	0.00	0.335	4.356	0.00
min	0.83	2.66	15.95	0.00	7.15	0.00	14.62	0.00	0.00	0.00	0.32	0.00	4.77	0.00	0.00	0.00	9.85	1.91	0.00	0.00	2.07	0.00
max	1.59	5.75	34.18	0.00	22.59	0.67	25.75	5.81	0.50	0.00	2.17	0.00	8.14	0.00	0.00	0.33	26.09	6.85	0.00	0.78	12.69	0.00

Scaphopod facies

sample	aggl. f.	mil. f.	hyal. f.	spong	corals	bryo	mol	worm	crust	ostr	echi	vert	red	green	plant	pellets	comp	crypto	ooid	non-ca	unident	matrix
B3	2.01	4.95	19.19	0.00	0.62	0.93	42.26	0.00	0.46	0.46	1.08	0.00	0.62	0.00	0.00	0.15	5.26	3.25	0.00	0.00	13.62	5.11

Table 4 (continued): Frequency (%) of sediment constituents and some statistical parameters of microfacies.

limestone) or show signs of abrasion.

Distribution: All four samples come from the “East area”, however, they originate from three different areas (Fig. 17). They are, nevertheless, located in marginal positions between basins and submarine elevations: three samples (B 28, B 49, B 41) in the more central parts between the north and south basin of the “East”, B 57 from the western margin of the southern basin. All come from water depth > 40 m.

5.9. *Halimeda* facies (Pl. 13, Fig. 2)

The sample B 51, with a percentage of 59.4 % of green algae, is completely different from all other samples. The green algae are exclusively represented by fragments of *Halimeda*. The amount of unidentified grains is with >32 % high and reflects the otherwise relatively fine grained sediment. In addition, only matrix and foraminifera exceed 1 %.

Distribution: The single sample comes from the “East area” and is located near the western margin of the submarine ridge connecting Ras Abu Soma and Safaga island which also acts as separation between the bay and the open sea (Fig. 17).

5.10. Soritid facies (Pl. 14, Fig. 1)

The samples of this facies (n = 10) are clearly dominated by foraminifera (32.8 %), in particular by miliolids (26.7 %). Besides unidentified grains (21.9 %), non-carbonate grains (15.9 %) and molluscs (10.8 %) exceed 10 %. Compound grains and cryptocrystalline grains together also reach 10 %.

The miliolid foraminifera are dominated by soritids, however, *Borelis* and sometimes peneroplids are also abundant. Hyaline foraminifera (4.5 %) are characterized by *Amphistegina*, in some samples planorbulinids and *Operculina* may also occur. The range of non-carbonate grains is very wide (4.1–46.4 %; s = 13.98 %). Striking is the highest amount of crustaceans (1 %) among all microfacies. Compound grains usually are of a dense type without interparticle porosity.

Distribution: The largest area covered by this facies parallels the western and main part of the northern margin of the “North area” and continues into the south to the “West area” covering the large shallow water area at the west coast except for a narrow coastal strip (Fig. 17). Another larger area parallels the west coast of the northern “Southwest channel”. Both coasts of the southern “Southwest channel” are also represented by this microfacies.

5.11. *Operculina* – soritid facies

Two thin sections (A 4, A 12) are different from all other samples in having more than 52 % of foraminifera. Not one major group dominates since both hyaline (27.5 %) as well as miliolid (22.0 %) foraminifera are very abundant, both with a small variance; in addition, agglutinated forms are relatively abundant with 3.4 %. Besides foraminifera,

molluscs (15.8 %) and unidentified grains (20.5 %) exceed 10 %; non-carbonate grains exceed 5 %.

The hyaline foraminifera are dominated by *Amphistegina* and *Operculina*, the miliolids by soritids and *Borelis*. Compound grains are of fine grained non-porous type.

Distribution: The location of the two samples represents the transitional character of the facies as they are located at the margin of the Foraminiferan sand facies in the southern part of the “Southwest channel” (Fig. 17).

5.12. Foraminiferan sand facies (Pl. 14, Fig. 2; Pl. 15, Fig. 1)

This large sample group (n = 16), belonging to the fine grained main group, is characterized by a relatively high percentage of foraminifera (18.9 %). Besides more than 40 % of unidentified grains, only non-carbonate grains exceed 10 % (Tab. 4); molluscs (just below 10 %) and compound grains (7.8 %) exceed 5 %. The variance of all major constituents is relatively high, reflecting the inhomogenous composition of this facies (Tab. 4).

Foraminifera are well represented by all three major groups: agglutinated forms reach the highest percentage of all facies (3.8 %), however, they range between 0 and 9.4 %. The samples with higher abundances comprise mainly large paraperforate *Textularia*, but smaller forms may be also common. Miliolid forms range between 2.7 and 17.5 %, the majority of which consists of small forms of *Quinqueloculina*-*Triloculina* type without obvious dominance of soritids, peneroplids and *Borelis*. Hyaline foraminifera (range 0.9–23.1 %) are represented by *Operculina* in the samples with higher frequencies

Distribution: Three relatively large areas belong to this microfacies (Fig. 17): The first covers the main part of the northern basin and the areas connecting to the southern basin of the “East”. The second area covers the east of the “North area” located north of Tubya al-Hamra. The third area is in the axis of the northern part of the “Southwest channel”

5.13. Coralgal mud facies (Pl. 15, Fig. 2)

A frequency of 42 % of unidentified grains and nearly 10 % of matrix assigns this facies (7 samples) to the fine grained group. The frequency of corals (13.9 %), red algae (5.5 %), molluscs (9.3 %), and compound grains (5.7 %) clearly point in the direction of Coralgal-molluscan facies. Foraminifera occur with 8.2 %.

Among foraminifera, hyaline forms dominate represented on the one hand by *Operculina* (although not abundant), but also by acervulinids, planorbulinids and *Heterostegina* on the other.

Distribution: All samples of this facies come from a marginal position of areas with pronounced topographic relief. These are located on the one hand along the eastern

Peloolitic molluscan facies

sample	aggl. f.	mil. f.	hyal. f.	spong	corals	bryo	mol	worm	crust	ostr	echi	vert	red	green	plant	pellets	comp	crypto	ooid	non-ca	unident	matrix
B28	1.86	1.86	7.97	0.00	4.07	0.00	30.00	0.00	0.17	1.19	0.00	1.53	0.00	7.46	18.47	1.53	4.07	4.07	12.88	2.88		
B41	1.39	5.56	13.49	0.00	4.03	0.00	19.61	0.28	0.42	0.28	0.00	0.83	0.00	3.34	20.03	7.65	1.67	3.48	16.27	0.28		
B49	1.73	4.32	12.97	0.00	3.60	0.00	19.02	0.29	0.00	0.29	0.00	0.87	0.00	5.33	20.03	10.66	1.44	1.59	13.40	2.59		
B57	0.71	3.01	4.60	0.00	2.48	0.00	39.47	0.89	0.35	0.00	1.77	0.00	6.55	0.00	1.42	20.89	3.36	0.89	3.54	10.09	0.00	
n=4																						
mean	1.423	3.688	9.758	0.00	3.545	0.00	27.025	0.365	0.193	0.185	0.00	2.445	0.00	4.388	19.855	5.80	2.018	3.17	13.16	1.438		
st. dev.	0.515	1.603	4.244	0.00	0.741	0.00	9.709	0.375	0.224	0.135	0.301	0.00	2.755	0.00	2.597	1.008	4.132	1.407	1.086	2.532	1.507	
min	0.71	1.86	4.60	0.00	2.48	0.00	19.02	0.00	0.00	0.00	1.19	0.00	0.83	0.00	1.42	18.47	1.53	0.89	1.59	10.09	0.00	
max	1.86	5.56	13.49	0.00	4.07	0.00	39.47	0.89	0.42	0.29	1.87	0.00	6.55	0.00	7.46	20.89	10.66	4.07	4.07	16.27	2.88	

Halimeda facies

sample	aggl. f.	mil. f.	hyal. f.	spong	corals	bryo	mol	worm	crust	ostr	echi	vert	red	green	plant	pellets	comp	crypto	ooid	non-ca	unident	matrix
B51	0.29	1.17	1.17	0.00	0.29	0.00	0.73	0.00	0.00	0.15	0.00	0.00	0.00	59.38	0.00	0.29	0.59	0.29	0.00	0.59	32.11	2.93

Soritid facies

sample	aggl. f.	mil. f.	hyal. f.	spong	corals	bryo	mol	worm	crust	ostr	echi	vert	red	green	plant	pellets	comp	crypto	ooid	non-ca	unident	matrix
A2	0.87	35.59	2.88	0.00	17.00	0.00	13.11	0.00	0.14	0.58	0.00	2.74	0.00	0.00	0.00	5.76	0.00	0.00	5.62	15.71	0.00	
A5	2.12	32.90	10.10	0.00	1.79	0.00	10.42	2.61	1.47	0.00	0.33	0.00	0.00	0.65	0.00	7.82	1.63	0.00	4.07	21.98	2.11	
A8	0.64	16.85	5.30	0.00	10.11	0.80	13.16	0.32	0.80	0.16	0.96	0.00	2.41	0.00	0.32	0.00	12.84	1.93	0.00	10.59	22.79	0.00
A11	2.01	31.90	4.31	0.00	2.73	0.14	11.35	0.72	0.86	0.00	0.14	0.00	0.29	0.00	0.29	0.00	5.46	0.57	0.00	9.63	28.74	0.00
A11	1.90	21.75	6.71	0.00	0.29	0.00	12.12	0.44	0.15	0.44	0.15	0.00	0.44	0.00	0.15	0.00	1.90	0.15	0.00	46.42	7.01	0.00
A19	2.91	27.01	6.51	0.00	1.11	0.00	10.11	1.80	0.28	0.14	1.25	0.00	0.55	0.14	0.00	0.00	2.91	8.73	0.00	6.65	29.64	0.28
A25	1.65	21.20	4.36	0.00	0.90	0.00	13.38	1.35	0.30	0.00	0.30	0.00	0.00	0.00	0.00	0.00	9.77	5.71	0.00	11.13	27.07	0.45
A30	1.35	33.38	2.70	0.00	2.16	0.00	5.27	1.35	0.41	0.00	1.08	0.00	0.00	0.27	0.00	0.00	5.00	10.00	0.00	5.13	31.49	0.41
B17	0.78	24.14	1.40	0.00	2.96	0.00	7.17	0.00	2.03	0.00	1.40	0.00	0.00	0.16	0.00	4.98	0.31	0.00	36.60	16.51	0.00	
C16	0.68	22.72	1.22	0.00	3.54	0.00	11.70	0.82	1.36	0.14	0.27	0.00	0.68	0.00	0.00	0.00	8.57	6.94	0.00	23.40	17.96	0.00
n=10																						
mean	1.491	26.744	4.549	0.00	4.259	0.094	10.779	0.941	1.007	0.131	0.718	0.00	0.836	0.014	0.184	0.016	6.501	3.597	0.00	15.924	21.89	0.325
st. dev.	0.757	6.354	2.732	0.00	5.255	0.252	2.683	0.839	0.881	0.145	0.45	0.00	1.015	0.044	0.209	0.051	3.286	3.865	0.00	14.733	7.68	0.654
min	0.64	16.85	1.22	0.00	0.29	0.00	5.27	0.00	0.00	0.00	0.15	0.00	0.00	0.00	0.00	0.00	1.90	0.00	0.00	4.07	7.01	0.00
max	2.91	35.59	10.10	0.00	17.00	0.80	13.38	2.61	2.71	0.44	1.40	0.00	2.74	0.14	0.65	0.16	12.84	10.00	0.00	46.42	31.49	2.11

Operculina-soritid facies

sample	aggl. f.	mil. f.	hyal. f.	spong	corals	bryo	mol	worm	crust	ostr	echi	vert	red	green	plant	pellets	comp	crypto	ooid	non-ca	unident	matrix
A4	2.75	22.17	30.42	0.00	0.32	0.00	19.09	0.00	0.00	0.65	0.00	0.00	0.00	0.00	0.00	3.56	0.00	0.00	5.18	14.56	1.29	
A12	4.00	21.76	24.64	0.00	1.28	0.00	12.48	0.00	0.00	0.16	0.48	0.00	0.00	0.00	0.00	0.32	0.00	0.00	5.28	26.40	3.04	
n=2																						
mean	3.375	21.965	27.53	0.00	0.80	0.00	15.785	0.00	0.08	0.565	0.00	0.00	0.08	0.00	0.00	1.94	0.00	0.00	5.23	20.48	2.16	
st. dev.	0.884	0.29	4.087	0.00	0.679	0.00	4.674	0.00	0.00	0.113	0.12	0.00	0.00	0.00	0.00	2.291	0.00	0.00	0.071	8.372	1.23	

Table 4 (continued): Frequency (%) of sediment constituents and some statistical parameters of microfacies.

margin of the basin of the “West” on the other in small isolated depressions of different areas (Fig. 17).

5.14. *Operculina* facies (Pl. 16, Fig. 1)

The high percentage of unidentified grains (48.2 %) and matrix (7.3 %) in connection with 15.9 % of hyaline foraminifera discriminates this large sample group (16 samples) from other facies. Besides these three categories, molluscs are present in higher frequencies (10.7 %). Foraminifera as a whole reach 21.7 %. The sediment ranges predominantly in the fine sand and in silt fraction. A further differentiation into two groups (a sand and a mud group) would be possible, however, without a sharp distinction.

Hyaline foraminifera are clearly dominated by *Operculina*, however, their frequency range is remarkably high (7.5–33.5 %). Agglutinated forms are characterized by large textulariids; miliolids are variable in diversity.

Distribution: The most characteristic area for this microfacies is found in the southern basin of the “East area” where nearly all samples belong into this facies (Fig. 17). The northeastern part of the northern basin also belongs herein. An additional typical area is a narrow strip along the western margin of the basin of the “West” as well as the axial part of the southern “Southwest channel”

5.15. Mud facies (Pl. 16, Fig. 2)

The 10 samples classified in this microfacies are completely dominated by fine grained sediment, expressed by the high percentages of unidentified grains (62.5 %) and matrix (29.6 %). Among the remaining constituents, non-carbonate grains (2.8 %), foraminifera (2.7 %) and molluscs (1.1 %) exceed 1 %.

Small sized as well as zonally structured pellets are worth mentioning, but are volumetrically unimportant. Relatively large elphidiids and *Quinqueloculina-Triloculina* type forms are conspicuous among the rare foraminifera. The rare molluscs seem to be dominated by gastropods.

Distribution: The entire basin of the “West area” is covered by this facies which projects for a short distance into the northernmost part of the “Southwest channel” (Fig. 17).

5.16. Mixed mud facies

Those four samples which have a relatively high percentage of unidentified grains (40.5 %) and matrix (32.8 %) combined with, at least, one more abundant particle category (> 5 %) are classed in this microfacies. It is in fact a transitional group: the general characteristic of the sediment resembles that of the mud facies, whereas the higher amount of one grain category points to another microfacies (e.g., foraminiferan sand or coralgan mud facies). Their classification in a separate microfacies represents a compromise.

Distribution: All four samples occur in marginal position along the basin of the “West area”

5.17. Terrigenous facies (Pl. 17, Figs. 1, 2; Pl. 18, Figs. 1, 2)

The samples of this microfacies (n = 11) are distinctly separated from all other samples by their high percentage of non-carbonate particles (77.9 %) with a relatively low variance (s = 11 %). No other particle category exceeds 5 %, foraminifera (3.8 %), unidentified particles (3.3 %), cryptocrystalline particles (3.3 %), and compound grains (3.1 %) exceed 3 %, however, showing high variances. Two subgroups can be separated on the basis of the amount of non-carbonate particles (supported also by cluster analysis). One group is characterized by more than 80 % non-carbonate grains, the second by percentages between 64 and 72 %.

Grain size is variable with respect to sand fraction, reaching from fine sand dominated samples to coarse sand samples with a considerable amount of gravel. Roundness is also highly variable.

Distribution: The Terrigenous facies is represented by a continuous relatively narrow strip along the main coast from the “Southwest channel” to the western coast of Ras Abu Soma. A second area is on the tidal flat and mangal west of Safaga island (Fig. 17).

6. Microfacies interpretation and relations to bottom facies

One of the main goals of this study is to detect the degree of compatibility between field observations, documented in the bottom facies distribution (PILLER & PERVESLER, 1989), and the results of the thin section analysis (Figs. 17 and 18).

The **Coralgal microfacies** clearly reflects the immediate neighbourhood of corals and coralline algae to the sample localities. Compared with the bottom facies it corresponds with coral reefs, coral carpet, and sand with coral patches. Its main distributional area is therefore in shallow water. A further distinction between very shallow water and somewhat deeper water samples (e.g., B 56, B 59, B 60, B 61) could be possible in differentiating between scleractinians and octocorallians. The amount of the latter seems to be considerably higher in the samples from deeper water.

The **Heterostegina microfacies** is restricted to relatively deep water (below 45 m) and is similar in composition to the Coralgan facies. The high percentage of *Heterostegina*, however, is diagnostic and reflects the availability of hard substrates, the main microhabitat of this large hyaline foraminifer. An increase in abundance of *Heterostegina* with depth was also reported from the Gulf of Aqaba (HOTTINGER, 1977; REISS & HOTTINGER, 1984).

Foraminiferan sand facies

sample	aggli. f.	mil. f.	hyal. f.	spong.	corals	bryo	mol	worm	crust	ostr	echi	vert	red	green	plant	pellets	comp	crypto	ooid	non-ca	unident	matrix
A20	7.01	4.27	20.27	0.00	0.76	0.00	21.34	0.00	0.76	0.00	0.31	0.31	0.00	0.15	0.00	1.98	0.91	0.00	13.87	27.29	0.76	
A21	5.24	9.52	5.24	0.00	2.76	0.00	8.83	0.00	0.83	0.14	0.15	0.00	0.00	0.00	0.00	6.48	3.59	0.00	12.28	36.62	2.76	
A22	1.59	2.71	23.13	0.00	1.43	0.00	11.16	0.00	1.12	0.00	0.96	0.00	0.16	0.00	0.00	0.64	0.48	0.00	26.79	27.59	2.23	
A23	3.60	8.07	5.33	0.00	0.29	0.00	8.79	0.29	0.58	0.00	0.43	0.00	0.00	0.00	0.00	5.47	5.62	0.14	25.79	34.01	1.59	
B6	7.21	10.97	13.42	0.00	2.60	0.14	6.49	0.00	0.58	0.14	0.87	0.00	1.15	0.00	0.00	8.66	2.17	1.30	4.33	39.25	0.72	
B9	1.52	5.94	1.01	0.00	0.51	0.00	1.90	0.13	0.00	0.13	0.38	0.00	1.14	0.00	0.00	0.25	15.17	0.00	1.77	65.87	4.05	
B18	3.10	6.51	2.61	0.00	15.80	0.00	12.38	0.33	0.33	0.16	1.14	0.00	4.23	0.16	0.00	12.21	3.26	0.00	2.12	35.34	0.33	
B42	7.17	4.88	10.21	0.00	1.52	0.31	14.02	0.31	0.31	0.61	1.22	0.00	0.46	0.00	0.00	1.52	6.25	2.29	2.44	42.38	2.89	
B48	8.77	4.87	7.95	0.16	1.95	0.00	17.37	0.49	0.16	0.00	0.81	0.00	1.30	0.16	0.00	0.16	9.90	2.92	4.22	3.90	33.28	0.00
C4	9.43	5.39	4.34	0.15	0.00	17.22	0.30	0.90	0.30	0.00	0.15	0.00	0.00	0.00	0.00	0.15	9.58	1.05	0.45	3.59	42.51	4.34
C6	0.00	10.27	1.04	0.15	5.80	0.00	4.61	0.30	0.45	0.15	0.15	0.00	2.83	0.15	0.00	0.15	7.74	11.01	2.08	21.43	30.95	0.74
C7	0.00	4.77	1.06	0.00	1.72	0.13	2.65	0.80	0.13	0.00	0.00	0.00	1.06	0.00	0.00	0.00	3.32	2.25	0.13	21.09	56.90	3.98
C12	0.53	14.70	1.71	0.00	9.58	0.13	5.12	1.44	0.26	0.66	0.00	0.79	0.00	0.00	0.00	12.20	8.79	0.00	2.49	41.08	0.26	
C20	0.72	17.49	2.46	0.00	2.89	0.00	6.21	0.29	0.15	0.00	0.00	0.29	0.00	0.00	0.00	14.45	2.46	0.00	3.18	48.27	1.01	
C23	0.79	16.25	0.92	0.13	0.79	0.00	12.45	0.52	0.00	0.00	0.65	0.00	0.26	0.00	0.92	0.00	10.09	4.19	0.00	0.79	49.28	1.96
C26	3.72	7.97	6.11	0.00	3.19	0.00	9.43	0.00	0.13	0.00	1.19	0.00	1.06	0.00	0.00	0.27	15.14	5.05	1.19	15.94	29.35	0.27
<i>n=16</i>																						
mean	3.775	8.411	6.676	0.037	3.234	0.044	9.998	0.325	0.418	0.128	0.651	0.029	1.05	0.039	0.058	0.156	7.773	4.451	0.671	10.113	40.123	1.743
st. dev.	3.271	4.485	6.891	0.066	4.11	0.089	5.577	0.375	0.343	0.163	0.502	0.084	1.158	0.069	0.23	0.376	4.635	4.013	1.148	9.40	10.765	1.476
min	0.00	2.71	0.92	0.00	0.15	0.00	1.90	0.00	0.00	0.00	0.00	0.00	0.00	0.00	0.00	0.25	0.48	0.00	0.79	27.29	0.00	
max	9.43	17.49	23.13	0.16	15.80	0.31	21.34	1.44	1.12	0.61	1.65	0.31	4.23	0.16	0.92	1.52	15.14	15.17	4.22	26.79	65.87	4.34

Coralgal mud facies

sample	aggli. f.	mil. f.	hyal. f.	spong.	corals	bryo	mol	worm	crust	ostr	echi	vert	red	green	plant	pellets	comp	crypto	ooid	non-ca	unident	matrix
A29	0.66	1.18	3.55	0.00	16.43	0.13	6.05	1.58	0.00	0.79	0.00	4.47	0.00	0.00	0.00	4.21	1.58	0.00	1.46	42.18	15.77	
B7	0.61	6.59	8.28	0.00	7.36	0.00	8.74	0.46	0.15	0.61	0.00	7.68	0.31	0.00	0.00	4.14	0.31	0.00	0.00	52.45	1.84	
B8	0.69	5.65	3.31	0.00	8.40	0.00	16.80	1.24	0.00	0.41	0.96	0.00	5.79	0.14	0.00	0.55	3.72	7.30	0.00	2.07	39.39	3.58
B13	0.41	1.10	1.78	0.27	20.27	0.00	6.71	0.00	0.00	0.14	0.27	0.00	3.15	0.00	0.00	1.64	10.14	0.82	0.00	0.14	21.78	31.37
B24	0.50	3.66	4.33	0.00	10.48	0.17	9.15	1.83	0.33	0.00	0.83	0.00	4.33	0.00	0.00	7.15	3.16	0.00	0.00	48.92	5.76	
B30	1.43	0.02	6.29	0.14	16.45	0.14	11.02	1.29	0.43	0.01	0.00	7.15	0.43	0.00	0.29	5.01	3.00	0.00	0.71	38.77	4.15	
C14	1.20	1.33	2.80	0.00	17.71	0.00	6.39	1.33	0.53	0.13	0.00	5.86	0.00	0.00	0.13	5.33	3.20	0.00	0.67	50.60	2.80	
<i>n=7</i>																						
mean	0.786	3.073	4.334	0.059	13.871	0.063	9.266	1.104	0.206	0.637	0.00	5.49	0.126	0.00	0.373	5.671	2.767	0.00	0.721	42.013	9.324	
st. dev.	0.38	2.274	2.234	0.107	5.045	0.079	3.77	0.644	0.224	0.186	0.374	0.00	1.615	0.178	0.00	0.594	2.273	2.316	0.00	0.79	10.466	10.791
min	0.41	1.10	1.78	0.00	7.36	0.00	6.05	0.00	0.00	0.00	0.00	0.00	3.15	0.00	0.00	3.72	0.31	0.00	0.00	21.78	1.84	
max	1.43	6.59	8.28	0.27	20.27	0.17	16.80	1.83	0.53	0.46	0.01	0.00	7.68	0.43	0.00	1.64	10.14	7.30	0.00	2.07	52.45	31.37

Table 4 (continued): Frequency (%) of sediment constituents and some statistical parameters of microfacies.

Due to these requirements, the occurrence of this facies is restricted to the bottom facies classified as Rock bottom and Sand with macrooids respectively. The relatively deep occurrence of this facies is also documented in the relatively high amount of alcyonarian spicules.

The **Scaphopod microfacies** is related to the *Heterostegina* microfacies, genetically as well as from their location. The primary reason for their differentiation may be the amount of finer sediment, the higher percentage of which produces a softer substrate providing a favourable habitat for scaphopods and a lower offer of hard substrate for *Heterostegina*. The reason for the higher amount of fine grained sediment is the position west of the submarine ridge separating the bay from the open sea. This position is somewhat deeper than the ridge producing a current shade which causes the deposition of fine grained material out of the suspension.

Compound grain and cryptocrystalline grain microfacies are interpreted as being genetically very similar, although, their visual appearance can differ widely (Pl. 11, Figs. 1, 2). There is, nevertheless, a continuous transition between compound grains and cryptocrystalline particles on the one hand and single superficially micritized grains and cryptocrystalline grains on the other. Although the degree of micritization is studied only in a semiquantitative way, a strong coincidence in the distributional pattern with compound grains (of grapestone type) and cryptocrystalline grains respectively is obvious. The best correspondence exists between the degree of micritization and the distribution of samples of compound grain and cryptocrystalline grain microfacies. The compound and cryptocrystalline particles as well as strong micritization are most abundant in shallow water which occurs predominantly in the "North area" and around the Tubya islands. This facies is consequently strongly restricted to very shallow water of the above mentioned areas. The degree of compound grain formation as well as the degree of micritization is a reflection of micritic cement precipitation, which thus only occurs in very shallow water. The weak degree of micritization in samples from the southern basin of the "East area" clearly points to different origin of the compound and cryptocrystalline grains of this area (see below). As mentioned above (chap. 5.5.), the **Soritid–compound grain microfacies** is a transition between the compound grain and soritid microfacies. Its location also favours this interpretation. Genetically it is an area of compound grain facies with a stock of seagrass. The latter, as a preferred substrate for some soritids, is responsible for the higher abundance of these large porcellaneous foraminifers.

The **Peloolitic molluscan microfacies** is one of the most interesting and problematic facies in the study area. The samples are located in the "East area" in water depth

>40 m. In addition to the four samples of this microfacies, two samples (B 42, B 48) show some similarities with respect to pellets and ooids and also come from the same area. Besides molluscs, compound grains are relatively important. These compound grains are not of the grapestone type and represent, at least partly, lithoclasts. Another feature, typical for these and most other samples of the basins of the "East area" are blackened particles (Fig. 19). This means that particles (e.g., ooids, compound grains) have a black or very dark cortex. This cortex usually has a transitional inner margin grading into the "unaltered" particle what is similar to micritic envelopes. The micritic envelopes present in shallow water samples of the bay (see above), however, never show this black color. Another characteristic feature of ooids and compound grains as well as of pellets are irregular surfaces. Taking all these characters into account for the interpretation of the depositional environment of this microfacies leads to following conclusion:

Multilamellar ooids, one of the diagnostic characters of the microfacies, are typically not produced in water depths > 40 m under quiet water conditions.

Blackened particles occur, except those under discussion, in the study area in several localities. Most of these are in a transitional position where pronounced topographic relief occurs (Fig. 19): at the base of coral covered pinnacles (e.g., B 45) and along the western margin of the basin of the "West" (e.g., B 15). They can, additionally, be abundant in the muddy sands of the axial part of the "Southwest channel". Most of the blackened particles show an irregular surface pointing to mechanical and/or biological abrasion. The blackening together with abrasion may therefore be a sign of reworking and no or reduced sedimentation. These particles may represent reworked limestone (partly oolitic) fragments or grains which are exposed on the sediment surface for a prolonged period.

The samples of this microfacies are therefore thought to represent relict sediments probably generated in very shallow water – as documented by the occurrence of ooids and cryptocrystalline grains – during a sea level lowstand. This interpretation is also supported by the results of quartz grain surface investigations (PILLER & MANSOUR, 1994).

Compared with bottom facies the samples of this microfacies belong to the sand and sand with seagrass respectively (B 49).

The **Soritid microfacies** covers a relatively large area (Fig. 17). Compared with the distribution of bottom facies, it corresponds well with the occurrence of seagrass and sand with seagrass (Fig. 18). The preferred microhabitat of the soritids are seagrass leaves. Although seagrass is not well preserved in recent sediment and has no fossilization potential, the original stock of seagrass is also detectable in fossil sediments by the frequent abundance of these epiphytic foraminifers.

Operculina facies

sample	aggl. f.	mil. f.	hyal. f.	spong.	corals	bryozo.	mol.	worm	crust	str.	echi	vert	red	green	plant	pellets	comp	crypto	oid	non-ca	unident	matrix
A14	2.20	6.75	27.47	0.00	0.00	16.48	0.00	0.79	0.00	0.63	0.00	0.16	0.00	0.00	0.00	0.79	2.98	0.00	8.63	30.61	2.51	
A26	0.60	1.94	10.01	0.00	1.05	0.00	16.44	0.00	0.60	0.00	1.05	0.00	0.00	0.00	0.00	0.15	2.39	0.00	11.06	50.22	4.48	
B20	1.91	2.05	8.19	0.00	1.09	0.00	11.87	0.55	0.00	2.05	0.00	0.68	0.00	0.00	0.14	1.50	4.50	0.00	2.73	55.25	7.51	
B32	5.53	1.80	10.68	0.00	0.26	0.00	9.14	0.39	0.13	0.00	0.39	0.00	0.13	0.00	0.77	4.89	1.67	0.00	0.77	54.18	9.27	
B33	1.33	0.80	14.53	0.00	0.00	3.47	0.13	0.13	0.00	0.40	0.00	0.40	0.00	0.00	1.20	8.93	2.80	0.00	0.53	62.53	2.80	
B34	2.25	3.38	33.49	0.00	0.48	0.00	5.31	0.48	0.16	0.00	0.48	0.00	0.00	0.00	0.16	7.73	0.97	0.00	0.81	38.00	6.28	
B35	0.13	2.92	17.84	0.13	0.41	0.00	17.84	0.00	0.27	0.27	0.81	0.00	0.27	0.00	0.00	0.41	2.16	2.70	0.00	1.08	39.39	13.51
B36	1.48	4.72	16.44	0.00	1.48	0.27	11.86	0.13	0.00	1.35	0.00	0.54	0.00	0.00	0.13	1.75	2.69	0.00	1.21	46.36	9.44	
B37	1.93	6.35	17.38	0.00	0.97	0.00	12.83	0.41	0.00	0.14	0.69	0.00	0.55	0.00	0.00	0.14	3.72	1.65	0.14	3.86	43.86	5.38
B38	2.07	4.79	16.97	0.00	1.94	0.00	11.92	0.13	0.78	0.00	0.13	0.00	0.00	0.00	0.13	0.39	4.53	0.00	17.62	28.37	10.10	
B52	1.33	3.20	18.40	0.13	4.40	0.00	12.93	0.53	0.40	0.13	0.40	0.00	0.40	0.00	0.00	0.27	3.87	2.27	0.00	0.67	44.93	5.73
B53	1.44	2.23	19.76	0.00	0.52	0.00	6.15	0.13	0.00	0.13	0.65	0.00	0.39	0.00	0.00	0.26	1.44	1.44	0.00	1.83	56.15	7.46
B54	1.82	3.76	7.52	0.00	0.13	0.00	11.28	0.00	0.26	0.13	0.26	0.00	0.00	0.00	0.17	4.41	3.37	0.52	1.56	57.72	6.10	
B69	3.35	3.17	7.57	0.00	0.18	0.00	16.55	0.00	0.35	0.53	0.59	0.00	0.18	0.00	0.00	0.06	2.29	0.00	7.22	55.28	0.70	
C2	2.22	7.53	17.73	0.00	0.00	3.55	0.00	0.15	0.15	0.29	0.00	0.00	0.44	0.00	0.59	1.77	1.03	0.00	0.00	52.14	12.41	
C3	2.63	4.71	10.94	0.14	0.00	0.00	4.02	0.14	0.00	0.14	0.00	0.00	0.39	0.00	0.41	2.49	2.49	0.00	0.14	56.37	13.44	
n=16																						
mean	2.014	3.756	15.993	0.025	0.807	0.017	10.728	0.189	0.286	0.101	0.707	0.00	0.223	0.123	0.008	0.361	2.941	2.486	0.041	3.733	48.21	7.32
st. dev.	1.206	1.922	7.13	0.054	1.123	0.068	4.938	0.208	0.27	0.142	0.548	0.00	0.24	0.356	0.033	0.386	2.538	1.046	0.132	4.962	9.994	3.848
min	0.13	0.80	7.52	0.00	0.00	3.47	0.00	0.00	0.13	0.00	0.00	0.00	0.00	0.00	0.15	0.97	0.00	0.00	0.00	28.37	0.70	
max	5.53	7.53	33.49	0.14	4.40	0.27	17.84	0.55	0.79	0.53	2.05	0.00	0.68	1.39	0.13	1.20	8.93	4.53	0.52	17.62	62.53	13.51

Mud facies

sample	aggl. f.	mil. f.	hyal. f.	spong.	corals	bryozo.	mol.	worm	crust	str.	echi	vert	red	green	plant	pellets	comp	crypto	oid	non-ca	unident	matrix
A18	0.75	2.74	2.49	0.00	0.00	2.37	0.00	0.00	0.25	0.00	0.00	0.00	0.00	0.00	0.37	0.50	0.50	0.00	4.61	74.69	10.72	
B14	0.37	0.87	0.87	0.00	0.00	0.25	0.00	0.00	0.13	0.00	0.00	0.50	0.00	0.13	0.00	2.00	61.75	33.13				
B16	0.17	1.70	1.19	0.00	0.17	0.00	1.53	0.00	0.17	0.68	0.00	0.00	0.51	0.00	0.00	0.17	2.04	57.89	33.79			
B21	0.28	2.27	1.42	0.00	0.57	0.00	1.71	0.00	0.71	1.85	0.00	0.43	0.00	0.00	0.99	1.42	0.00	7.24	76.42	4.69		
B22	0.13	0.25	0.75	0.00	0.00	0.37	0.00	0.00	0.13	0.25	0.00	0.00	0.00	0.00	1.12	0.13	0.37	0.00	0.50	73.07	22.94	
B43	0.00	0.25	2.41	0.00	0.00	0.51	0.00	0.00	0.25	0.89	0.00	0.00	0.00	0.00	0.76	0.13	0.00	0.00	3.05	57.11	43.01	
B44	0.13	0.38	0.89	0.00	0.00	0.89	0.00	0.00	0.13	0.64	0.00	0.00	0.00	0.00	0.89	0.00	1.02	0.00	2.67	56.69	35.67	
B46	0.12	0.00	0.36	0.00	0.00	0.48	0.00	0.00	0.12	0.36	0.00	0.00	0.00	0.00	0.00	0.00	0.00	0.00	2.65	38.72	57.18	
B70	0.14	0.86	2.43	0.00	0.00	0.71	0.00	0.00	0.71	0.00	0.00	0.00	0.00	0.00	0.14	0.00	0.00	0.00	2.15	61.23	31.62	
D6	0.00	1.37	1.12	0.00	0.00	1.87	0.00	0.00	0.13	0.25	0.00	0.00	0.00	0.00	1.00	0.37	2.24	0.00	1.00	67.62	23.04	
n=10																						
mean	0.209	1.069	1.393	0.00	0.074	0.00	1.069	0.063	0.00	0.164	0.601	0.00	0.043	0.00	0.00	0.515	0.226	0.568	0.017	2.791	62.519	29.579
st. dev.	0.221	0.929	0.777	0.00	0.182	0.00	0.741	0.199	0.00	0.209	0.507	0.00	0.136	0.00	0.00	0.424	0.318	0.764	0.054	1.922	11.215	15.187
min	0.00	0.00	0.36	0.00	0.00	0.25	0.00	0.00	0.00	0.13	0.00	0.00	0.00	0.00	0.00	0.00	0.00	0.00	0.50	38.72	4.69	
max	0.75	2.74	2.49	0.00	0.57	0.00	2.37	0.63	0.00	0.71	1.85	0.00	0.43	0.00	0.00	1.12	0.99	2.24	0.17	7.24	76.42	57.18

Table 4 (continued): Frequency (%) of sediment constituents and some statistical parameters of microfacies.

Foraminiferan sand microfacies is heterogenous compared with bottom facies: Of the 16 samples 7 were classified with muddy sand, 5 with seagrass, 3 with sand with seagrass, and 1 with sand. Comparing the spatial distribution, however, the area of foraminiferan sand is mainly located in muddy sand area. This sediment represents “normal” sedimentary and ecologic conditions ranging between areas with mass occurrences of *Operculina* (represented in *Operculina* facies) and soritids (Soritid facies).

***Operculina* microfacies** represents a soft bottom muddy sand substrate with a high standing crop of *Operculina* settling on the sediment surface. Compared with bottom facies, the samples represent part of the muddy sand area. Only one sample was classified with mud bottom (B 20: at the western margin of the basin of the “West area”) and one with sand with seagrass (C 3) due to a sparse seagrass stock.

***Halimeda* microfacies** is represented only by one sample which originates from a dense *Halimeda* meadow. This dense *Halimeda* stock grows in a depression inside a large coral carpet area on muddy substrate. It was the only dense *Halimeda* stock observed in the entire bay. Due to its restricted distribution, it was not documented separately on the bottom facies map (PILLER & PERVESLER, 1989, enclosure 1).

Coralgal – molluscan and **Coralgal mud microfacies** are both transitional facies differing basically in their amount of fine sediment. All samples of these two facies come from marginal positions either from the margins between coral covered areas and muddy basin bottoms or from sediment filled small depressions within hard bottoms (coral carpet or coral covered rock bottom). The samples of Coralgal – molluscan facies come generally from locations where the boundary between hard and soft substrate is less sharp due to a more gentle relief (e.g., west margin of the basin of the “West”: B 15; coral patches in seagrass: B 12). Samples of Coralgal mud facies typically originate from sharp boundaries due to a very pronounced relief (e.g., east and north margin of the basin of the “West area”: B 13; small depressions in coral carpet: B 7, B 30). In spite of this transitional character, such samples are easy to classify due to a pronounced bimodal grain size distribution: fine grained matrix and sand to gravel sized coralgal particles. The origin of these microfacies can easily be explained by broken coralgal fragments fallen down into neighboured fine grained sediment. Of subordinate importance may also be an additional transport of molluscs. However, the later seem to originate from mainly primary inhabitants of the fine grained sediment. The transitional character and the marginal position of the samples is also documented in comparison with bottom facies: 4 samples of Coralgal mud facies are grouped with coral carpet, 3 with muddy sand; 3 samples of Coralgal – molluscan facies are classed with coral carpet, 3 with muddy sand, one with sand, and one with seagrass.

Mud microfacies corresponds with the distribution of mud bottom facies and is restricted to the basin of the “West area”. As pointed out by PILLER & PERVESLER (1989, p. 123), the mud is deposited in this depression due to the general current regime and the steep bordering flanks framing the basin. The latter produces a current gradient resulting in sedimentation of the suspended material. **Mixed mud microfacies** comprises mud samples with a higher content of one or two components which may represent autochthonous as well as allochthonous elements. These samples are located in marginal positions (north and east margin of the basin of the “West” and at the western margin of the central axis of the northern “Southwest channel”).

The **Terrigenous microfacies** is produced by transport of mainly non-carbonate material from the hinterland either by fluvial or aeolian transport mechanisms or by reworking of underlying rocks. This origin is clearly reflected by the coastal distribution of this facies (compare also PILLER & MANSOUR, 1994). Most of these samples were classified as pure sands in bottom facies, one was classified with seagrass, one with sand with seagrass, and two samples come from the mangrove.

7. Microfacies versus sedimentary facies

The grain size, coarse component and mineral analyses of PILLER & MANSOUR (1990) led to a classification of the samples in 8 “sedimentary facies”. As the 120 thin sections studied in this microfacies investigation originate from the same samples as the material studied by PILLER & MANSOUR (1990) a direct comparison is of particular interest.

Comparing the general pattern of the facies distributions of both studies (Fig. 17 herein and Fig. 53 of PILLER & MANSOUR, 1990) reveals a relatively good coincidence. Some differences occur, however, in several respects: The coralgal sedimentary facies can be subdivided by the data of the microfacies study into Coralgal, *Heterostegina*, and – partly – Coralgal-molluscan microfacies. Most samples of the compound grain microfacies and that of cryptocrystalline grain microfacies were also grouped within coralgal sedimentary facies. Only two samples were classified with compound grain sedimentary facies. The reason for this more detailed classification is mainly founded in the restricted grain size fractions studied in coarse grain analyses ($>250 \mu\text{m}$) and by the fact that compound grains may easier be detected in thin section. The distribution of compound grains in grain size fractions (Fig. 28 in PILLER & MANSOUR, 1990), already, pointed to their underestimation by coarse grain analysis due to pronounced increase in frequency with decreasing grain size. Completely undetected by the coarse grain

Mixed mud facies

sample	aggl. f.	mil. f.	hyal. f.	spong.	corals	bryo	mol	worm	crust	ostr	echi	vert	red	green	plant	pellets	comp	crypto	ooid	non-ca	unident	matrix
A22	0.49	10.59	2.74	0.00	0.49	0.00	21.05	0.00	0.62	0.00	0.13	0.00	0.00	0.00	0.13	0.25	3.61	0.00	0.49	36.74	22.66	
B23	0.00	1.47	4.11	0.00	8.07	0.44	4.84	0.73	0.00	0.73	0.00	1.76	0.00	1.17	0.73	1.17	0.00	0.15	29.47	45.16		
D5	0.25	1.24	1.24	0.25	3.85	0.25	14.41	0.37	0.00	0.12	0.75	0.00	2.48	0.00	1.24	1.37	0.25	0.00	0.00	59.01	12.92	
D9	0.57	1.92	0.79	0.00	0.00	0.11	6.78	0.00	0.11	0.11	0.23	0.00	0.00	0.00	0.00	1.13	0.00	0.00	1.13	36.73	50.39	
n=4																						
mean	0.328	3.805	2.22	0.063	3.103	0.20	11.77	0.275	0.183	0.058	0.46	0.00	1.06	0.00	0.635	0.87	1.258	0.00	0.443	40.488	32.783	
st. dev.	0.257	4.532	15.11	0.125	3.728	0.19	7.439	0.35	0.296	0.067	0.326	0.00	1.259	0.00	0.661	0.49	1.647	0.00	0.502	12.814	17.891	
min	0.00	1.24	0.79	0.00	0.00	0.00	4.84	0.00	0.00	0.00	0.13	0.00	0.00	0.00	0.00	0.25	0.00	0.00	0.00	29.47	12.92	
max	0.57	10.59	4.11	0.25	8.07	0.44	21.05	0.73	0.62	0.12	0.75	0.00	2.48	0.00	0.00	1.24	1.37	3.61	0.00	1.13	59.01	50.39

Terrigenous facies

sample	aggl. f.	mil. f.	hyal. f.	spong.	corals	bryo	mol	worm	crust	ostr	echi	vert	red	green	plant	pellets	comp	crypto	ooid	non-ca	unident	matrix
A6	0.00	1.13	0.28	0.00	0.99	0.00	8.09	0.00	0.00	0.28	0.00	1.13	0.00	0.00	0.14	0.99	0.28	0.71	82.98	2.98	0.00	
A7	0.00	0.17	0.17	0.00	3.51	0.00	1.51	0.00	0.00	0.17	0.00	0.00	0.00	0.00	0.00	4.51	4.01	0.00	85.95	0.00	0.00	
A9	0.00	16.59	0.32	0.00	0.48	0.00	1.91	0.00	0.00	0.00	0.00	1.12	0.00	0.00	0.16	0.00	3.19	7.65	0.00	65.87	2.71	0.00
A10	0.00	4.97	0.28	0.00	5.26	0.00	3.13	0.00	0.00	0.00	0.00	2.70	0.00	0.00	0.00	0.00	3.55	7.67	0.00	71.31	1.14	0.00
A15	1.12	6.98	1.26	0.00	0.00	0.00	1.68	0.56	0.28	0.00	0.00	0.28	0.00	0.00	0.00	0.00	2.23	0.42	0.00	71.79	13.41	0.00
A32	0.14	3.78	0.56	0.00	3.78	0.00	3.08	0.00	0.00	0.00	0.00	2.24	0.00	0.00	0.00	0.00	2.38	8.26	2.52	64.43	8.82	0.00
A33	0.00	0.00	0.00	0.00	0.00	0.00	1.09	0.00	0.00	0.00	0.00	0.00	0.00	0.00	0.54	0.00	1.77	0.00	0.00	95.24	1.36	0.00
C9	0.00	0.58	0.00	0.00	0.29	0.00	0.72	0.00	0.00	0.29	0.00	0.14	0.00	0.00	0.00	1.87	0.72	0.00	95.25	0.14	0.00	
C13	0.00	1.15	0.14	0.00	0.43	0.00	1.73	0.00	0.00	0.00	0.00	0.43	0.00	0.00	0.14	7.49	2.88	12.97	71.90	0.72	0.00	
C21	0.00	1.16	0.29	0.00	7.85	0.00	9.01	0.00	0.00	0.00	0.00	2.62	0.00	0.00	0.00	5.67	0.29	1.60	66.28	5.23	0.00	
D1	0.00	0.99	0.14	0.00	4.52	0.00	1.41	0.00	0.00	0.00	0.00	0.57	0.00	0.00	0.00	0.00	4.38	2.26	85.59	0.14	0.00	
n=11																						
mean	0.115	3.409	0.313	0.00	2.465	0.00	3.033	0.051	0.025	0.00	0.067	0.00	1.021	0.00	0.064	0.025	3.059	3.354	1.824	77.872	3.332	0.00
st. dev.	0.336	4.903	0.352	0.00	2.664	0.00	2.832	0.169	0.084	0.00	0.119	0.00	1.041	0.00	0.165	0.057	2.16	3.294	3.823	11.53	4.275	0.00
min	0.00	0.00	0.00	0.00	0.00	0.00	0.72	0.00	0.00	0.00	0.00	0.00	0.00	0.00	0.00	0.00	0.00	0.00	64.43	0.00	0.00	
max	1.12	16.59	1.26	0.00	7.85	0.00	9.01	0.56	0.28	0.00	0.29	0.00	2.70	0.00	0.54	0.14	7.49	8.26	12.97	95.25	13.41	0.00

Table 4 (continued): Frequency (%) of sediment constituents and some statistical parameters of microfacies.

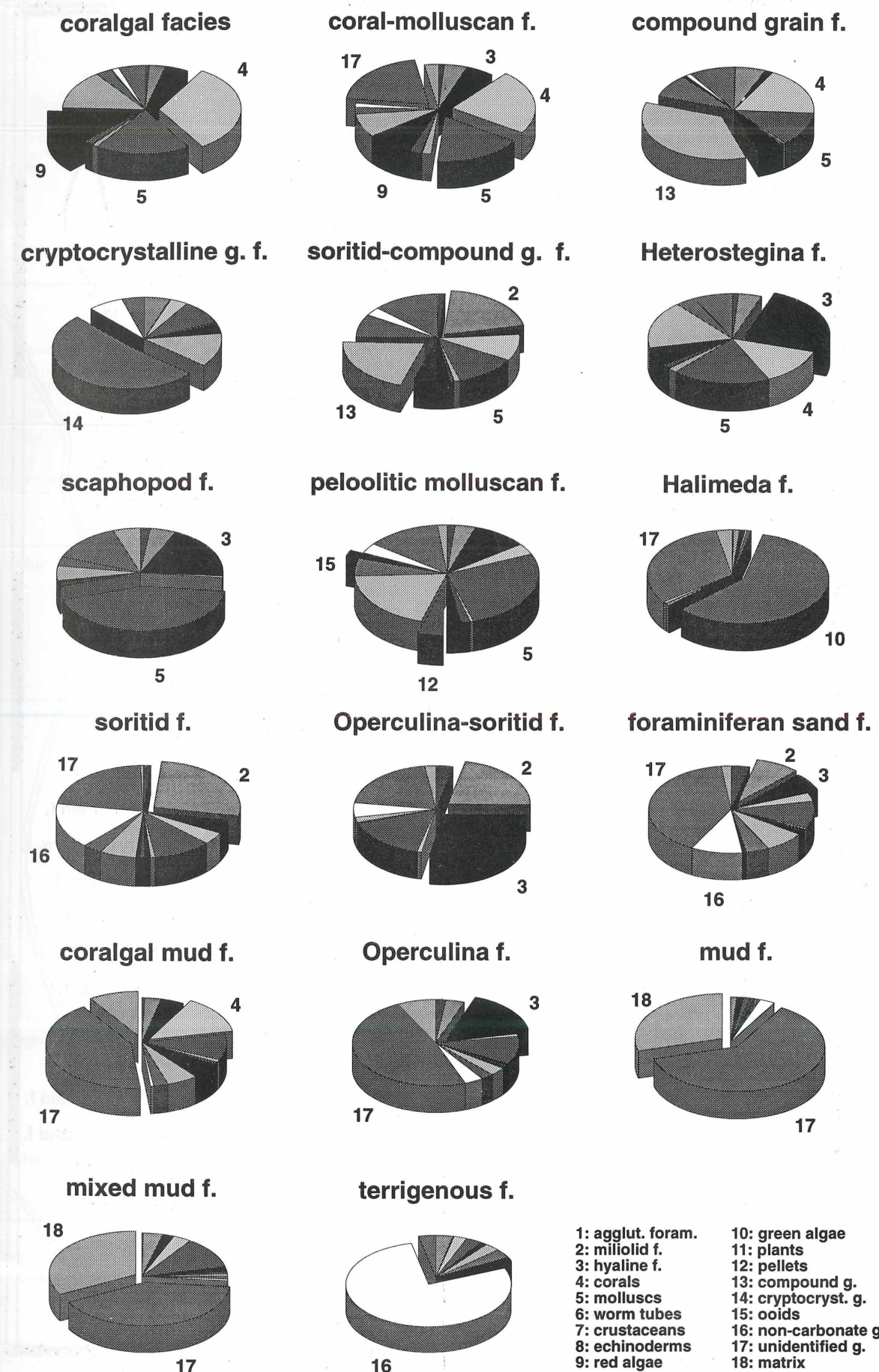


Figure 16: Diagrammatic representation of microfacies. The most important microfacial constituents are extracted. Numbers refer to constituents as listed in the legend.

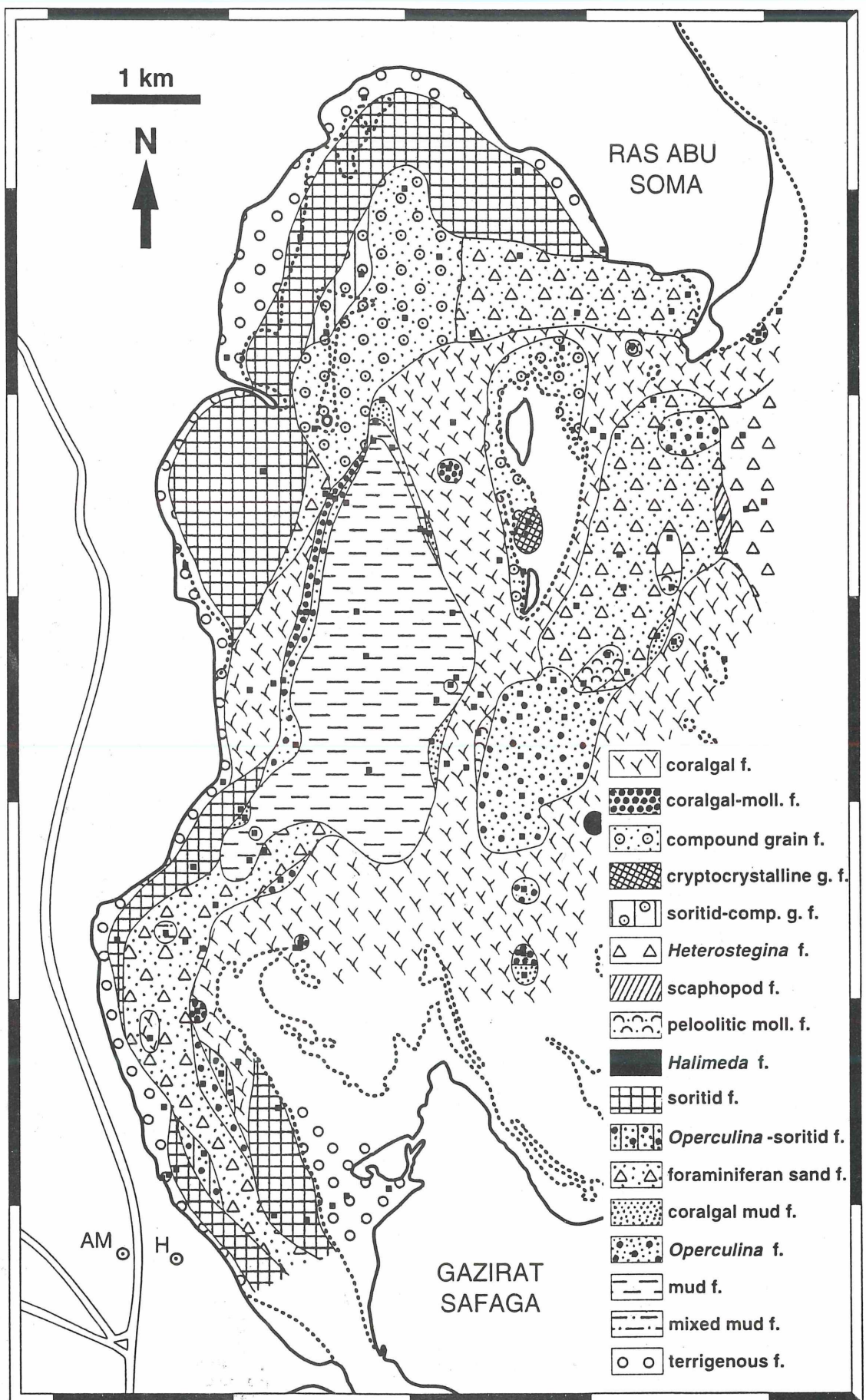


Figure 17: Distribution of microfacies.

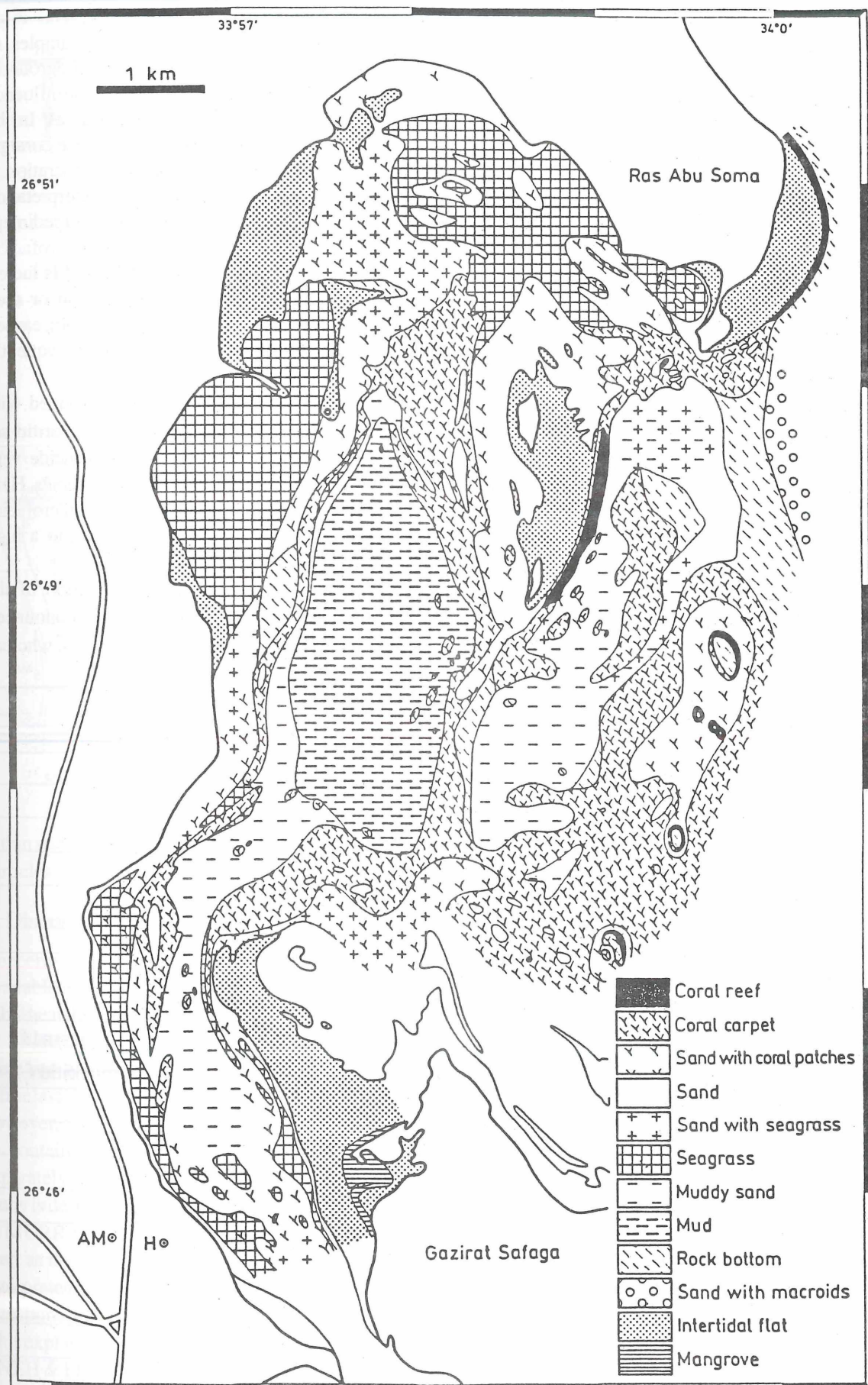


Figure 18: Distribution of bottom facies (according to PILLER & PERVESLER, 1989).

analysis was the peloolitic molluscan facies; 3 samples were grouped with coralgal sedimentary facies and one with molluscan sedimentary facies. The small size of pellets as well as ooids together with their relatively infrequent occurrence are also responsible for being missed. The greatest differences between both methods are recognized with foraminiferan sand facies and molluscan sedimentary facies respectively. Most samples now classified with foraminiferan sand microfacies were grouped within the molluscan facies (11 of 16). This is due to the coarse fraction analysis, because molluscs dominate in coarse fraction and decrease drastically with grain size (PILLER & MANSOUR, 1990, p. 35). Thin section analysis reveals that they are replaced by foraminifera in many samples. However, some of the samples of the soritid sedimentary facies are now also grouped with foraminiferan sand facies. This re-grouping results from the fact, that miliolids were more or less equated with soritids. In some of these samples, however, smaller miliolid foraminifers dominate. These samples cover a relatively large area in the "North area"

Concerning the mud dominated samples coincidence exists in the basin of the "West area". The loose sediment study incorporates the mud sedimentary facies in a broader

sense than is done in microfacies analysis. This is an important difference, because the transitional samples, as well as the samples from small depressions in hardgrounds, were grouped with mud without any hint as to the influence of the surrounding coralgal characterized areas. In the microfacies analysis, a clear separation of these coralgal influenced mud samples is possible. This separation is very important with respect to the geological interpretation of such samples. The samples of the *Operculina* sedimentary facies were also united in the *Operculina* microfacies, with the inclusion of much more samples in this facies, which formerly were found in the molluscan or mud sedimentary facies. This difference is, once more, caused in the small size of some *Operculina* which consequently are missing in coarse grain analysis.

Except the area in the "North", which is grouped with foraminiferan sand microfacies (see above), soritid sedimentary facies and soritid microfacies coincide very well. The same holds true for the terrigenous facies. Here only one sample is now grouped into the soritid microfacies due to a high content of soritids in addition to a high amount of non-carbonate grains.

The greatest difference in general composition of the sediments using these two methods is the pronounced dominance of molluscs in coarse grain analysis, whereas

Persian Gulf	Northern Bay of Safaga
Lamellibranch sand	Coralgal-molluscan facies (?)
Compound grain/lamellibranch sand	Compound grain facies
Large perforate-foraminiferal sand	<i>Heterostegina</i> facies
Coralgal/algal sand	Coralgal facies
	Cryptocrystalline grain facies
Imperforate foraminiferal/pelletoidal sand	p.p. Foraminiferan sand facies
Gastropod sand	Soritid facies (?)
Ooidal sand (oolite)	(p.p. Terrigenous facies)
Lamellibranch muddy sand	p.p. <i>Operculina</i> f., Coralgal mud f., Foraminiferan sand f.
Gastropod muddy sand	(p.p. Peloolitic mol. f., soritid f., <i>Operculina</i> -soritid f.)
	<i>Halimeda</i> facies
	Scaphopod facies
	<i>Operculina</i> -soritid facies
	Soritid-compound grain facies
Lamellibranch mud	Mud facies, Mixed mud facies
Argillaceous lamellibranch mud	(p.p. Peloolitic molluscan facies)
Imperforate foraminiferal/gastropod mud	p.p. Foraminiferan sand facies
Quartz sand and muddy quartz sand	Terrigenous facies
Sedimentary gypsum	

Table 5: Comparison between microfacies of the Southern Persian Gulf (according to WAGNER & VAN DER TOGT, 1973) and the Northern Bay of Safaga.



Figure 19: Distribution of blackened particles.

in thin section analysis foraminifera are the most abundant particles.

8. Discussion

Concerning other parts of the Red Sea, some data are available from an east-west transect from the Strait of Jubal near the southern end of the Gulf of Suez (ROBERTS & MURRAY, 1988). The main sediment constituents there are also foraminifera, followed by molluscs and intraclasts, a detailed microfacial differentiation is, however, not provided. The category "intraclasts" seems to contain a variety of particles, which were treated separately in this study (e.g., a pellet in the sense of this study is designated as intraclast in Fig. 24B in ROBERTS & MURRAY, 1988). Ooids are reported from shallow as well as deeper parts of the Strait of Jubal. The latter are interpreted as having formed in nearshore areas and being transported to the deeper areas by aeolian mechanisms. This explanation was adopted from SASS et al. (1972) and SNEH & FRIEDMAN (1984). The occurrence of deeper water ooids in the Northern Bay of Safaga, however, is explained as being relict (early Holocene to Pleistocene) – due to blackening and corrosion features of several

particles – probably reflecting a relative sea-level lowstand (see also below).

The greatest similarities in sediment composition can be detected with the Southern Persian Gulf from where WAGNER & VAN DER TOGT (1973) described 14 sediment types (Tab. 5). Their Coral/algal sand mainly corresponds with Coralgal facies in the Bay of Safaga, their Compound grain/lamellibranch sand with Compound grain facies. The Gulf's Imperforate foraminiferal/pelletoidal sand is extremely variable (WAGNER & VAN DER TOGT, 1973, p. 136) and has probably no direct expression in the Safaga Bay, especially as pelletoids are not as frequent as in this Persian Gulf sediment type. It may partly be comparable to the Foraminiferan sand facies. The Gastropod sand of the Gulf coincides partly with the Soritid facies, whereas no real Ooidal sand is developed in the Bay of Safaga. Some samples of the Terrigenous facies may come close to the Ooidal sand (e.g., C13). Their Large perforate-foraminiferal sand may be comparable to the *Heterostegina* facies, because not only larger hyaline foraminifera but also coralline algae are relatively abundant. The *Heterostegina* facies, however, occurs in slightly deeper water. The muddy sands of the Persian Gulf are subdivided into a Lamellibranch muddy sand and a Gastropod muddy sand, in the Bay of Safaga they would be represented in part by *Operculina* facies, Coralgal mud facies, and Foraminiferan sand facies, perhaps also in part by Peloolitic molluscan facies, Soritid facies, and *Operculina*-soritid facies. Also *Halimeda* facies would be classified with a muddy sand sediment type, however, there is no expression in the Persian Gulf due to the absence of *Halimeda* (HUGHES CLARKE & KEIJ, 1973; LEES, 1975). In general, for the sediments of the Safaga Bay the grain size differentiation between sand and muddy sand was not considered as being so important and more emphasis was placed on the particle composition. Also the usage of the grain size composition in the Persian Gulf was not consistently applied, as one example of the Argillaceous lamellibranch mud (Fig. 16) represents a muddy sand. This example corresponds with the sediments united in the Peloolitic molluscan facies in the Safaga Bay. The mud sediments were subdivided into Lamellibranch mud, Argillaceous lamellibranch mud and Imperforate foraminiferal/gastropod mud in the Southern Persian Gulf. Lamellibranch mud and Argillaceous lamellibranch mud are separated on the basis of insoluble residue (< or > 10 %). Such a distinction was not applied to the Safaga samples, however, all of the samples summarized in Mud and Mixed mud facies have non-carbonate contents $\geq 10\%$, and would therefore match the Argillaceous lamellibranch mud. The Imperforate foraminiferal/gastropod mud may in part be compared with the Foraminiferan sand facies (e.g., sample B9). The Terrigenous facies is equivalent to the Quartz sand, the

muddy quartz sand of the Persian Gulf has no expression in the Bay of Safaga as well as Sedimentary gypsum. These sediment types change not only on a large scale along the gentle slope of the ramp away from the Arabian coastline ("Arabian homoclinal"), but also on a small scale due to irregular bottom topography as documented by PURSER (1973). As in the Northern Bay of Safaga, this irregular bottom topography is primarily mainly caused structurally, with different subsequent modifications (KASSLER, 1973; PURSER, 1973, p.159).

Besides these general similarities between sediment types of the Persian Gulf and microfacies of the Bay of Safaga, blackened particles (WAGNER & VAN DER TOGT, 1973) and blackened ooids in particular are also abundant in the Persian Gulf (LOREAU & PURSER, 1973). These blackened particles are C^{14} -dated and show – at least for the ooids – that they are relict. This absolute dating supports the relict-interpretation of the blackened particles in the Bay of Safaga.

Compared to other tropical carbonate sedimentation areas, the carbonate sediments of the Northern Bay of Safaga are distinguished by a distinct dominance of skeletal components, whereas non-skeletal particles are of subordinate importance. The latter are dominated by compound and cryptocrystalline grains, with pellets and ooids occurring rarely. This clearly separates the Northern Bay of Safaga from the "classical" shallow water carbonates of the Bahama Banks, for example, although the general parameters would be appropriate also in the Red Sea (LEES, 1975, Fig. 8). The reasons for these differences could be caused by the different bottom morphology: large, extremely shallow water areas with monotonous topography on the one hand (e.g., Bahama Banks: PURDY, 1963a, b; Belize: PUSEY, 1975) and small scaled, ragged morphology with greater depth variations on the other. This prevents formation of non-skeletal carbonate particles on a larger scale.

Another obvious difference to well known carbonate production areas is the abundance of green algae. *Halimeda*, in particular, is one of the major carbonate sediment producers (e.g., Great Barrier Reef Province: FLOOD & ORME, 1988; ORME & SALAMA, 1988), especially in the Caribbean realm (e.g., Belize: MACINTYRE et al., 1987; Jamaica: BOSS & LIDDELL, 1987). In the Bay of Safaga this alga can also be a dominating sediment constituent in isolated samples (B 51, which represents *Halimeda* facies), however, its spatial coverage remains low, compared to other areas, for example the Northern Belize Shelf (PUSEY, 1975). It occurs extremely patchy in only a few places and must generally be considered unimportant for carbonate production (compare also PILLER & MANSOUR, 1990).

9. Conclusion

Using complete bulk samples (without removing small grain sizes by sieving), the most abundant sediment constituents in thin section analysis of the samples of the Northern Bay of Safaga are unidentified particles. This somewhat unusual result pointing to methodological inconsistencies reflects, in fact, the amount of fine grained material together with the percentage of mud (fine sand to mud fraction). The use of unsieved loose sediment samples for producing artificial rocks, is, however, thought to be a more adequate method than coarse grain analysis for comparisons with results originating from thin section analyses of natural rocks.

Among identifiable sediment constituents foraminifera, molluscs and corals dominate the skeletal grains. Compound grains clearly prevail among non-skeletal carbonate grains and, in addition, non-carbonate particles reach more than 10 %, reflecting the character of this mixed carbonate/siliciclastic depositional environment. The non-carbonate content, however, is highly variable due to its prevailing occurrence along the main coast. Compared to the coarse grain analysis (PILLER & MANSOUR, 1990), molluscs are by far not so important as reflected by grain size fractions $>250 \mu\text{m}$. They are supplanted by foraminifera. Compound grains and pellets are much more abundant, with ooids as well as cryptocrystalline grains only being detected by thin section study. Ooids are, however, rare and, if at all, are recently produced only in very restricted, shallow water areas. At least some of the ooid occurrences, in particular in the basin of the "East area", seem to be relicts of ancient sea-level low stands.

Classification of the sediments in 17 microfacies is much more detailed than was possible by field observations (PILLER & PERVESLER, 1989) and coarse grain analysis respectively (PILLER & MANSOUR, 1990). Compared with coarse grain analysis, thin section analysis allows a more differentiated distinction concerning hard bottom sediments. In addition, in the marginal areas between hard grounds and muddy sediments, a differentiation of transitional facies was possible (or necessary). This documents that the close neighbourhood of highly different environments is well documented in the sediment, if the entire sediment is considered, and not only the coarse fractions.

Although non-skeletal carbonate grains were detected in higher quantities compared with coarse grain analysis they are rare compared with other tropical carbonate environments. The same holds true with green algae although they are of subordinate importance in thin section analysis.

The microfacies distribution shows a very similar general pattern to the distribution of bottom facies and sedimentary facies, being a reflection of sea bottom morphology which is highly influenced by tectonics. Due to this complex topography, the microfacies is highly variable laterally representing a different type of carbonate environment than represented by the large scaled shallow water platforms as for example the Bahama Banks. Great similarities exist between the microfacies of Safaga Bay and the sediment types of the Southern Persian Gulf (WAGNER & VAN DER TOGT, 1973).

10. Acknowledgements

This study was supported by projects P 5877 and P 7507-Geo of the Austrian "Fonds zur Förderung der wissenschaftlichen Forschung". The author is gratefully indebted to K. Kleemann, P. Pervesler, F.F. Steininger (all Inst. for Palaeontology, Univ. Vienna), A.M. Mansour (Dept. Geology, Univ. Assiut/Qena), C. Rupp (Geologische Bundesanstalt Vienna), J.H. Nebelsick (Inst. for Palaeontology, Univ. Tuebingen) for collaboration during field works. The kind help of the entire staff of the Austrian Cultural Institute of the Austrian Embassy in Cairo as well as of the Department of Geology of the University of Assiut/Qena made the organization of the field works possible. Thin sections were carefully prepared by F. Sattler, V. Perlinger and W. Simeth, photographs printed by R. Gold and some drawings supported by N. Frotzler (all Inst. for Palaeontology, Univ. Vienna). Special thanks are given to E. Flügel (Inst. for Palaeontology, Univ. Erlangen) and J.H. Nebelsick (Inst. for Palaeontology, Univ. Tuebingen) for critically reading the manuscript and improving the English.

11. References

BOSS, S.K. & LIDDELL, W.D., 1987. Patterns of sediment composition of Jamaican fringing reef facies. — *Sedimentology*, **34**:77–87, 6 Figs., Oxford.

BROMLEY, R.G., 1990. Trace fossils: biology and taphonomy. — XI+280 pp., London (Unwin Hyman).

FLOOD, P.G. & ORME, G.R., 1988. Mixed Siliciclastic/Carbonate Sediments of the Northern Great Barrier Reef Province, Australia. — [in:] DOYLE, L.J. & ROBERTS, H.H. (eds.) *Carbonate–Clastic Transitions. — Developments in Sedimentology*, **42**:175–205, 16 Fig., Amsterdam (Elsevier).

GINSBURG, R.N., 1956. Environmental relationships of grain size and constituent particles in some South Florida carbonate sediments. — *Amer. Assoc. Petroleum Geologists Bull.*, **40**:2384–2427, 10 Figs., Tulsa, Oklahoma.

HOTTINGER, L., 1977. Distribution of larger Peneroplidae, *Borelis* and Nummulitidae in the Gulf of Elat, Red Sea. — *Utrecht Micropaleontological Bulletins*, **15**:35–109, 36 Fig., Utrecht.

HUGHES CLARKE, M.W. & KEIJ, A.J., 1973. Organisms as Producers of Carbonate Sediment and Indicators of Environment in the Southern Persian Gulf. — [in:] PURSER, B.H. (ed.). *The Persian Gulf. Holocene Carbonate Sedimentation and Diagenesis in a Shallow Epicontinental Sea*. — 33–56, 6 Figs., 7 Pl., Berlin – Heidelberg – New York (Springer).

ILLING, L.V., 1954. Bahamian calcareous sands. — *Amer. Assoc. Petroleum Geologists Bull.*, **38**:1–95, 13 Figs., 9 Pl., Tulsa, Oklahoma.

KASSLER, P., 1973. The Structural and Geomorphologic Evolution of the Persian Gulf. — [in:] PURSER, B.H. (ed.). *The Persian Gulf. Holocene Carbonate Sedimentation and Diagenesis in a Shallow Epicontinental Sea*. — 11–32, 10 Fig., Berlin – Heidelberg – New York (Springer).

KLEEMANN, K., 1992. Coral Communities and Coral-Bivalve Associations in the Northern Red Sea at Safaga, Egypt. — *Facies*, **26**:125–134, 3 Pl., 1 Fig., Erlangen.

LEES, A., 1975. Possible influence of salinity and temperature on modern shelf carbonate sedimentation. — *Marine Geology*, **19**:159–198, 12 Fig., Amsterdam.

LOEBLICH, A.R. Jr. & TAPPAN, H., 1988. Foraminiferal genera and their classification. — vol. 1: XII + 970 pp.; vol 2: X + 212 pp., 847 pl., New York (Van Nostrand Reinhold Comp. Inc.).

LOREAU, J.-P. & PURSER, B.H., 1973. Distribution and Ultrastructure of Holocene Ooids in the Persian Gulf. — [in:] PURSER, B.H. (ed.). *The Persian Gulf. Holocene Carbonate Sedimentation and Diagenesis in a Shallow Epicontinental Sea*. — 279–328, 20 Figs., Berlin – Heidelberg – New York (Springer).

MACINTYRE, I.G., GRAUS, R.R., REINTHAL, P.N., LITTLER, M.M. & LITTLER, D.S., 1987. The Barrier Reef sediment apron: Tobacco Reef, Belize. — *Coral Reefs*, **6**:1–12, 12 Figs., Berlin – Heidelberg.

NEBELSICK, J.H., 1992 a. Echinoid Distribution by Fragment Identification in the Northern Bay of Safaga, Red Sea, Egypt. — *Palaios*, **7**:316–328, 8 Figs., Tulsa, Oklahoma.

NEBELSICK, J.H., 1992 b. The Northern Bay of Safaga (Red Sea, Egypt): an actuopalaeontological approach. III. Distribution of echinoids. — *Beitr. Paläont. Österr.*, **17**:5–79, 37 Figs., 8 Taf., Wien.

ORME, G.R. & SALAMA, M.S., 1988. Form and seismic stratigraphy of *Halimeda* banks in part of the northern Great Barrier Reef Province. — *Coral Reefs*, **6**:131–137, 5 Figs., Berlin – Heidelberg.

PILLER, W.E. & MANSOUR, A., 1990. The Northern Bay of Safaga (Red Sea, Egypt): an actuopalaeontological approach. II. Sediment analyses and sedimentary facies. — *Beitr. Paläont. Österr.*, **16**:1–102, 55 Figs., Wien.

PILLER, W.E. & MANSOUR, A.M., 1994. Origin and transport mechanisms of non-carbonate sediments in

a carbonate dominated environment (Northern Safaga Bay, Red Sea, Egypt). — *Jb. Geol. Bundesanstalt*, **50**:385–395, 6 Text-Figs., 1 Pl., Wien.

PILLER, W.E. & PERVESLER, P., 1989. The Northern Bay of Safaga (Red Sea, Egypt): An Actuopalaeontological Approach. I. Topography and Bottom Facies. — *Beitr. Paläont. Österr.*, **15**:103–147, Wien.

PURDY, E.G., 1963a. Recent Calcium Carbonate Facies of the Great Bahama Bank. 1. Petrography and Reaction Groups. — *J. Geology*, **71**:334–355, Chicago.

PURDY, E.G., 1963b. Recent Calcium Carbonate Facies of the Great Bahama Bank. 2. Sedimentary Facies. — *J. Geology*, **71**:472–497, Chicago.

PURSER, B.H. (ed.), 1973. The Persian Gulf. Holocene Carbonate Sedimentation and Diagenesis in a Shallow Epicontinental Sea. — **VII** + 471 pp., Berlin–Heidelberg – New York (Springer).

PURSER, B.H., 1973. Sedimentation around Bathymetric Highs in the Southern Persian Gulf. — [in:] PURSER, B.H. (ed.). The Persian Gulf. Holocene Carbonate Sedimentation and Diagenesis in a Shallow Epicontinental Sea. — 157–177, 13 Figs., Berlin – Heidelberg – New York (Springer).

PUSEY, W.C. III, 1975. Holocene Carbonate Sedimentation on Northern Belize Shelf. — *Amer. Assoc. Petrol. Geol., Studies in Geology*, **2**:131–233, 34 Figs., Tulsa, Oklahoma.

REISS, Z. & HOTTINGER, L., 1984. The Gulf of Aqaba. Ecological Micropaleontology. — **VIII** + 354 pp., Berlin – Heidelberg (Springer).

ROBERTS, H.H. & MURRAY, S.P. 1988. Gulfs of the Northern Red Sea: Depositional Settings of Abrupt Siliciclastic-Carbonate Transitions. — [in:] DOYLE, L.J. & ROBERTS, H.H. (eds.). Carbonate-Clastic Transitions. — *Developments in Sedimentology*, **42**:99–142, 26 Figs., Amsterdam (Elsevier).

SASS, E., WEILER, Y. & KATZ, A., 1972. Recent Sedimentation and Oolite Formation in the Ras Matarma Lagoon, Gulf of Suez. — [in:] STANLEY, D.J. (ed.). The Mediterranean Sea: A Natural Sedimentation Laboratory. — 279–292, 10 Figs., Stroudsburg, Pennsylvania (Dowden, Hutchinson & Ross, Inc.).

SCHUBÖ, W. & UEHLINGER, H.-M., 1986. SPSS^X: Handbuch der Programmversion 2.2. — **XIV** + 659 pp., Stuttgart – New York (G. Fischer).

SNEH, A. & FRIEDMAN, G.M., 1984. Spit complexes along the eastern coast of the Gulf of Suez. — *Sediment. Geol.*, **39**:211–226, 16 Figs., Amsterdam.

WAGNER, C.W. & VANDER TOGT, C., 1973. Holocene Sediment Types and Their Distribution in the Southern Persian Gulf. — [in:] PURSER, B.H. (ed.). The Persian Gulf. Holocene Carbonate Sedimentation and Diagenesis in a Shallow Epicontinental Sea. — 123–155, 20 Figs., Berlin – Heidelberg – New York (Springer).

sample	aggl. f.	mil. f.	hyal. f.	spong.	corals	bryo	mol.	worm	crust.	osfr	echi.	vert	red	green	plant	pellets	comp	crypto	oid	non-ca	unident	matrix
A2	0.87	35.59	2.88	0.00	17.00	0.00	13.11	0.00	0.00	0.14	0.58	0.00	2.74	0.00	0.00	0.00	5.76	0.00	0.00	5.62	15.71	0.00
A4	2.75	22.17	30.42	0.00	0.32	0.00	19.09	0.00	0.00	0.00	0.65	0.00	0.00	0.00	0.00	3.56	0.00	0.00	5.18	14.56	1.29	
A5	2.12	32.90	10.10	0.00	1.79	0.00	10.42	2.61	1.47	0.00	0.33	0.00	0.00	0.00	0.65	0.00	7.82	1.63	0.00	4.07	21.98	2.11
A6	0.00	1.13	0.28	0.00	0.99	0.00	8.09	0.00	0.00	0.28	0.00	1.13	0.00	0.00	0.14	0.98	0.28	0.71	82.98	2.98	0.00	
A7	0.00	0.17	0.17	0.00	3.51	0.00	1.51	0.00	0.00	0.00	0.17	0.00	0.00	0.00	0.00	4.51	4.01	0.00	85.95	0.00	0.00	
A8	0.64	16.85	5.30	0.00	10.11	0.80	13.16	0.32	0.80	0.16	0.96	0.00	2.41	0.00	0.32	0.00	12.84	1.93	0.00	10.59	22.79	0.00
A9	0.00	16.59	0.32	0.00	0.48	0.00	1.91	0.00	0.00	0.00	0.00	1.12	0.00	0.16	0.00	3.19	7.65	0.00	65.87	2.71	0.00	
A10	0.00	4.97	0.28	0.00	5.26	0.00	3.13	0.00	0.00	0.00	0.00	2.70	0.00	0.00	0.00	3.55	7.67	0.00	71.31	1.14	0.00	
A11	2.01	31.90	4.31	0.00	2.73	0.14	11.35	0.72	0.86	0.29	0.86	0.00	0.14	0.00	0.29	0.00	5.46	0.57	0.00	9.63	28.74	0.00
A12	4.00	21.76	24.64	0.00	1.28	0.00	12.48	0.00	0.00	0.16	0.48	0.00	0.00	0.00	0.16	0.00	0.32	0.00	0.00	5.28	26.40	3.04
A13	0.16	8.87	2.38	0.00	35.82	0.00	22.19	0.32	0.00	0.00	0.00	3.80	0.00	0.00	0.00	12.52	7.92	0.00	3.17	2.85	0.00	
A14	2.20	6.75	27.47	0.00	0.00	0.00	16.48	0.00	0.79	0.00	0.63	0.00	0.16	0.00	0.00	0.79	2.98	0.00	8.63	30.61	2.51	
A15	1.12	6.98	1.26	0.00	0.00	0.00	1.68	0.56	0.28	0.00	0.00	0.28	0.00	0.00	0.00	0.23	0.42	0.00	71.79	13.41	0.00	
A16	1.67	3.51	4.18	0.00	15.89	0.17	21.91	1.67	0.00	0.00	2.01	0.00	0.86	0.00	0.17	0.00	9.37	2.84	0.00	5.18	18.56	6.02
A17	0.71	1.61	2.68	0.00	41.25	0.18	18.39	0.54	0.36	0.00	0.71	0.00	10.89	0.00	0.00	0.00	18.57	0.71	0.00	0.00	3.39	0.00
A18	0.75	2.74	2.49	0.00	0.00	0.00	2.37	0.00	0.00	0.25	0.00	0.00	0.00	0.00	0.00	0.37	0.50	0.00	4.61	74.69	10.72	
A19	1.90	21.75	6.71	0.00	0.29	0.00	12.12	0.44	0.15	0.44	0.15	0.00	0.44	0.00	0.15	0.00	1.90	0.15	0.00	46.42	7.01	0.00
A20	7.01	4.27	20.27	0.00	0.76	0.00	21.34	0.00	0.76	0.00	0.31	0.00	0.15	0.00	0.00	1.98	0.91	0.00	13.87	27.29	0.76	
A21	5.24	9.52	5.24	0.00	2.76	0.00	8.83	0.00	0.83	0.14	1.65	0.00	2.07	0.00	0.00	0.00	6.48	3.59	0.00	12.28	38.62	2.76
A22	0.49	10.59	2.74	0.00	0.49	0.00	21.05	0.00	0.62	0.00	0.13	0.00	0.00	0.00	0.00	0.13	0.25	0.00	3.61	0.00	0.49	
A24	1.59	2.71	23.13	0.00	1.43	0.00	11.16	0.00	1.12	0.00	0.96	0.00	0.16	0.00	0.00	0.64	0.48	0.00	26.79	27.59	2.23	
A25	2.91	27.01	6.51	0.00	1.11	0.00	10.11	1.80	0.28	0.14	1.25	0.00	0.55	0.14	0.00	0.00	2.91	8.73	0.00	6.65	29.64	0.28
A26	0.60	1.94	10.01	0.00	1.05	0.00	16.44	0.00	0.60	0.00	1.05	0.00	0.00	0.00	0.00	0.15	0.00	0.00	0.00	11.06	50.22	
A27	3.60	8.07	5.33	0.00	0.29	0.00	8.79	0.29	0.58	0.00	0.43	0.00	0.00	0.00	0.00	0.00	5.47	5.62	0.14	25.79	34.01	1.59
A28	1.38	3.29	6.57	0.00	44.81	0.17	10.55	0.69	0.17	0.00	2.25	0.00	13.15	0.00	0.00	0.00	7.44	2.42	0.00	0.52	6.57	0.00
A29	0.66	1.18	3.55	0.00	16.43	0.13	6.05	1.58	0.00	0.00	0.79	0.00	4.47	0.00	0.00	0.00	4.21	1.58	0.00	1.46	42.18	15.77
A30	1.65	21.20	4.36	0.00	0.90	0.00	13.38	1.35	2.71	0.00	0.30	0.00	0.00	0.00	0.00	9.77	5.71	0.00	11.13	27.07	0.45	
A32	0.14	3.78	0.56	0.00	3.78	0.00	3.08	0.00	0.00	0.00	0.00	0.00	0.00	0.00	0.00	2.38	8.26	2.52	64.43	8.82	0.00	
A33	0.00	0.00	0.00	0.00	0.00	0.00	1.09	0.00	0.00	0.00	0.00	0.00	0.00	0.00	0.00	1.77	0.00	0.00	95.24	1.36	0.00	
B1	1.50	4.84	28.55	0.00	10.68	0.67	16.53	0.00	0.00	0.00	0.00	2.17	0.00	5.68	0.00	0.00	9.85	6.85	0.00	0.00	12.69	0.00
B2	0.83	2.66	15.95	0.00	22.59	0.17	14.62	5.81	0.50	0.00	1.99	0.00	8.14	0.00	0.00	0.00	15.95	3.65	0.00	0.17	6.65	0.00
B3	2.01	4.95	19.19	0.00	0.62	0.93	42.26	0.00	0.46	0.46	1.08	0.00	0.62	0.00	0.00	0.15	5.26	3.25	0.00	0.00	13.62	5.11
B4	1.24	5.75	17.39	0.00	10.87	0.00	18.48	0.47	0.00	0.00	1.40	0.00	7.14	0.00	0.00	0.00	26.09	2.64	0.00	0.78	7.61	0.00
B6	7.21	10.97	13.42	0.00	2.60	0.14	6.49	0.00	0.58	0.14	0.87	0.00	1.15	0.00	0.00	0.00	8.66	2.17	1.30	4.33	39.25	0.72
B7	0.61	6.59	8.28	0.00	7.36	0.00	8.74	0.46	0.15	0.46	0.61	0.00	7.68	0.31	0.00	0.00	4.14	3.31	0.00	0.00	52.45	1.84
B8	0.69	5.65	3.31	0.00	8.40	0.00	16.80	1.24	0.00	0.41	0.96	0.00	5.79	0.14	0.00	0.00	0.55	3.72	0.00	2.07	39.39	3.58
B9	1.52	5.94	1.01	0.00	0.51	0.00	1.90	0.00	0.13	0.00	0.38	0.00	1.14	0.00	0.00	0.00	0.25	15.17	0.00	1.77	65.87	4.05
B10	0.00	1.24	4.43	0.00	34.16	0.18	22.30	0.18	0.18	0.00	1.59	0.00	18.23	0.18	0.00	0.00	12.92	0.00	0.00	0.00	4.42	0.00
B11	0.35	1.76	7.92	0.00	27.82	0.35	5.99	1.06	0.53	0.00	4.40	0.00	30.99	0.00	0.00	0.00	11.09	0.88	0.00	0.18	6.69	0.00
B12	1.95	9.40	2.43	0.00	23.34	0.16	9.08	0.65	0.32	0.16	3.89	0.00	15.07	0.16	0.49	0.00	6.81	2.92	0.00	0.16	23.01	0.00
B13	0.41	1.10	1.78	0.27	20.27	0.00	6.71	0.00	0.00	0.14	0.27	0.00	3.15	0.00	0.00	0.00	1.64	10.14	0.82	0.00	0.14	21.78
B14	0.37	0.87	0.87	0.00	0.00	0.00	0.25	0.00	0.00	0.00	0.13	0.00	0.00	0.00	0.00	0.50	0.00	0.13	0.00	2.00	61.75	
B15	0.31	5.00	4.06	0.00	15.94	0.00	27.66	0.78	0.47	0.00	1.72	0.00	4.69	0.00	0.00	0.00	11.09	2.34	0.00	0.78	20.00	5.16

Appendix 1: Frequency (%) of sediment constituents of 120 samples (thin sections).

sample	aggl. f.	mil. f.	hyal. f.	spong.	corals	bryo	mol.	worm	crust	ostr.	echi.	vert	red	green	plant	pellets	comp	crypto	oid	non-ca	unident	matrix
B16	0.17	1.70	1.19	0.00	0.17	0.00	1.53	0.00	0.00	0.17	0.66	0.00	0.00	0.00	0.51	0.00	0.00	0.17	2.04	57.89	33.79	
B17	1.35	33.38	2.70	0.00	2.16	0.00	5.27	1.35	0.41	0.00	1.08	0.00	0.00	0.27	0.00	5.00	10.00	0.00	5.13	31.49	0.41	
B18	3.10	6.51	2.61	0.00	15.80	0.00	12.38	0.33	0.33	0.16	1.14	0.00	4.23	0.16	0.00	0.00	12.21	3.26	0.00	2.12	35.34	0.33
B19	1.85	2.86	8.91	0.00	12.77	0.00	29.08	1.35	0.17	0.00	2.69	0.00	6.39	0.00	0.00	0.00	12.61	2.69	0.00	3.53	12.10	3.03
B20	1.91	2.05	8.19	0.00	1.09	0.00	11.87	0.55	0.00	0.00	2.05	0.00	0.68	0.00	0.00	0.14	1.50	4.50	0.00	2.73	55.25	7.51
B21	0.28	2.27	1.42	0.00	0.57	0.00	1.71	0.00	0.00	0.71	1.85	0.00	0.43	0.00	0.00	0.99	1.42	0.00	7.24	76.42	4.69	
B22	0.13	0.25	0.75	0.00	0.00	0.00	0.37	0.00	0.00	0.13	0.25	0.00	0.00	0.00	0.00	1.12	0.13	0.37	0.00	0.50	73.07	22.94
B23	0.00	1.47	4.11	0.00	8.07	0.44	4.84	0.73	0.00	0.00	0.73	0.00	1.76	0.00	0.00	1.17	0.73	1.17	0.00	0.15	29.47	45.16
B24	0.50	3.66	4.33	0.00	10.48	0.17	9.15	1.83	0.33	0.00	0.83	0.00	4.33	0.00	0.00	7.15	3.16	0.00	0.00	48.92	5.76	
B25	0.66	1.33	2.98	0.00	25.99	0.00	24.01	0.17	0.00	0.00	0.33	0.00	12.75	0.00	0.00	14.73	11.92	0.99	0.33	3.48	0.00	
B26	0.33	1.81	0.49	0.00	8.07	0.00	7.25	0.00	0.00	0.00	0.66	0.00	5.93	0.00	0.00	51.73	14.83	5.60	2.14	1.15	0.00	
B28	1.86	1.86	7.97	0.00	4.07	0.00	30.00	0.00	0.00	0.17	1.19	0.00	1.53	0.00	0.00	7.46	18.47	1.53	4.07	12.88	2.88	
B30	1.43	2.00	6.29	0.14	16.45	0.14	11.02	1.29	0.43	0.29	1.00	0.00	7.15	0.43	0.00	0.29	5.01	3.00	0.00	0.71	38.77	4.15
B31	1.25	3.06	5.01	0.14	37.47	0.14	14.07	0.70	0.14	0.00	0.84	0.00	7.80	0.00	0.00	4.32	1.53	0.00	0.00	23.26	0.28	
B32	5.53	1.80	10.68	0.00	0.26	0.00	9.14	0.39	0.13	0.00	0.39	0.00	0.13	0.00	0.00	0.77	4.89	1.67	0.00	0.77	54.18	9.27
B33	1.33	0.80	14.53	0.00	0.00	0.00	3.47	0.13	0.13	0.00	0.40	0.00	0.40	0.00	0.00	1.20	8.93	2.80	0.00	0.53	62.53	2.80
B34	2.25	3.38	33.49	0.00	0.48	0.00	5.31	0.48	0.16	0.00	0.48	0.00	0.00	0.00	0.00	0.16	7.73	0.97	0.00	0.81	38.00	6.28
B35	0.13	2.92	17.84	0.13	0.41	0.00	17.84	0.00	0.27	0.27	0.81	0.00	0.27	0.00	0.00	0.41	2.16	2.70	0.00	1.08	39.39	13.51
B36	1.48	4.72	16.44	0.00	1.48	0.27	11.86	0.13	0.00	0.13	1.35	0.00	0.54	0.00	0.00	0.13	1.75	2.69	0.00	1.21	46.36	9.44
B37	1.93	6.35	17.38	0.00	0.97	0.00	12.83	0.41	0.00	0.14	0.69	0.00	0.55	0.00	0.00	0.14	3.72	1.65	0.14	3.86	43.86	5.38
B38	2.07	4.79	16.97	0.00	1.94	0.00	11.92	0.13	0.78	0.00	0.13	0.00	0.00	0.00	0.13	0.13	0.39	4.53	0.00	17.62	28.37	10.10
B41	1.39	5.56	13.49	0.00	4.03	0.00	19.61	0.28	0.42	0.28	1.67	0.00	0.83	0.00	0.00	3.34	20.03	7.65	1.67	3.48	16.27	0.28
B42	7.17	4.88	10.21	0.00	1.52	0.31	14.02	0.31	0.61	1.22	0.00	0.46	0.00	0.00	1.52	6.25	2.29	1.22	2.44	42.38	2.89	
B43	0.00	0.25	2.41	0.00	0.00	0.51	0.63	0.00	0.25	0.89	0.00	0.00	0.00	0.00	0.76	0.13	0.00	0.00	3.05	57.11	43.01	
B44	0.13	0.38	0.89	0.00	0.00	0.00	0.89	0.00	0.00	0.13	0.64	0.00	0.00	0.00	0.00	0.89	0.00	1.02	0.00	2.67	56.69	35.67
B45	1.21	1.56	3.64	0.00	23.05	0.17	10.40	2.77	0.00	0.00	1.39	0.00	12.13	0.00	0.00	0.52	5.37	1.21	0.00	0.35	30.50	5.72
B46	0.12	0.00	0.36	0.00	0.00	0.48	0.00	0.00	0.12	0.36	0.00	0.00	0.00	0.00	0.00	0.00	0.00	0.00	0.00	2.65	38.72	
B48	8.77	4.87	7.95	0.16	1.95	0.00	17.37	0.49	0.16	0.00	0.81	0.00	1.30	0.16	0.00	0.16	9.90	2.92	4.22	3.90	33.28	0.00
B49	1.73	4.32	12.97	0.00	3.60	0.00	19.02	0.29	0.00	0.29	1.87	0.00	0.87	0.00	0.00	5.33	20.03	10.66	1.44	1.59	13.40	2.59
B51	0.29	1.17	1.17	0.00	0.29	0.00	0.73	0.00	0.00	0.15	0.00	0.00	0.00	0.00	0.00	59.38	0.00	0.29	0.00	0.59	32.11	2.93
B52	1.33	3.20	18.40	0.13	4.40	0.00	12.93	0.53	0.40	0.13	0.40	0.00	0.40	0.00	0.00	0.27	3.87	2.27	0.00	0.67	44.93	5.73
B53	1.44	2.23	19.76	0.00	0.52	0.00	6.15	0.13	0.00	0.13	0.65	0.00	0.39	0.00	0.00	0.26	1.44	1.44	0.00	1.83	56.15	7.46
B54	1.82	3.76	7.52	0.00	0.13	0.00	11.28	0.00	0.26	0.13	0.26	0.00	0.00	0.00	0.00	1.17	4.41	3.37	0.52	1.56	57.72	6.10
B56	0.41	1.83	7.71	0.00	29.21	0.00	16.23	1.42	0.20	0.00	0.61	0.00	17.65	0.00	0.00	0.00	17.85	3.25	0.00	0.81	2.84	0.00
B57	0.71	3.01	4.60	0.00	2.48	0.00	39.47	0.89	0.35	0.00	1.77	0.00	6.55	0.00	0.00	1.42	20.89	3.36	0.89	3.54	10.09	0.00
B58	0.93	6.79	3.70	0.00	30.25	0.00	21.14	1.70	0.31	0.00	0.77	0.00	13.43	0.00	0.00	12.35	2.93	0.00	0.77	4.94	0.00	
B59	3.44	3.14	4.71	0.00	29.80	0.00	15.88	1.57	0.98	0.00	0.78	0.00	18.04	0.20	0.00	15.88	0.78	0.00	0.00	5.29	0.00	
B60	0.94	0.19	2.63	0.00	22.33	0.00	34.15	1.69	0.19	0.00	1.13	0.00	15.20	0.00	0.00	16.51	3.57	0.00	0.19	1.31	0.00	
B61	1.16	0.58	3.47	0.00	29.54	0.00	25.87	1.35	0.77	0.19	0.77	0.00	11.00	0.00	0.00	18.15	0.97	0.00	0.00	6.18	0.00	
B67	1.99	7.14	1.33	0.00	25.25	0.17	21.76	1.83	0.50	0.00	1.16	0.00	8.47	0.33	0.00	14.78	3.99	0.00	1.66	9.63	0.00	
B68	0.93	6.79	3.70	0.00	30.25	0.00	21.14	1.70	0.31	0.00	0.77	0.00	13.43	0.00	0.00	12.35	2.93	0.00	0.77	4.94	0.00	
B69	3.35	3.17	7.57	0.00	0.18	0.00	16.55	0.00	0.35	0.53	0.53	0.00	0.18	0.00	0.00	1.06	2.29	0.00	7.22	55.28	0.70	
B70	0.14	0.86	2.43	0.00	0.00	0.71	0.00	0.00	0.00	0.71	0.00	0.00	0.00	0.00	0.00	0.14	0.00	0.00	2.15	61.23	31.62	
B73	0.74	4.82	4.82	0.00	41.93	0.19	9.28	0.37	0.56	0.00	3.90	0.00	20.78	0.00	0.00	6.12	2.41	0.00	0.00	4.08	0.00	
B74	0.00	5.55	0.15	0.00	3.50	0.00	9.63	0.00	0.00	0.00	0.88	0.00	3.50	0.00	0.00	12.99	52.12	0.00	0.00	4.53	0.00	

Appendix 1 (continued): Frequency (%) of sediment constituents of 120 samples (thin sections).

sample	aggl. f.	mill. f.	hyal. f.	spong.	corals	byvo	mol.	worm	crust.	ostr.	echi.	vert.	red	green	plant	pellets	comp	crypto	oid	non-oid	unident	matrix	
C1	1.59	4.77	34.18	0.00	7.15	0.48	25.75	0.95	0.00	0.32	0.00	4.77	0.00	0.32	15.42	1.91	0.00	0.32	2.07	0.00	0.00		
C2	2.22	7.53	17.73	0.00	0.00	0.00	3.55	0.00	0.15	0.15	0.29	0.00	0.44	0.00	0.59	1.77	1.03	0.00	0.00	52.14	12.41		
C3	2.63	4.71	10.94	0.14	0.00	0.00	4.02	0.14	0.55	0.00	0.14	0.00	1.39	0.00	0.41	2.49	0.00	0.14,	56.37	13.44			
C4	9.43	5.39	4.34	0.15	0.15	0.00	17.22	0.30	0.90	0.30	0.00	0.15	0.00	0.00	0.15	9.58	1.05	0.45	3.59	42.51	4.34		
C5	1.19	2.84	4.33	0.00	22.24	0.15	17.31	0.30	0.15	0.00	1.49	0.00	6.27	0.00	0.30	14.78	4.03	1.64	13.43	9.55	0.00		
C6	0.00	10.27	1.04	0.15	5.80	0.00	4.61	0.30	0.45	0.15	0.15	0.00	2.83	0.15	0.00	7.74	11.01	2.08	21.43	30.95	0.74		
C7	0.00	4.77	1.06	0.00	1.72	0.13	2.65	0.80	0.13	0.00	0.00	0.00	1.06	0.00	0.00	3.32	2.25	0.13	21.09	56.90	3.98		
C8	1.11	9.34	3.07	0.00	18.13	0.00	13.39	1.12	0.00	0.14	0.42	0.14	2.93	0.00	0.00	20.08	3.49	0.00	1.95	24.69	0.00		
C9	0.00	0.58	0.00	0.29	0.00	0.72	0.00	0.00	0.00	0.29	0.00	0.14	0.00	0.00	0.00	1.87	0.72	0.00	95.25	0.14	0.00		
C10	0.17	5.41	2.20	0.00	30.24	0.00	14.02	1.18	0.00	0.00	0.85	0.00	2.87	0.00	0.00	0.00	30.24	4.05	0.00	0.34	8.45	0.00	
C11	0.00	3.47	0.73	0.00	7.31	0.00	17.73	0.18	0.00	0.18	0.00	0.18	2.19	0.00	0.00	0.00	66.36	0.00	0.00	0.18	1.65	0.00	
C12	0.53	14.70	1.71	0.00	9.58	0.13	5.12	1.44	0.26	0.26	0.66	0.00	0.79	0.00	0.00	0.00	12.20	8.79	0.00	2.49	41.08	0.26	
C13	0.00	1.15	0.14	0.00	0.43	0.00	1.73	0.00	0.00	0.00	0.00	0.43	0.00	0.00	0.14	7.49	2.88	12.97	71.90	0.72	0.00		
C14	1.20	1.33	2.80	0.00	17.71	0.00	6.39	1.33	0.33	0.13	0.00	0.00	5.86	0.00	0.00	0.13	5.33	3.20	0.00	0.67	50.60	2.80	
C15	0.82	21.75	1.65	0.00	8.90	0.00	7.91	0.33	0.33	0.00	0.33	0.00	4.45	0.00	9.06	0.00	13.84	13.01	0.33	2.80	14.00	0.49	
C16	0.78	24.14	1.40	0.00	2.96	0.00	7.17	0.00	2.03	0.00	1.40	0.00	1.40	0.00	0.16	4.98	0.31	0.00	36.60	16.51	0.00		
C17	2.00	19.08	2.00	0.00	10.92	0.15	16.31	1.69	0.61	0.00	0.31	0.00	1.39	0.00	0.00	0.00	27.08	3.39	0.00	2.92	12.15	0.00	
C18	0.30	8.71	1.50	0.00	27.48	0.15	14.71	0.15	0.00	0.15	0.75	0.00	5.25	0.00	0.15	0.00	27.03	3.60	0.00	0.90	9.16	0.00	
C19	0.68	22.72	1.22	0.00	3.54	0.00	11.70	0.82	1.36	0.14	0.27	0.00	0.68	0.00	0.00	0.00	8.57	6.94	0.00	23.40	17.96	0.00	
C20	0.72	17.49	2.46	0.00	2.89	0.00	6.21	0.29	0.15	0.15	0.00	0.00	0.29	0.00	0.00	0.00	14.45	2.46	0.00	3.18	48.27	1.01	
C21	0.00	1.16	0.29	0.00	7.85	0.00	9.01	0.00	0.00	0.00	0.00	0.00	2.62	0.00	0.00	0.00	5.67	0.29	1.60	66.28	5.23	0.00	
C22	0.79	16.25	0.92	0.13	0.79	0.00	12.45	0.52	0.00	0.00	0.65	0.00	0.26	0.00	0.92	0.00	10.09	4.19	0.00	0.79	49.28	1.96	
C23	0.00	5.30	2.06	0.00	20.18	0.00	7.81	0.15	0.15	0.00	0.74	0.00	5.30	0.00	0.00	0.00	33.58	12.52	0.00	0.29	11.93	0.00	
C24	3.72	7.97	6.11	0.00	3.19	0.00	9.43	0.00	0.13	0.00	1.19	0.00	1.06	0.00	0.00	0.00	0.27	15.14	5.05	1.19	15.94	29.35	0.27
C25	0.35	1.57	10.26	0.00	41.22	0.00	14.78	1.04	0.00	0.00	4.17	0.00	9.39	0.00	0.17	0.00	10.78	2.26	0.00	0.87	3.13	0.00	
C26	0.45	1.37	10.47	0.00	29.13	0.45	5.77	0.91	0.61	0.00	3.03	0.00	12.59	0.00	0.00	0.00	6.37	4.25	0.00	0.61	23.98	0.00	
D1	0.00	0.99	0.14	0.00	4.52	0.00	1.41	0.00	0.00	0.00	0.00	0.00	0.57	0.00	0.00	0.00	0.00	4.38	2.26	85.59	0.14	0.00	
D2	1.11	8.43	0.95	0.00	15.10	0.00	15.42	0.16	0.64	0.00	0.95	0.00	8.90	0.00	1.27	0.00	16.06	22.89	0.32	1.27	6.52	0.00	
D3	0.60	8.62	6.01	0.00	26.05	0.00	21.04	3.41	0.40	0.00	2.41	0.00	5.61	0.20	0.00	0.00	12.63	1.80	0.00	0.40	10.42	0.40	
D4	0.25	1.24	0.25	0.25	3.85	0.25	14.41	0.37	0.00	0.12	0.75	0.00	2.48	0.00	0.00	1.24	1.37	0.00	0.25	0.00	59.01	12.92	
D5	0.00	1.37	1.12	0.00	0.00	1.87	0.00	0.00	0.13	0.25	0.00	0.00	0.00	0.00	1.00	0.37	2.24	0.00	1.00	67.62	23.04		
D6	0.19	3.31	4.87	0.00	37.04	1.17	19.49	1.56	0.00	0.00	0.97	0.00	4.87	0.00	0.00	0.00	13.65	4.48	0.00	0.78	7.60	0.00	
D7	0.57	1.92	0.79	0.00	0.00	0.11	6.78	0.00	0.11	0.11	0.23	0.00	0.00	0.00	0.00	1.13	0.00	0.00	0.00	1.13	36.73		
D8	0.57	1.92	0.79	0.00	0.00	0.11	6.78	0.00	0.11	0.11	0.23	0.00	0.00	0.00	0.00	1.13	0.00	0.00	0.00	1.13	36.73		

Appendix 1 (continued): Frequency (%) of sediment constituents of 120 samples (thin sections).

PLATE 1
Foraminifera

Fig. 1. Biserial agglutinated foraminifer (*?Spiroplectammina* sp.). – Sample B 3.

Fig. 2. Large biserial agglutinated foraminifer with parapores. – Sample C 4.

Fig. 3. Two peripheral sections through agglutinated foraminifers with different wall structures. The upper individual shows a thick test wall with large agglutinated grains and parapores, the lower one a thin test wall with parapores. – Sample B 12.

Fig. 4. A sessile agglutinated foraminifer (*Haddonia* sp.) on a gastropod shell. – Sample B 33.

Fig. 5. Oblique section through two chambers of an agglutinated, paraperforate foraminifer. – Sample B 67.

Fig. 6. Section through an agglutinated, paraperforate foraminiferal test wall fragment. – Sample B 48.

Fig. 7. Section through a wall fragment of an agglutinated, paraperforate foraminiferal test. – Sample B 48.

Fig. 8. Two porcellaneous foraminifers of quinqueloculine type in subaxial sections. – Sample B 34.

Fig. 9. Subaxial section of a planispiral, porcellaneous foraminifer (*Spirolucina* sp.). Bottom left: octocorallian spicule. – Sample B 67.

Fig. 10. Axial-subaxial section of a quinqueloculine, porcellaneous foraminifer. The outer test wall shows open or partially filled microborings. – Sample C 11.

Fig. 11. Oblique section of a small, thin walled, porcellaneous foraminifer (quinqueloculine type). To its left a sponge spicule. – Sample 16.

Fig. 12. Transverse section of a porcellaneous foraminifer with high amount of agglutinated particles (*Schlumbergerina* sp.) – Sample A 5.

Fig. 13. Median section of a peneroplid foraminifer with cibrate aperture (*Peneroplis* sp.). – Sample B 67.

Fig. 14. Subaxial, longitudinal section of a peneroplid foraminifer with cibrate aperture (*Peneroplis* sp.). – Sample A 4.

Fig. 15. Subequatorial section of *Borelis schlumbergeri* (REICHEL). – Sample C 14.

Fig. 16. Subaxial section of *Borelis schlumbergeri* (REICHEL) showing streptospirally enrolled initial whorls, and an oblique section through a coarse agglutinated foraminifer. – Sample A 5.

PLATE 1

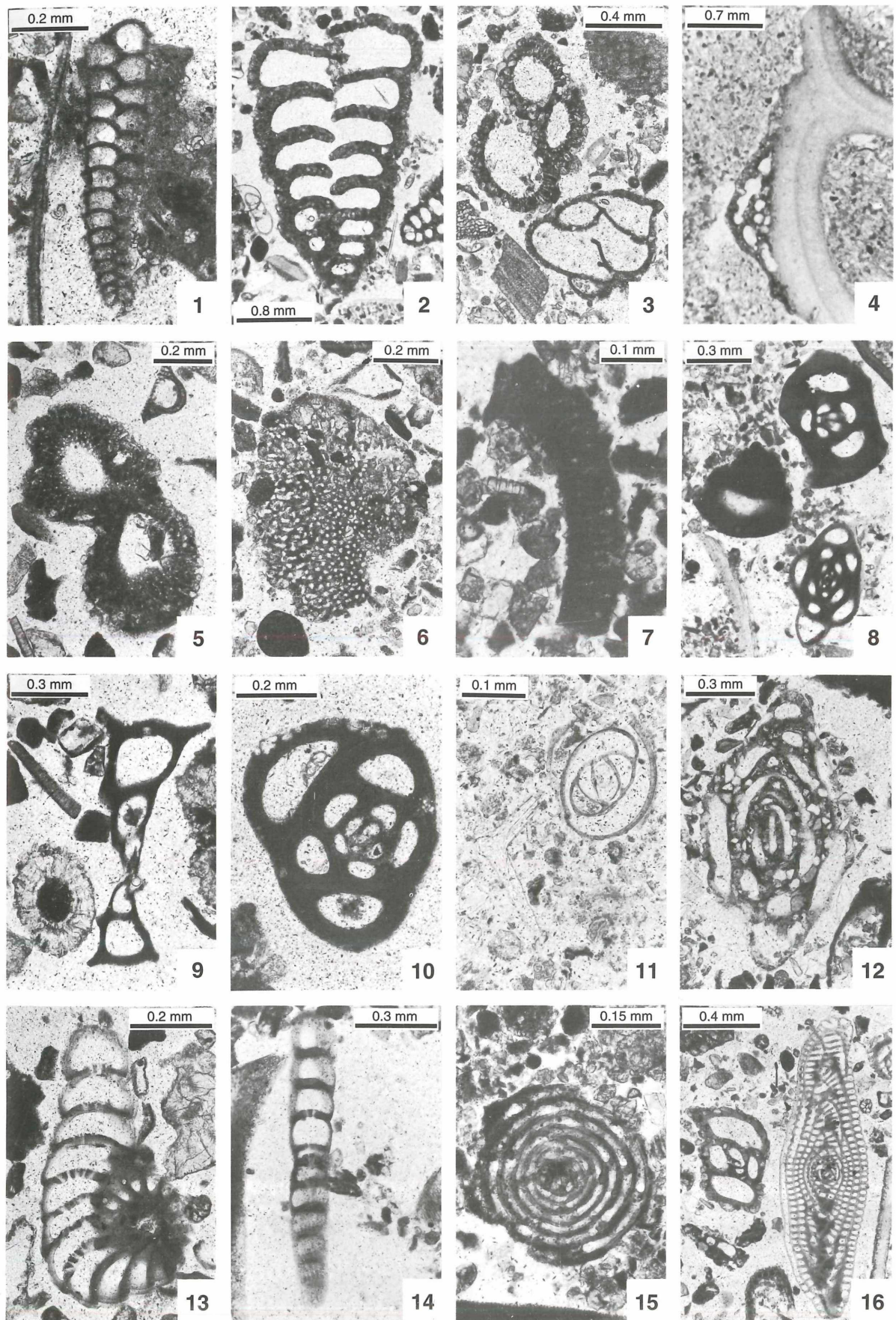


PLATE 2

Foraminifera

Fig. 1. Equatorial section through a soritid foraminifer (*Amphisorus hemprichii* EHRENBERG). – Sample C 16.

Fig. 2. Tangential section near the periphery of a soritid foraminiferal test. – Sample A 5.

Fig. 3. Oblique section through a test fragment of a soritid foraminifer. – Sample A 5.

Fig. 4. Three sections of larger hyaline foraminifera. The uppermost is an oblique section through *Heterostegina depressa* d'ORBIGNY, the two others are amphisteginids. – Sample C 1.

Fig. 5. Subaxial section of *Amphistegina lobifera* LARSEN. – Sample C 27.

Fig. 6. Axial section of *Amphistegina lessonii* d'ORBIGNY. – Sample B 42.

Fig. 7. Lateral, tangential section through *Amphistegina* showing the typically curved septa. – Sample C 27.

Fig. 8. Axial section of *Heterostegina depressa* d'ORBIGNY. – Sample C 1.

Fig. 9. Slightly oblique, nearly equatorial section of *Heterostegina depressa* d'ORBIGNY. – Sample C 1.

Fig. 10. Oblique section of *Heterostegina depressa* d'ORBIGNY. – Sample C 1.

Fig. 11. Oblique peripheral section through *Heterostegina depressa* d'ORBIGNY. – Sample B 30.

Fig. 12. Oblique section of *Heterostegina depressa* d'ORBIGNY. – Sample B 67.

Fig. 13. Equatorial section of *Operculina* (=*Assilina*) *ammonoides* (GRONOVIUS). – Sample B 34.

Fig. 14. Oblique peripheral section through *Operculina ammonoides* (GRONOVIUS) showing ornamentation. – Sample B 34.

Fig. 15. Section through a test wall fragment of *Operculina ammonoides* (GRONOVIUS) showing part of septa, pores and lamellation. – Sample B 42.

Fig. 16. Subaxial, tangential section through *Operculina ammonoides* (GRONOVIUS). – Sample A 4.

PLATE 2

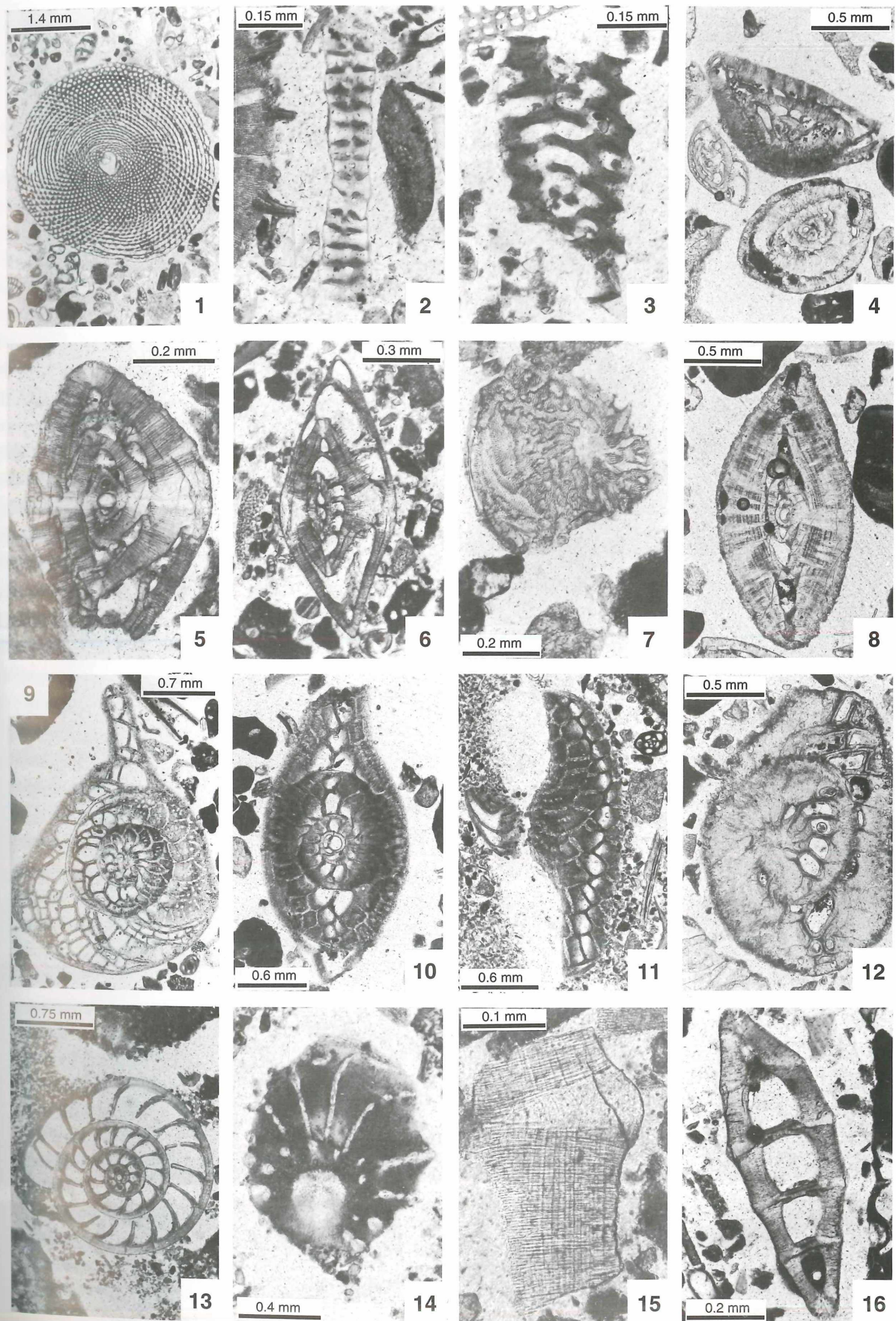


PLATE 3

Foraminifera and Sponges

Fig. 1. Subaxial section through an elphidiid foraminifer showing typical test wall interruptions. – Sample B 16.

Fig. 2. Transvers submedian section of *Neorotalia calcar* (d'ORBIGNY). – Sample B 12.

Fig. 3. Axial section of a rotaliid foraminifer. – Sample A 5.

Fig. 4. Subaxial section of a rotaliid foraminifer. – Sample C 15.

Fig. 5. Oblique sections of two planktic foraminifers. – Sample B 3.

Fig. 6. Section through a sessile homotrematid foraminifer. – Sample B 11.

Fig. 7. Section through a sessile homotrematid foraminifer overgrown by a thin crust of coralline algae. – Sample B 73.

Fig. 8. Section through a sessile homotrematid foraminifer. – Sample B 12.

Fig. 9. Axial section through *Planorbulinella* sp. – Sample B 73.

Fig. 10. Transverse equatorial section through *Planorbulinella* sp. – Sample B 73.

Fig. 11. Vertical section through sessile *Planorbulina* sp. – Sample A 5.

Fig. 12. Transverse section through sessile *Planorbulina* sp. – Sample A 5.

Fig. 13. Vertical section through a fragment of an acervulinid foraminifer. – Sample B 12.

Fig. 14. Peripheral section through a fragment of an acervulinid foraminifer. – Sample B 30.

Fig. 15. Vertical section through a sessile victoriellid foraminifer. Near the right margin: geniculate coralline algal gment. – Sample B 12.

Fig. 16. Triaxon sponge spicule. – Sample B 30.

PLATE 3

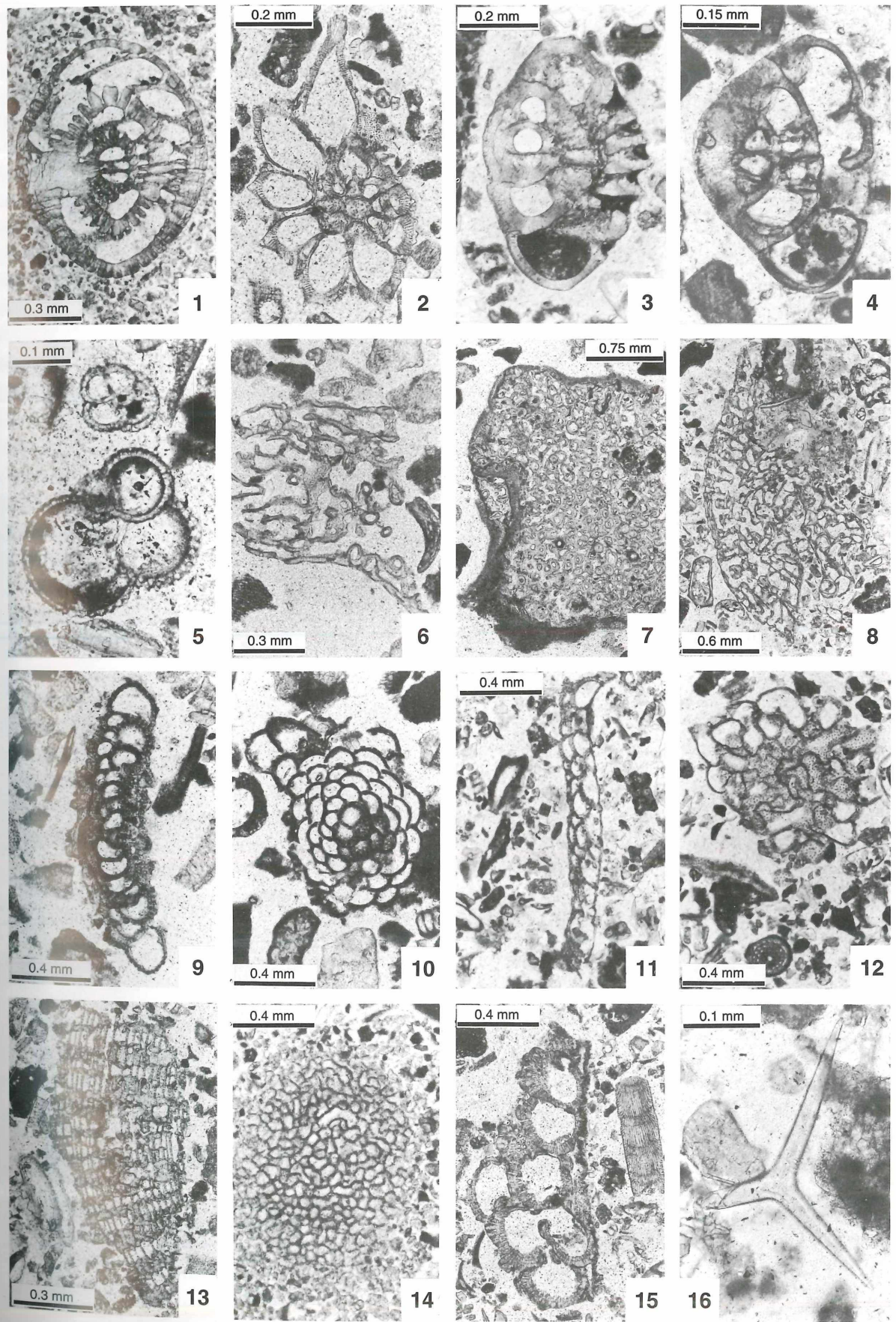


PLATE 4

Corals

Fig. 1. Scleractinian fragment with intraskeleton cavities filled with micritic cement. – Sample B 67.

Fig. 2. Scleractinian fragment with intraskeleton cavities filled with micritic cement. – Sample B 73.

Fig. 3. Scleractinian fragment with micritic cement on the external surface and in cavities. – Sample B 67.

Fig. 4. Cross section of a scleractinian coral branch. – Sample B 30.

Fig. 5. Longitudinal section through a scleractinian coral branch. – Sample A 17.

Fig. 6. Scleractinian fragment, overgrown by an acervulinid foraminifer. – Sample C 27.

Fig. 7. Longitudinal section through a scleractinian coral branch overgrown by coralline algae and acervulinid foraminifers. – Sample C 14.

Fig. 8. Scleractinian fragment with several borings. Cavities filled with micritic cement. – Sample B 74.

Fig. 9 – 11. Scleractinian fragments. – Sample B 30.

Fig. 12. Octocorallian spicule in longitudinal section. – Sample B 73.

Fig. 13. Octocorallian spicule in longitudinal section showing zonation and micritic envelope. – Sample B 73.

Fig. 14. Cross section of octocorallian spicule. – Sample C 27.

Fig. 15. Fragment of octocorallian spicule with micritic envelope and pore filling. – Sample C 15.

Fig. 16. Cross section of octocorallian spicule showing pronounced zonation. – Sample B 61.

PLATE 4

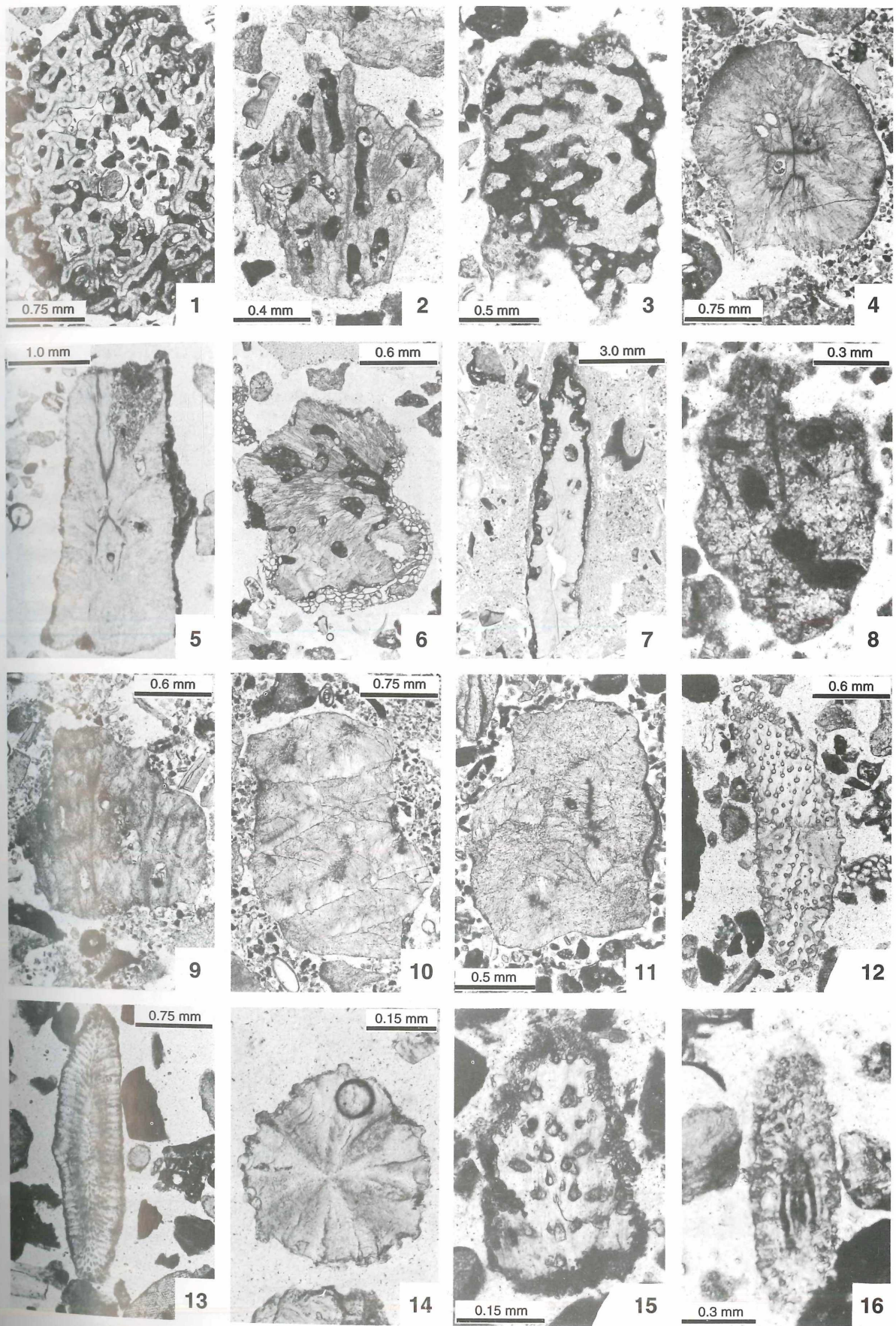


PLATE 5

Bryozoans and Molluscs

Fig. 1. Rameose bryozoan fragment in longitudinal section. – Sample B 1.

Fig. 2. Transverse section through a rameose bryozoan fragment. – Sample B 3.

Fig. 3. Oblique section through a bryozoan colony showing several zooecia. – Sample A 25.

Fig. 4. Rameose bryozoan fragment in longitudinal section. To the left and right scaphopod cross sections. Upper right corner: elphidiid foraminifer. – Sample B 3.

Fig. 5. Bifoliate cheilostomate bryozoan colony. Zooecia in lateral sections, partially infilled with sediment, showing large orifices. – Sample B 34.

Fig. 6. Cheilostomate bryozoan colony in section subparallel to the surface. Some of the zooecia show orifices, ascopores, and ovicells. – Sample A 8.

Fig. 7. Cheilostomate bryozoan colony in section subparallel to the surface. Most zooecia show differentiation in orifices, ascopores, and pseudopores. – Sample A 8.

Fig. 8. Cheilostomate bryozoan colony in section subparallel to the surface. Most zooecia show orifices and areoles. – Sample A 25.

Fig. 9. Gastropod shell in longitudinal section. – Sample B 73.

Fig. 10. Gastropod shell in cross section. – Sample B 1.

Fig. 11. Prismatic shell structure of a bivalve in section parallel to shell surface. – Sample A 28.

Fig. 12. Small bivalve fragment with prismatic shell structure cut perpendicular to shell surface. – Sample B 3.

Fig. 13. Small shell fragment exhibiting crossed-lamellar structure in oblique section. – Sample A 8.

Fig. 14. Complete bivalve shell in section parallel to commissure exhibiting ribbed ornamentation. – Sample B 31.

Fig. 15. Oblique section of a bivalve fragment with perforations (tubules) in cross section. – Sample B 2.

Fig. 16. Detail of a bivalve shell exhibiting tubules near the periphery of the shell. – Sample B 30.

PLATE 5

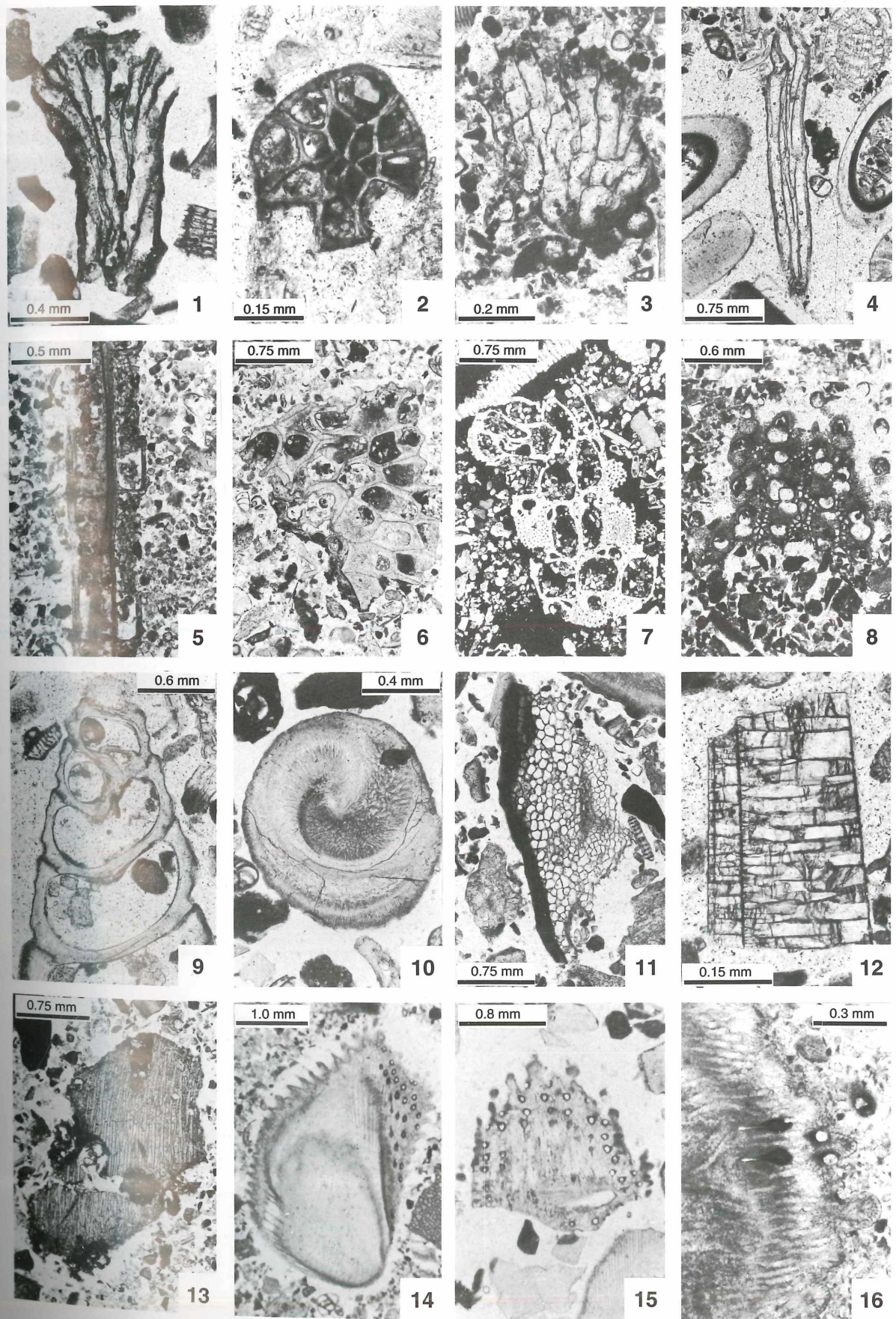


PLATE 6

Scaphopods, Annelids, Crustaceans, Echinoderms

Fig. 1. Oblique longitudinal section of a scaphopod shell with two layers. The inner layer typically exhibits bended lamellae. – Sample C 1.

Fig. 2. Transverse section of a scaphopod shell with its typical thick, bright, outer and thin, dark, inner layer. – Sample B 3.

Fig. 3. Oblique transverse section of a scaphopod shell exhibiting the two typical sublayers. These are overlain at the outer surface by a cellular layer representing the (?) periostracum. – Sample C 1.

Fig. 4. Longitudinal section of an annelid worm tube fragment composed of foliated calcite. – Sample B 30.

Fig. 5. Several transverse sections of an enrolled annelid worm tube exhibiting foliated structure. – Sample B 12.

Fig. 6. Oblique section through a worm tube fragment encrusted by an acervulinid foraminifer. – Sample B 11.

Fig. 7. Longitudinal section of an annelid worm tube fragment composed of foliated calcite. – Sample B 48.

Fig. 8. Typical section through a disarticulated decapod crustacean fragment with perforated prismatic structure. – Sample A 5.

Fig. 9. Oblique section through a decapod crustacean fragment with perforated prismatic structure. – Sample B 12.

Fig. 10. Section through a decapod crustacean fragment with perforated prismatic structure. – Sample B 67.

Fig. 11. Sculptured ostracod carapax with both shells articulated and prismatic structure in section perpendicular to hinge line. – Sample B 69.

Fig. 12. Ostracod shell sectioned parallel to hinge line (upper right). To its left a biserial (bolivinid) foraminifer, in the lower left corner a coralline algal fragment. – Sample B 36.

Fig. 13. Oblique transverse section through an echinoid spine fragment. – Sample D 3.

Fig. 14. Oblique longitudinal section through an echinoid spine. – Sample B 11.

Fig. 15. Longitudinal section through an echinoid spine with basal socket (bottom). – Sample C 28.

Fig. 16. Oblique section through an ophiuroid ossicle. – Sample B 73.

PLATE 6

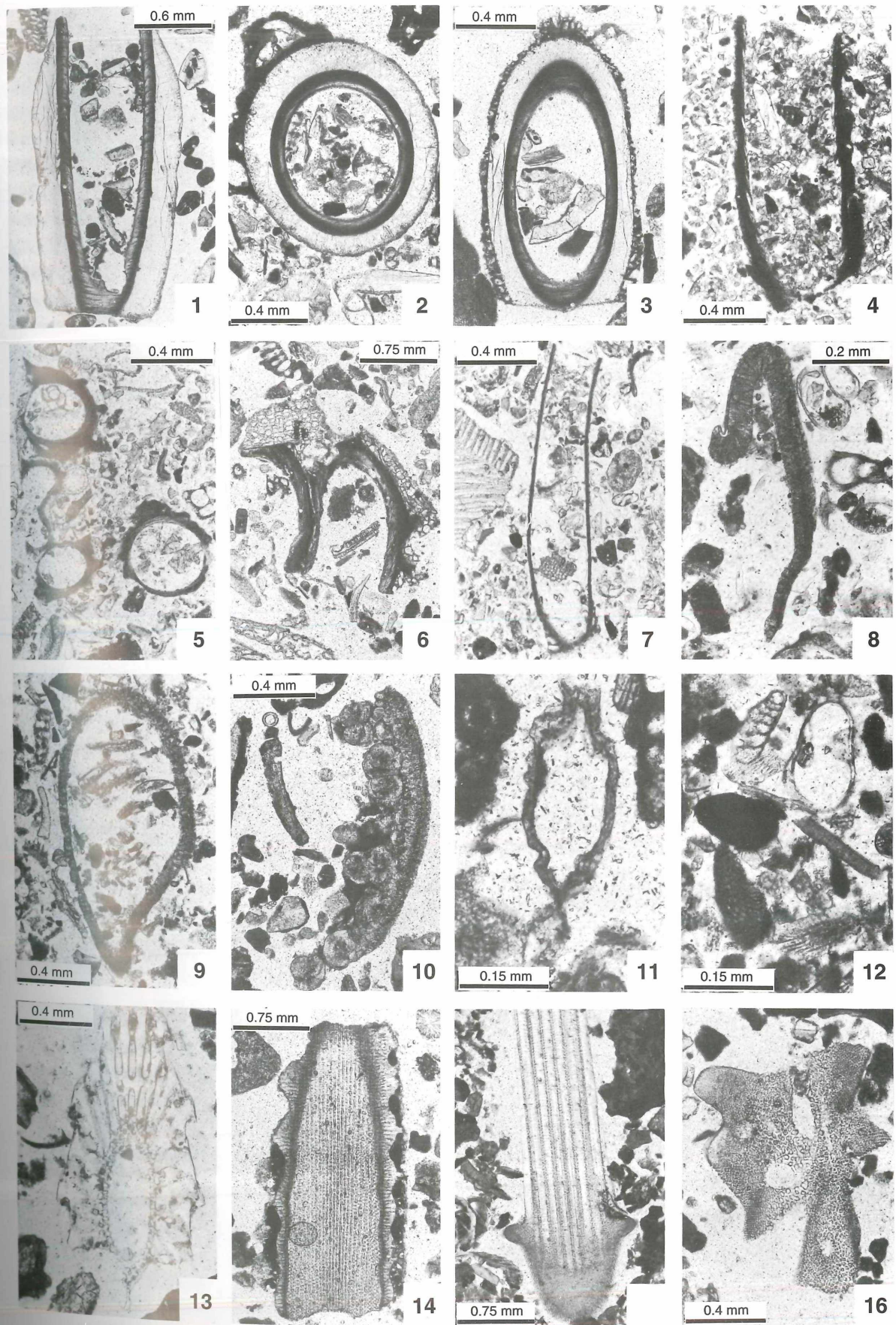


PLATE 7

Red algae, Green algae, Seagrass, Pellets

Fig. 1. Fragment of several crusts of coralline algae overgrowing each other in vertical section. – Sample C 14.

Fig. 2. Tiny, initial coralline algal rhodolith incorporating several components. – Sample B 48.

Fig. 3. Rhodolith fragment dominated by squamariaceans. – Sample C 1.

Fig. 4. Longitudinal (right) and oblique (left) section of geniculate coralline algae. – Sample B 12.

Fig. 5. Section through a disarticulated *Halimeda* segment exhibiting central medullary region and peripheral cortex. – Sample B 51.

Fig. 6. Section through *Halimeda* fragment composed mainly of cortical utricles. – B 51.

Fig. 7. Longitudinal section through *?Tydemania* sp. – B 67.

Fig. 8. Oblique transverse section through *?Tydemania* sp. – Sample B 30.

Fig. 9. Section through a seagrass leaf exhibiting cellular structure. – Sample C 15.

Fig. 10. Section through a terminal part of a seagrass leaf. In the upper part an oblique equatorial section through a soritid foraminifer. – Sample C 15.

Fig. 11. Oblique longitudinal section through an anomuran crustacean pellet with empty channels. – Sample C 13.

Fig. 12. Longitudinal section through an anomuran crustacean pellet with channels filled with sediment darker than the surrounding material. – Sample A 8.

Fig. 13. Pellets of large, ellipsoidal type composed of different particles but without internal structures. Lower right corner: quinqueloculine porcellaneous foraminifer. – Sample B 30.

Fig. 14. Pellet of large, ellipsoidal type composed of different particles without internal structures. – Sample C 13.

Fig. 15. Zonal pellet with dense outer cortex but small amount of particles and coarse grained core with high porosity. Around the zonal pellet occur several small, structureless pellets (type c). – Sample B 14.

Fig. 16. Two zonal pellets which are flattened by compaction. – Sample B 14.

PLATE 7

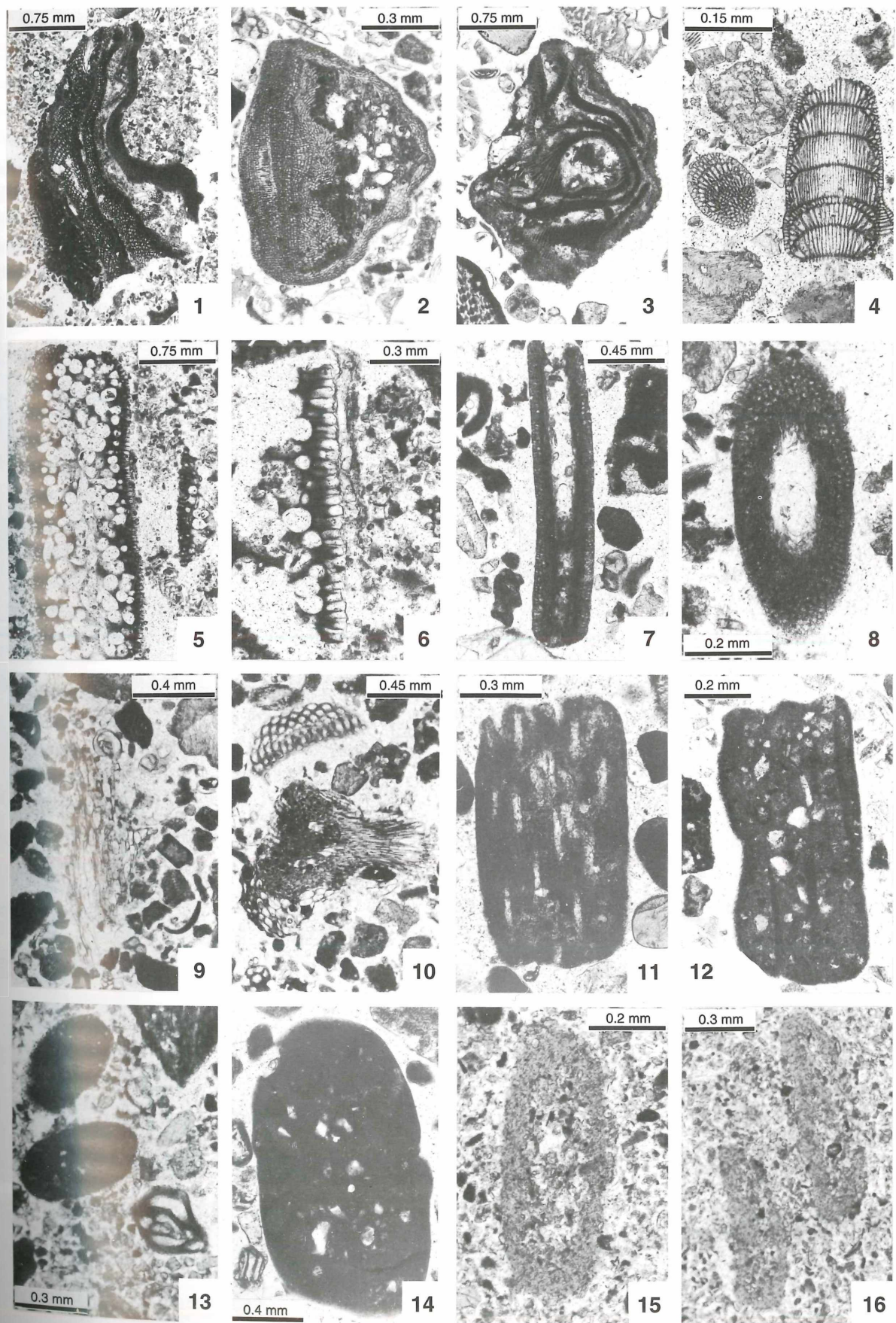


PLATE 8

Compound grains, Cryptocrystalline grains, Ooids

Fig. 1. Compound grain with relatively high amount of open interparticle pore space. The components are represented by several micritized skeletal grains and a hyaline foraminifer. – Sample B 48.

Fig. 2. Compound grain of grapestone type with very high proportion of open interparticle pore space. – Sample D 2.

Fig. 3. Compound grain with high amount of micritic cement, filling the main part of interparticle pore space. – Sample D 2.

Fig. 4. Compound grain of mud aggregate type composed of small components and high portion of matrix. The components are represented by small bioclasts, foraminifera and small pellets of type c. – Sample B 34.

Fig. 5. Compound grain of mud aggregate type which is encrusted by sessile foraminifers. – Sample B 34.

Fig. 6. Compound grain with relatively high abundance of ooids. Some of the components at the periphery of the aggregate are broken indicating transport. Thus, this type of aggregates can represent either relict compound grains or lithoclasts. – Sample B 48.

Fig. 7. Compound grain with high amount of micritic cement and abundant non-carbonate particles. – Sample C 13.

Fig. 8. Compound grain with high amount of micritic cement and ooids as dominating particles. – Sample C 13.

Fig. 9. Compound and cryptocrystalline grains. The compound grains are very small and of grapestone type; their components are predominantly cryptocrystalline grains. – Sample B 26.

Fig. 10. Several cryptocrystalline grains being completely micritized. – Sample B 74.

Fig. 11. Cryptocrystalline grain with several microborings. – Sample D 2.

Fig. 12. Ooid with multilamellar coating. – Sample B 48.

Fig. 13. Ooid with multilamellar coating and blackening. The blackening is stronger around the periphery. – Sample B 48.

Fig. 14. Multilamellar ooid with fecal pellet nucleus. – Sample B 48.

Fig. 15. Superficial ooid with quartz nucleus. – Sample C 6.

Fig. 16. Fragmented multilamellar ooid with blackened outer cortex. – Sample B 48.

PLATE 8

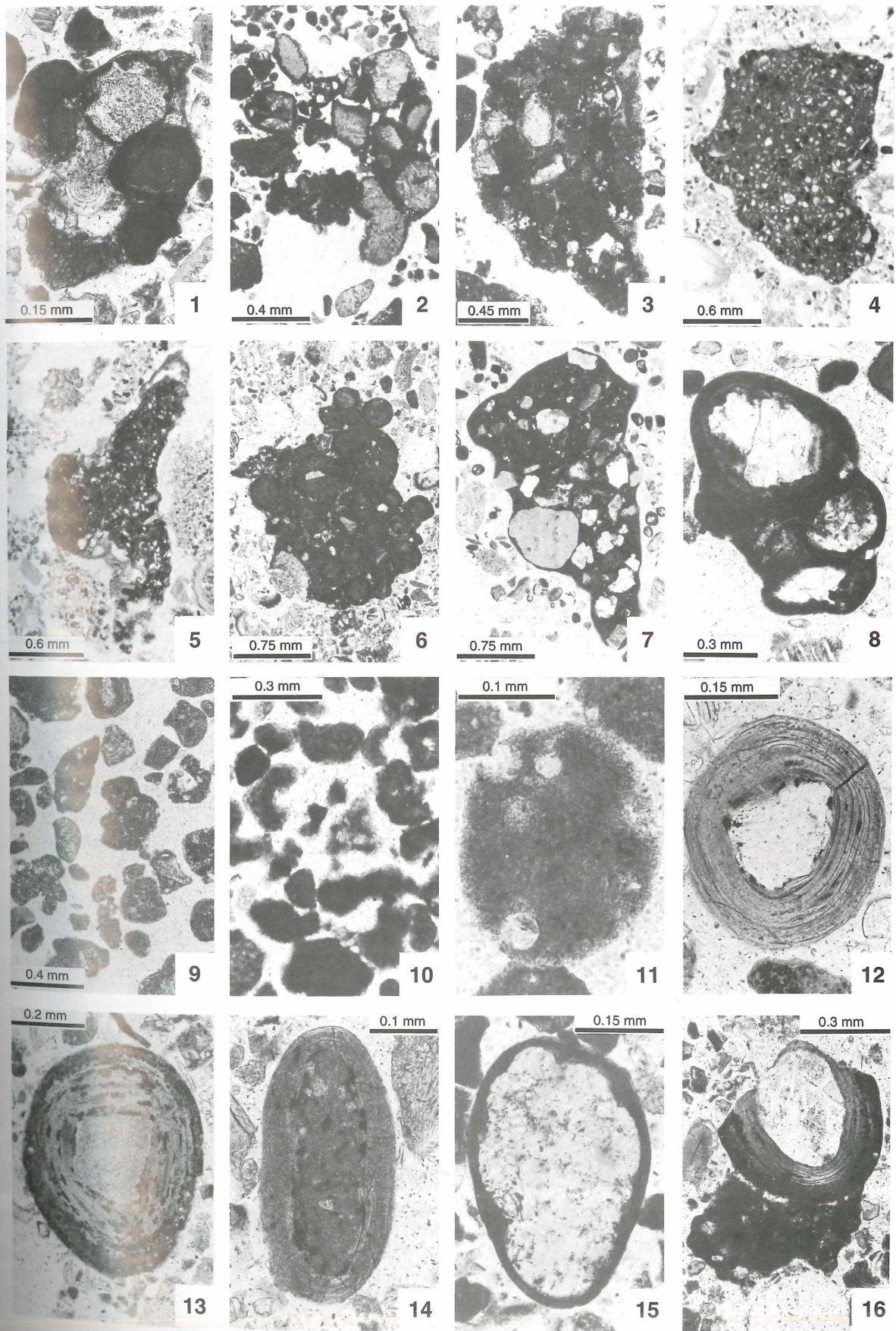


PLATE 9

Fig. 1. Coralgal facies. This sample is dominated by scleractinian bioclasts; coralline algae are represented mainly by smaller fragments and compound grains exhibit a high matrix content. The foraminiferal fauna is relatively diverse and dominated by porcellaneous forms like peneroplids, *Borelis*, and quinqueloculine miliolids; some agglutinated specimens are also present. – Sample B 67.

Fig. 2. Coralgal facies. Large fragments of corals and coralline algae characterize this thin section; molluscs, however, are also important. Foraminifera are represented by hyaline (amphisteginids, elphidiids) and porcellaneous forms. Many of the bioclasts show micritic envelopes and micritic cement in intraparticle cavities (especially coral fragments). – Sample A 17.

PLATE 9

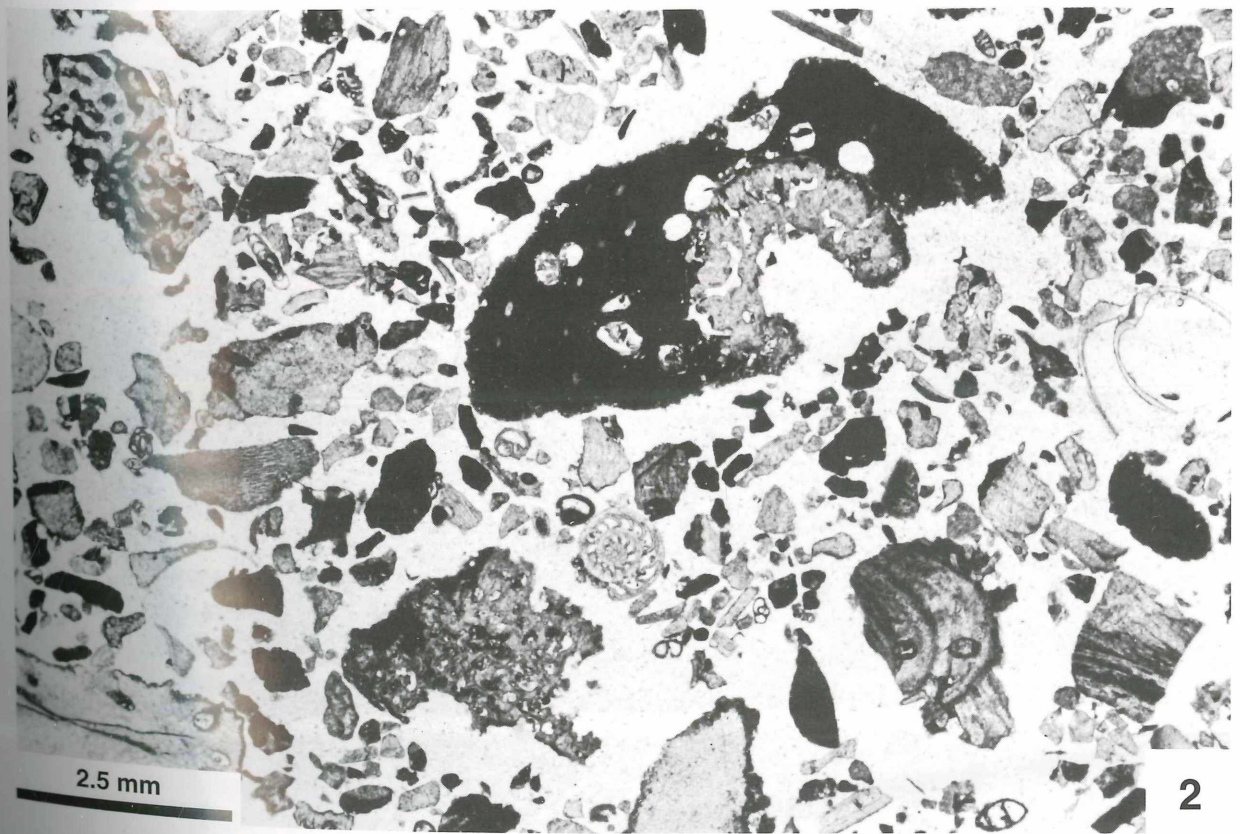
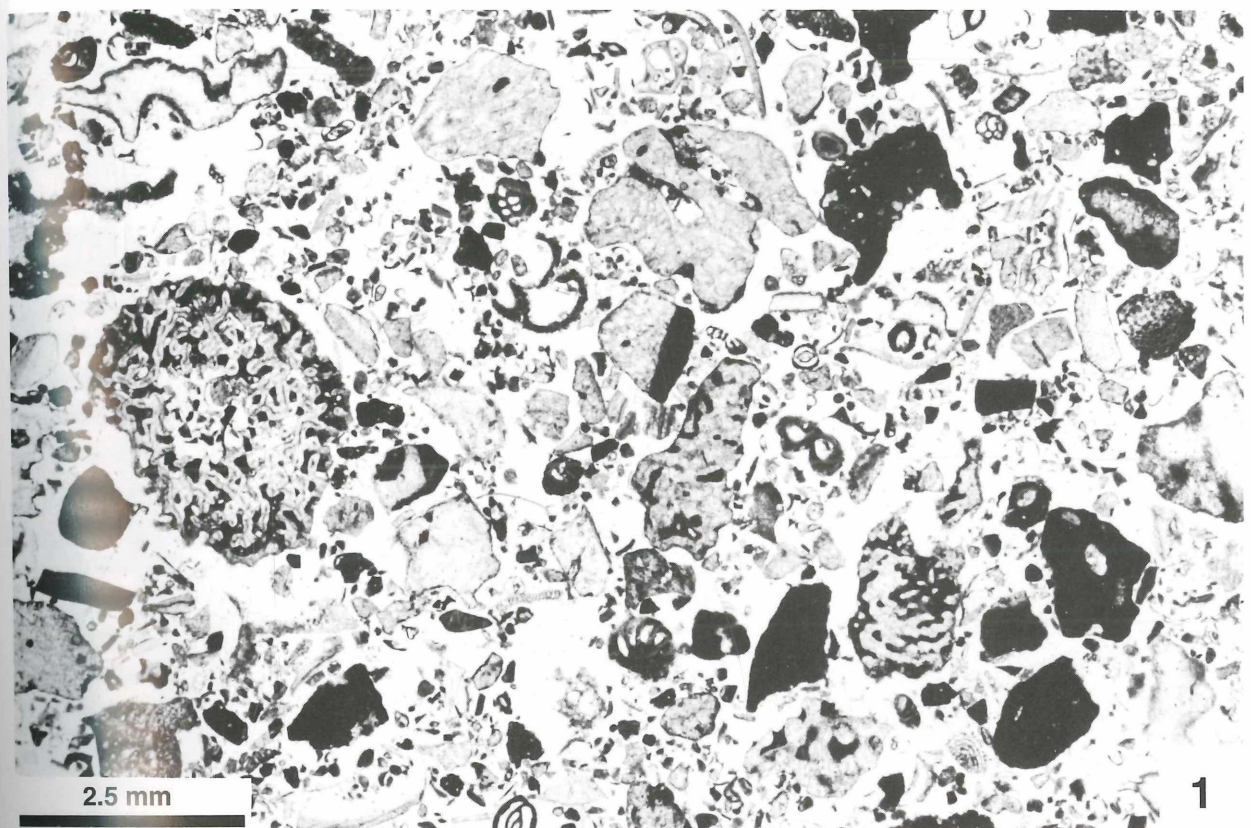


PLATE 10

Fig. 1. Coralgal-molluscan facies. Relatively coarse grained example with molluscs as well as corals and coralline algal crusts. Among corals the amount of octocorallian spicules is remarkably high. Foraminifera are represented by soritid, *Borelis*, *Heterostegina*, *Operculina*, and fragments of acervulinids. – Sample B 15.

Fig. 2. Coralgal-molluscan facies. Typical example with relatively high amount of fine grained particles. Molluscs are abundant, however, scleractinian fragments are dominating. The foraminiferan fauna is diverse with porcellaneous (quinqueloculine types and soritids) and hyaline (*Planorbulinella*, *Planorbulina*, abundant acervulinid crust fragments) forms. – Sample B 31.

PLATE 10

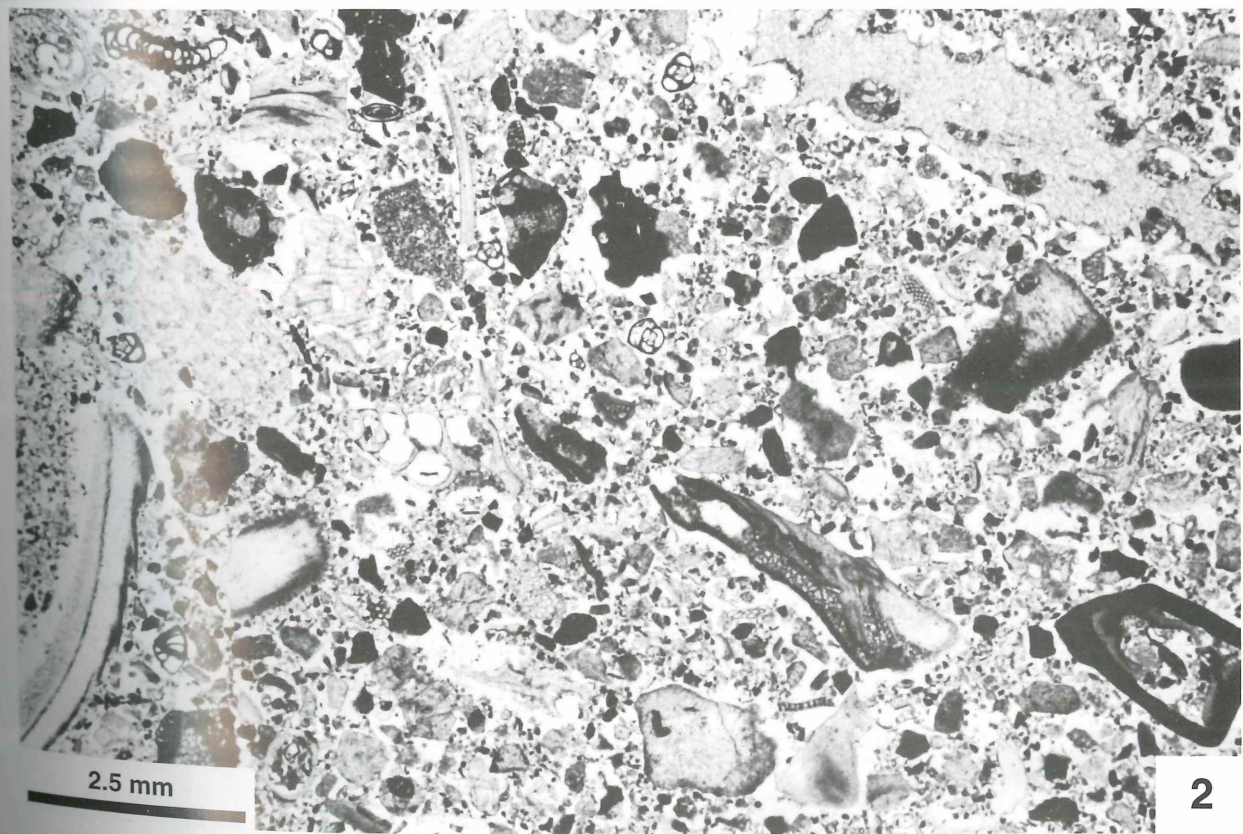
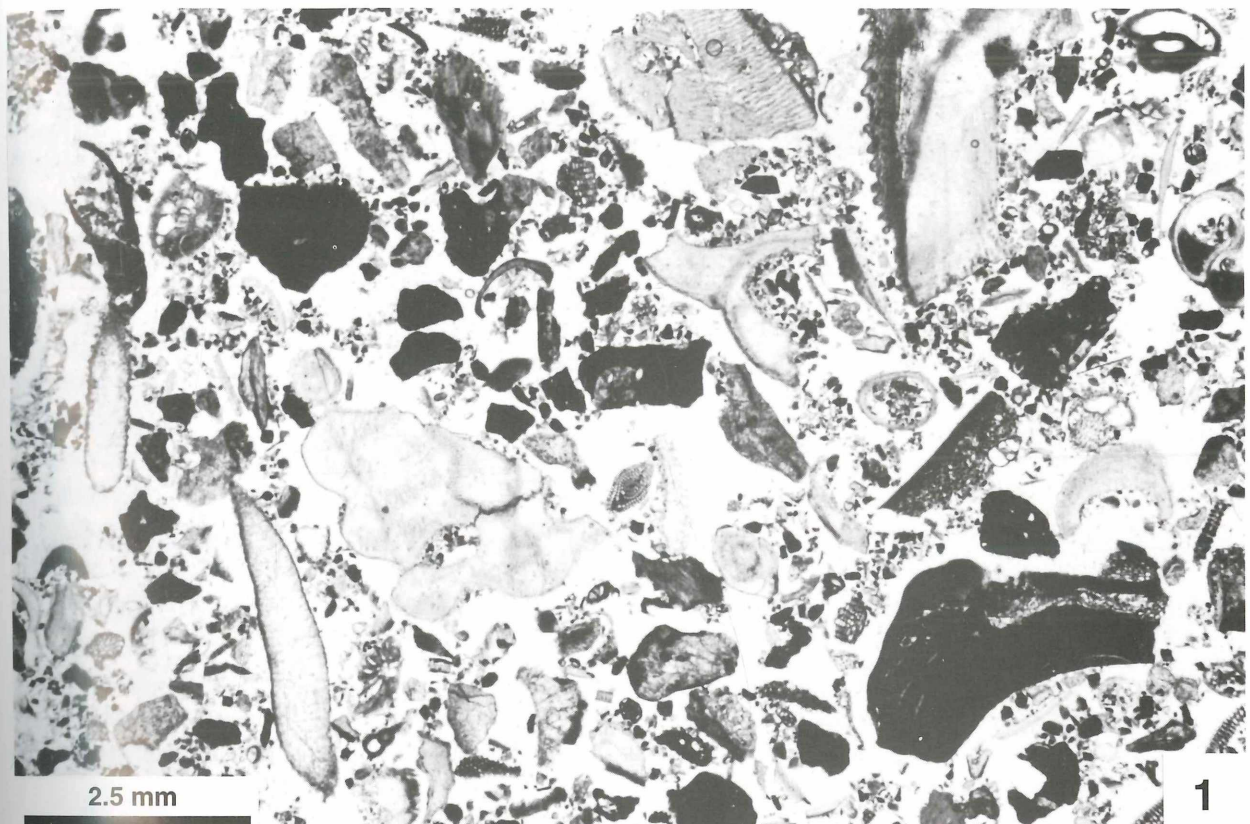


PLATE 11

Fig. 1. Compound grain facies. Most of the particles are bound together to form compound grains of grapestone type. The amount of micritic cement in the aggregates is variable, most particles are micritized, some are altered to cryptocrystalline grains. Skeletal grains are dominated by molluscs. Foraminifera are represented by quinqueloculine types (strongly affected by microborings and micritization) and by amphisteginids. – Sample C 11.

Fig. 2. Cryptocrystalline grain facies. The thin section is completely dominated by fine grained cryptocrystalline grains; compound grains are rare and characterized by a high amount of micritic cement. Skeletal grains are represented by molluscs and foraminifers. The latter are dominated by porcellaneous forms of quinqueloculine type and by soritids. – Sample B 74.

PLATE 11

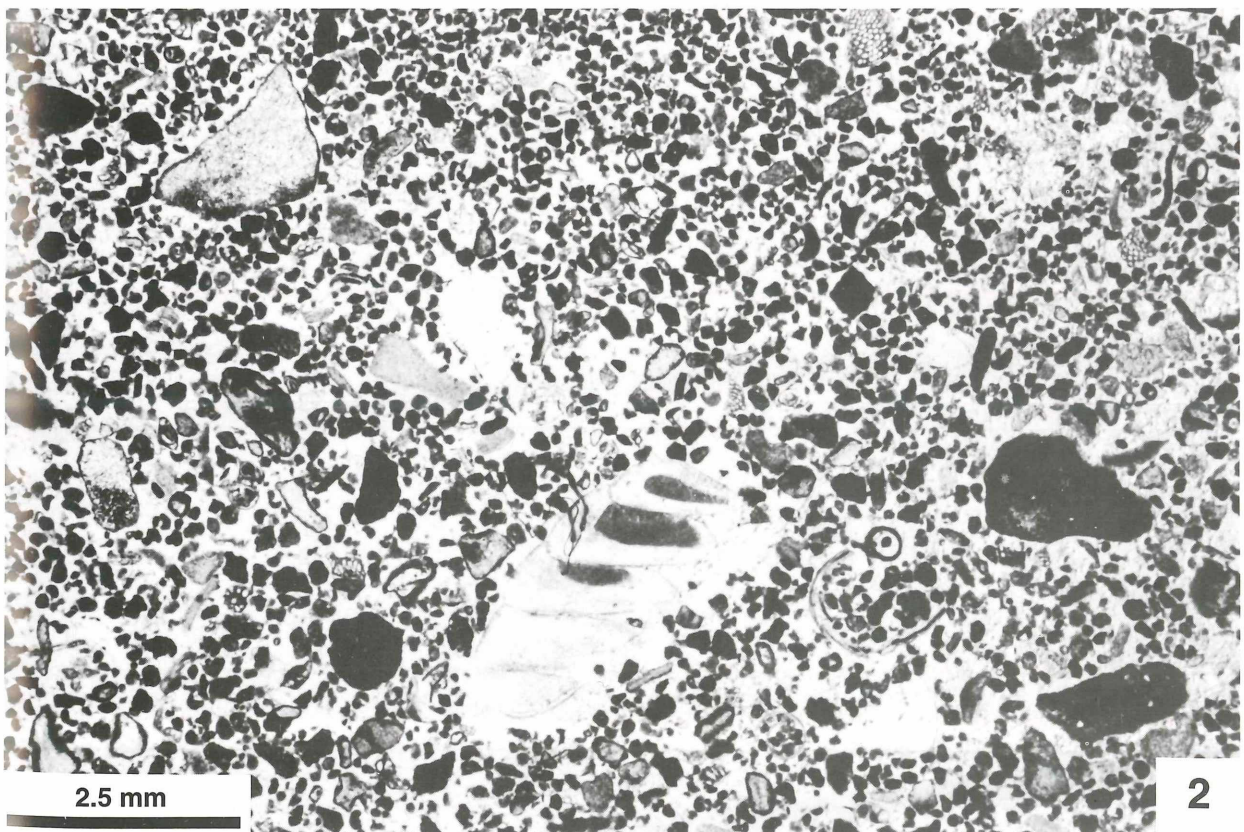
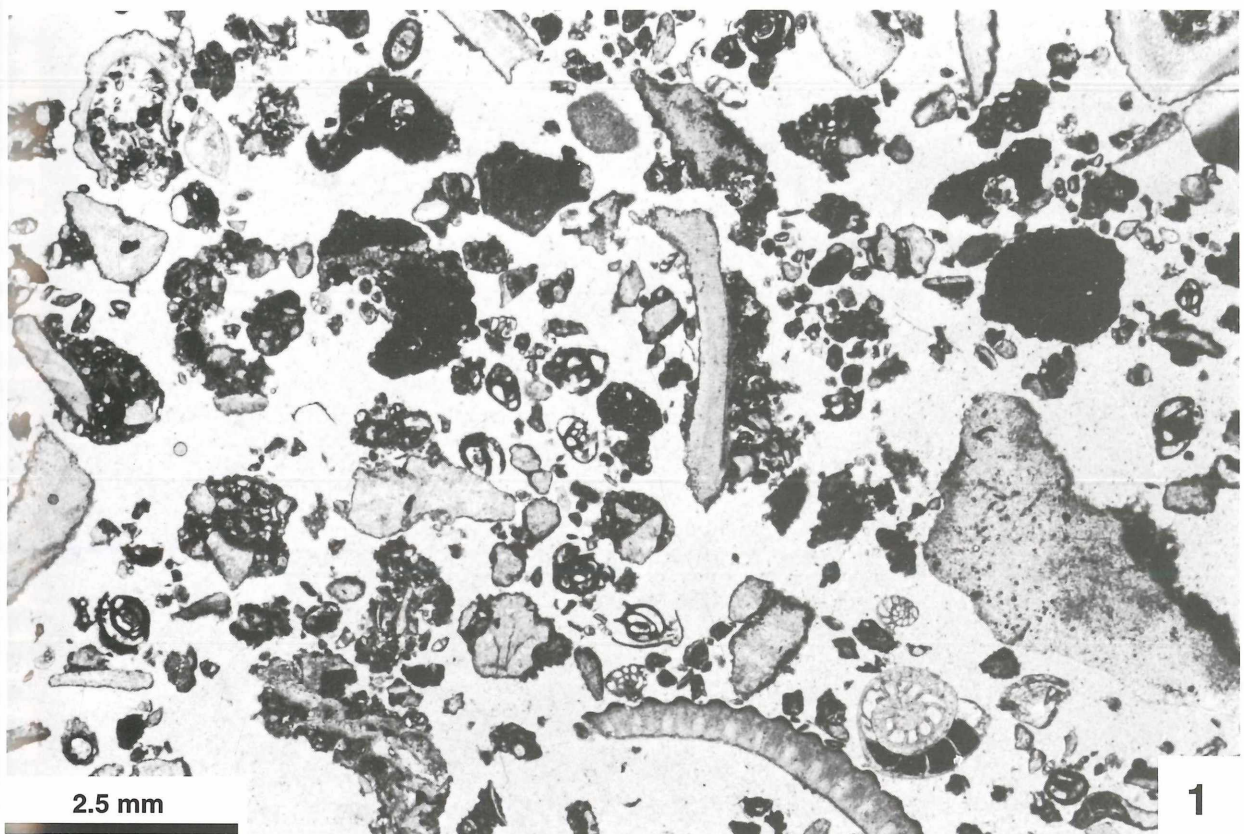


PLATE 12

Fig. 1. *Heterostegina* facies. The most obvious constituent of this thin section are larger foraminifera of the species *Heterostegina depressa*. Besides these, also some amphisteginids and porcellaneous forms are present. Additional skeletal grains are molluscs (gastropods, bivalves and scaphopods), bryozoans and coralline algae. Compound grains are rare and micritization is common. – Sample C 1.

Fig. 2. Scaphopod facies. The entire thin section is dominated by longitudinal and transverse sections through scaphopod shells. Grain size between shells is relatively small. Among foraminifera all three main groups are represented. – Sample B 3.

PLATE 12

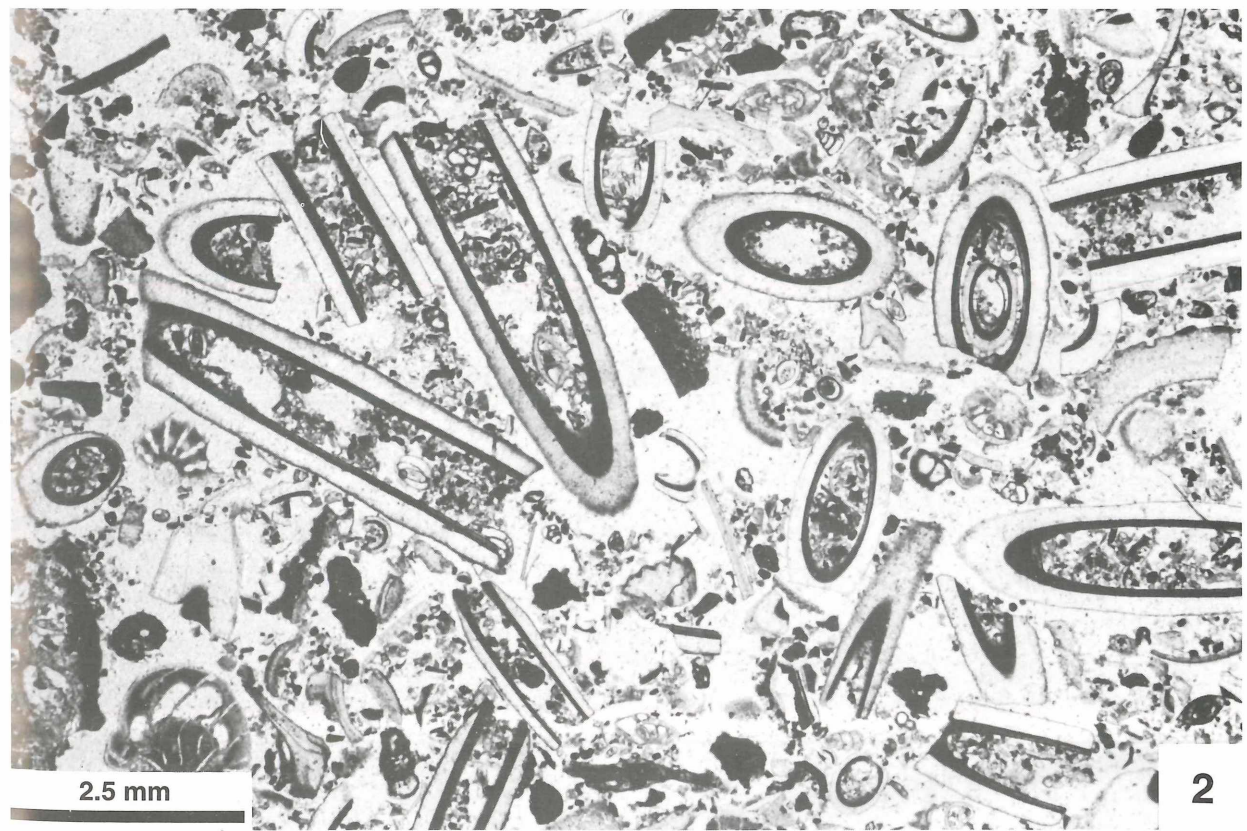
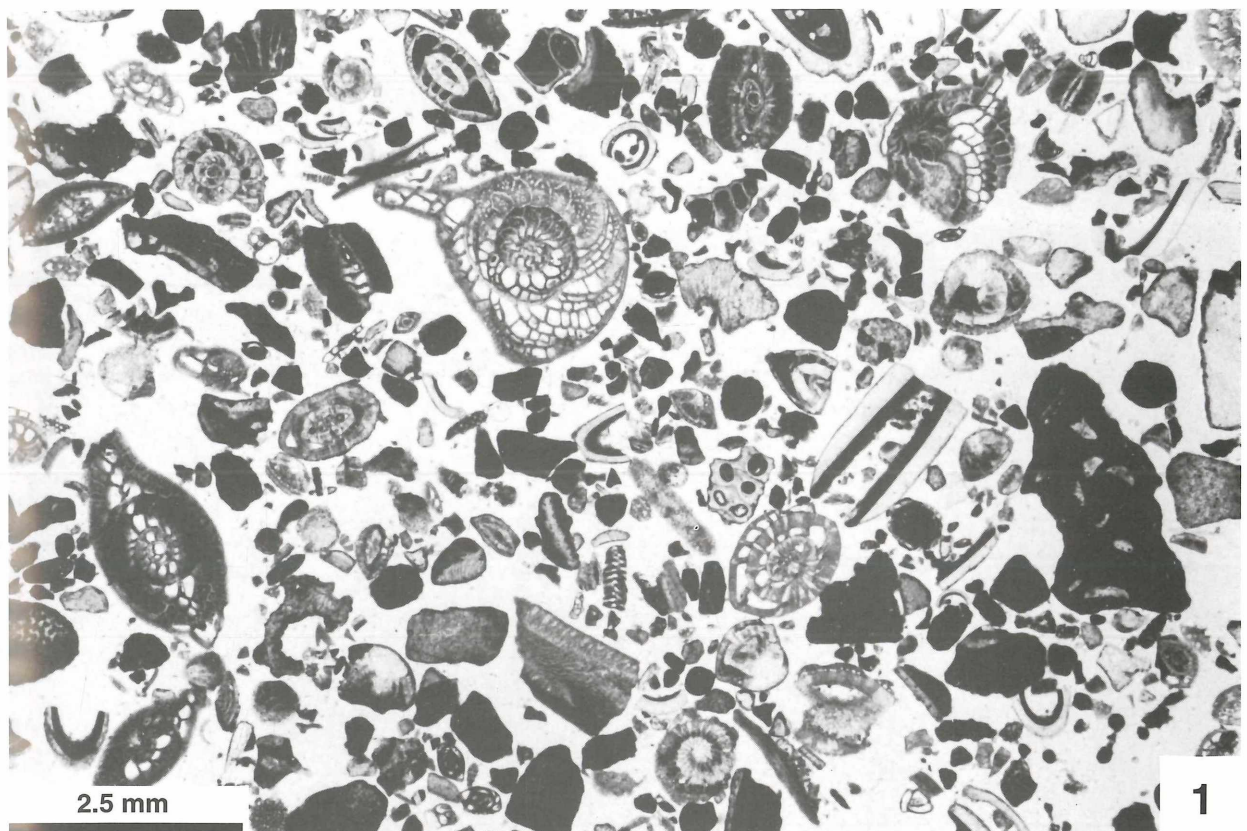


PLATE 13

Fig. 1. Peloolitic molluscan facies. The dominating constituents in this thin section are molluscan fragments; a large compound grain is also obvious. The most characteristic particles, however, are ooids and faecal pellets of the large type. Except molluscs, many blackened particles are present. Foraminifera are mainly represented by agglutinated and hyaline forms, the latter by *Operculina*. – Sample B 49.

Fig. 2. *Halimeda* facies. The thin section is completely dominated by *Halimeda* fragments, the sediment in between is relatively fine grained. Foraminifera are rare and belong to the agglutinated and porcellaneous group. – Sample B 51.

PLATE 13

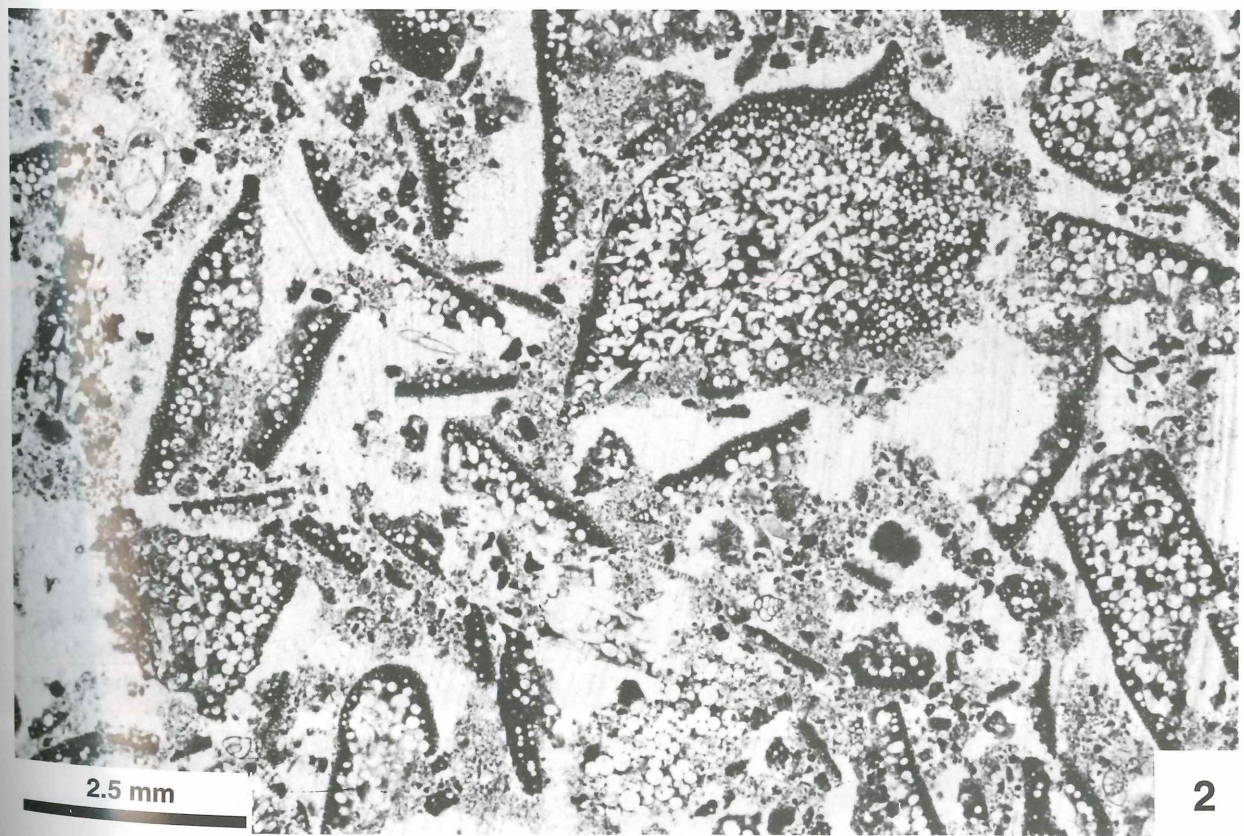
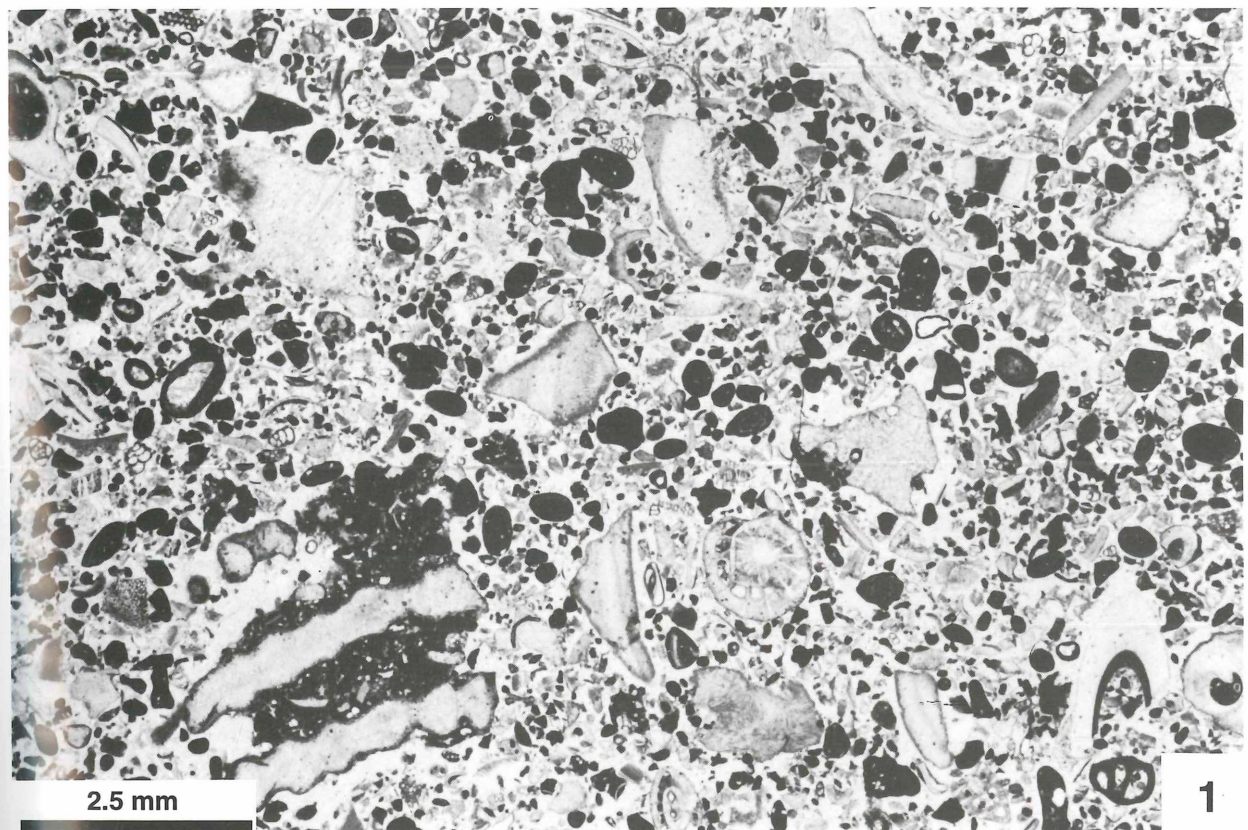


PLATE 14

Fig. 1. Soritid facies. The dominating constituents in this facies are porcellaneous foraminifera. Besides the prevailing soritids, *Borelis* is also abundant. Molluscs and compound grains are present as well as a relatively high amount of fine grained bioclastic particles. – Sample A 19.

Fig. 2. Foraminiferan sand facies. Fine grained example of this facies with extremely high number of small foraminifera belonging to the porcellaneous and agglutinated groups. The sediment in between is made up predominantly of unidentified particles. – Sample C 4.

PLATE 14

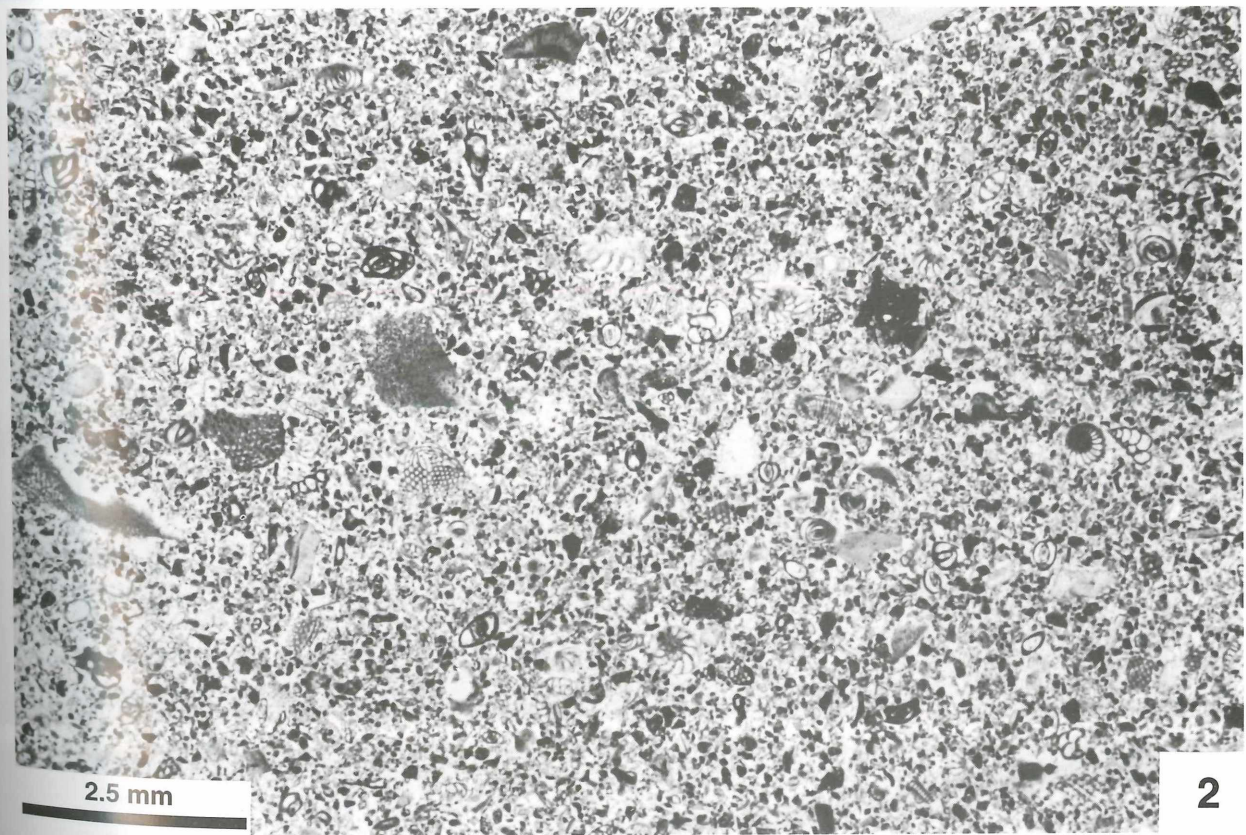
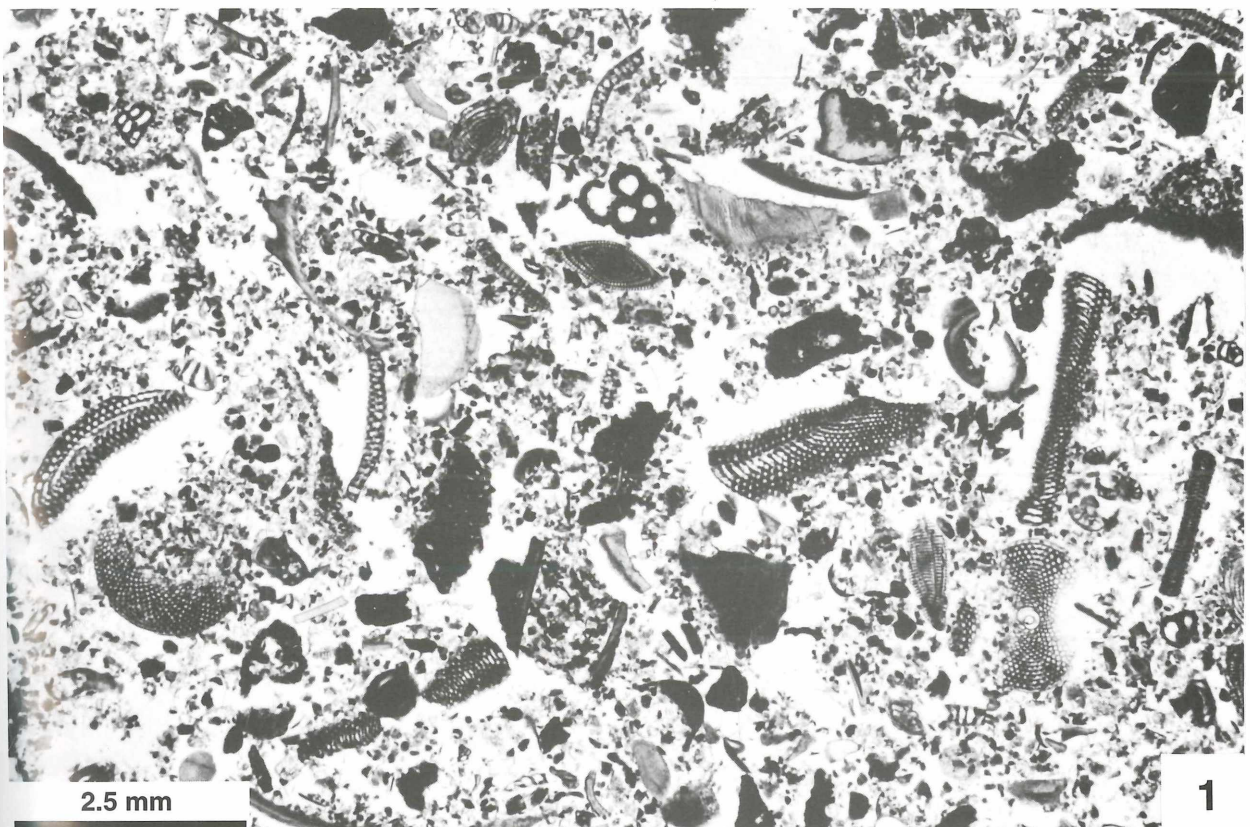


PLATE 15

Fig. 1. Foraminiferan sand facies. A coarser grained example of this facies, due to the occurrence of larger hyaline foraminifera (*Operculina*) as well as large agglutinated and porcellaneous forms. The amount of unidentified particles is high, however, also small compound grains are abundant. – Sample C 20.

Fig. 2. Coralgan mud facies. Relatively abundant fragments of scleractinian corals and coralline algae are present, surrounded by fine grained sediment. Porcellaneous foraminifera belong to quinqueloculine types, hyaline forms are represented by *Operculina*, *Planorbulina* and abundant fragments of acervulinids. – Sample

PLATE 15

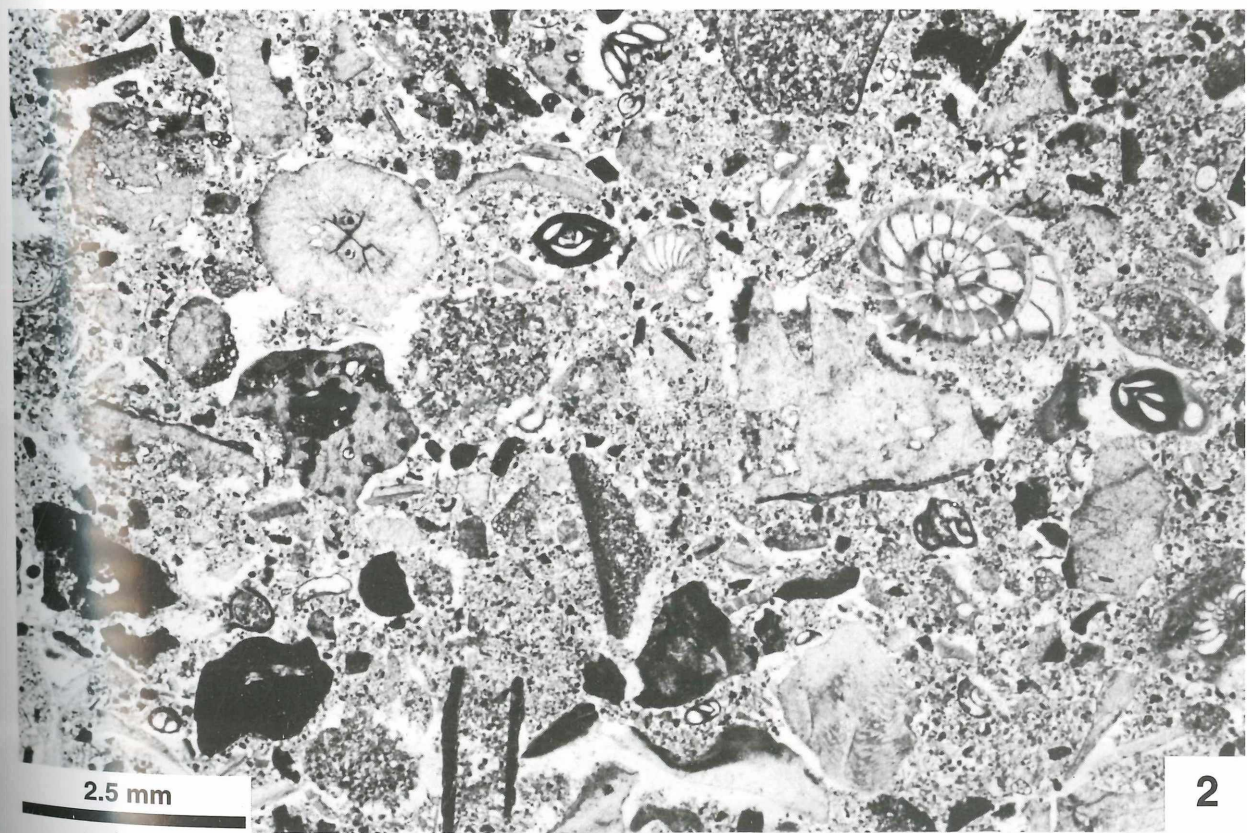
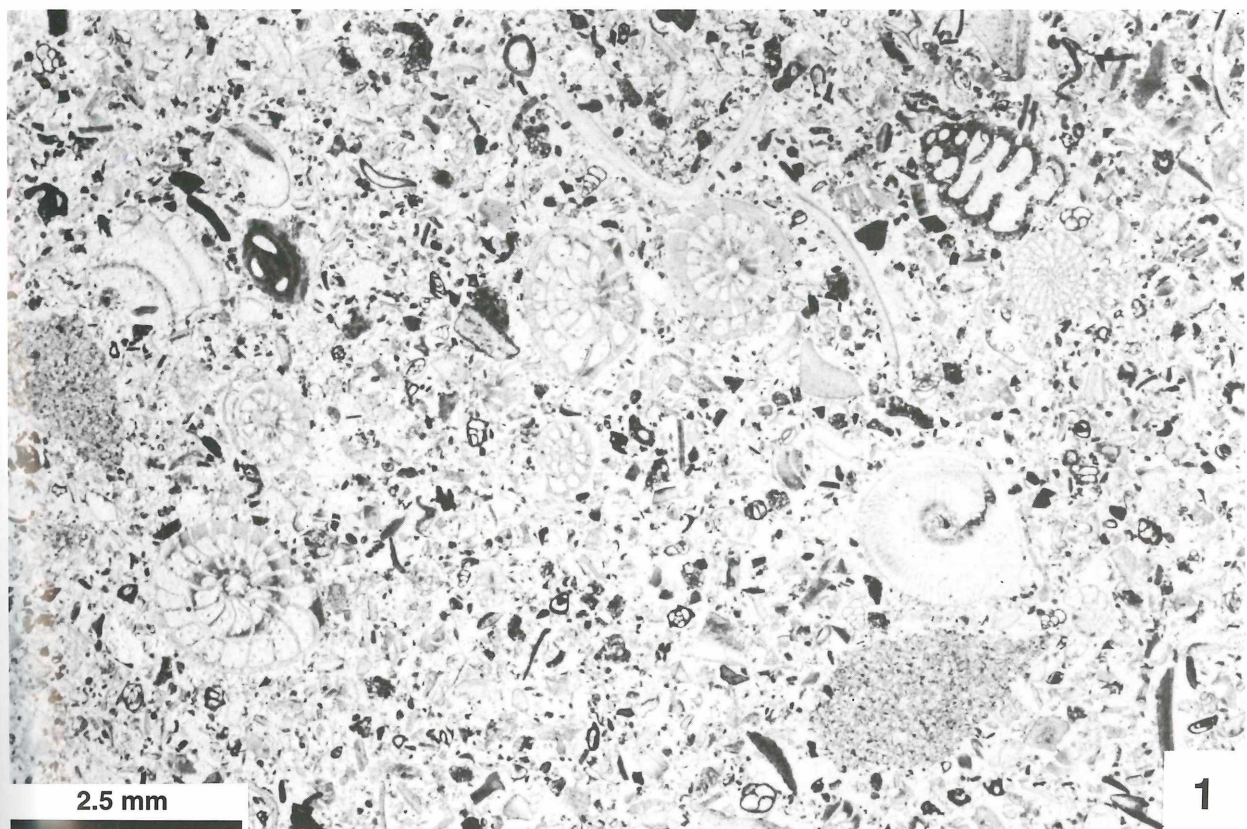
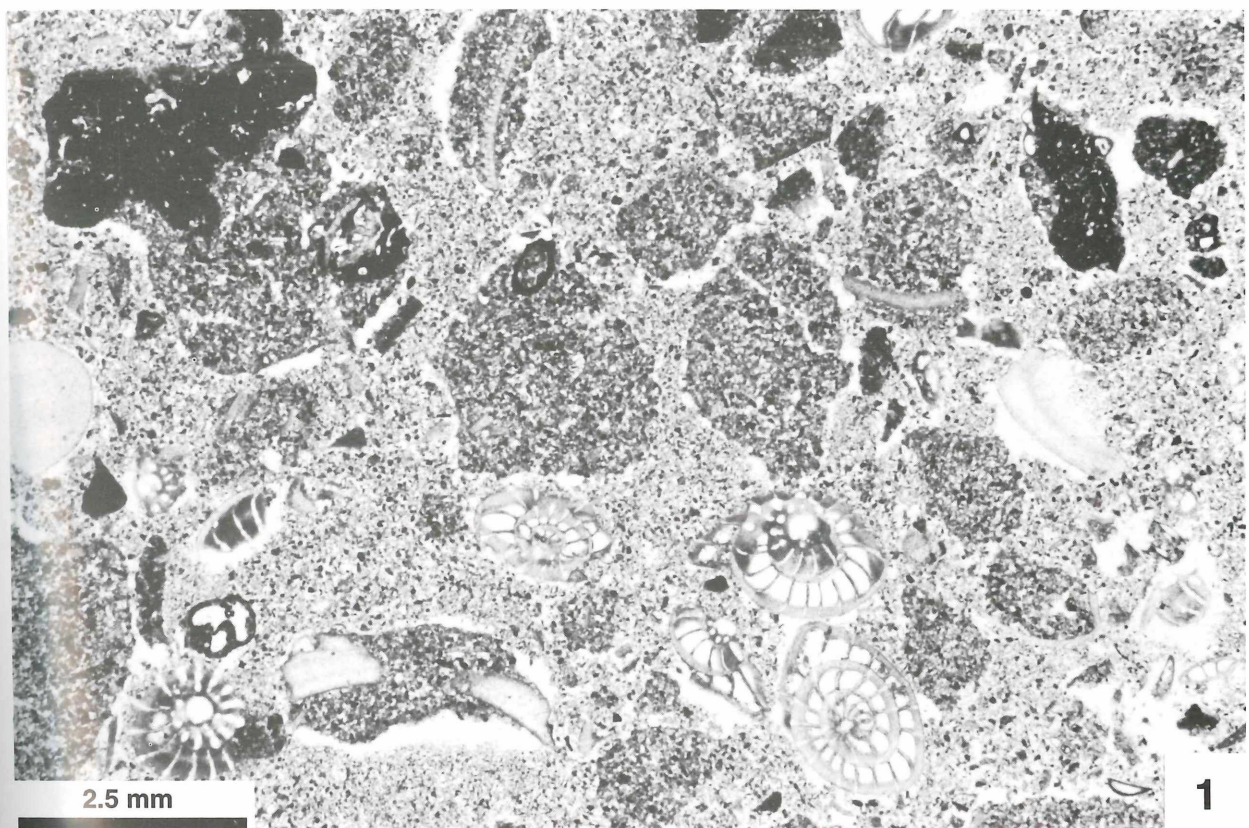


PLATE 16

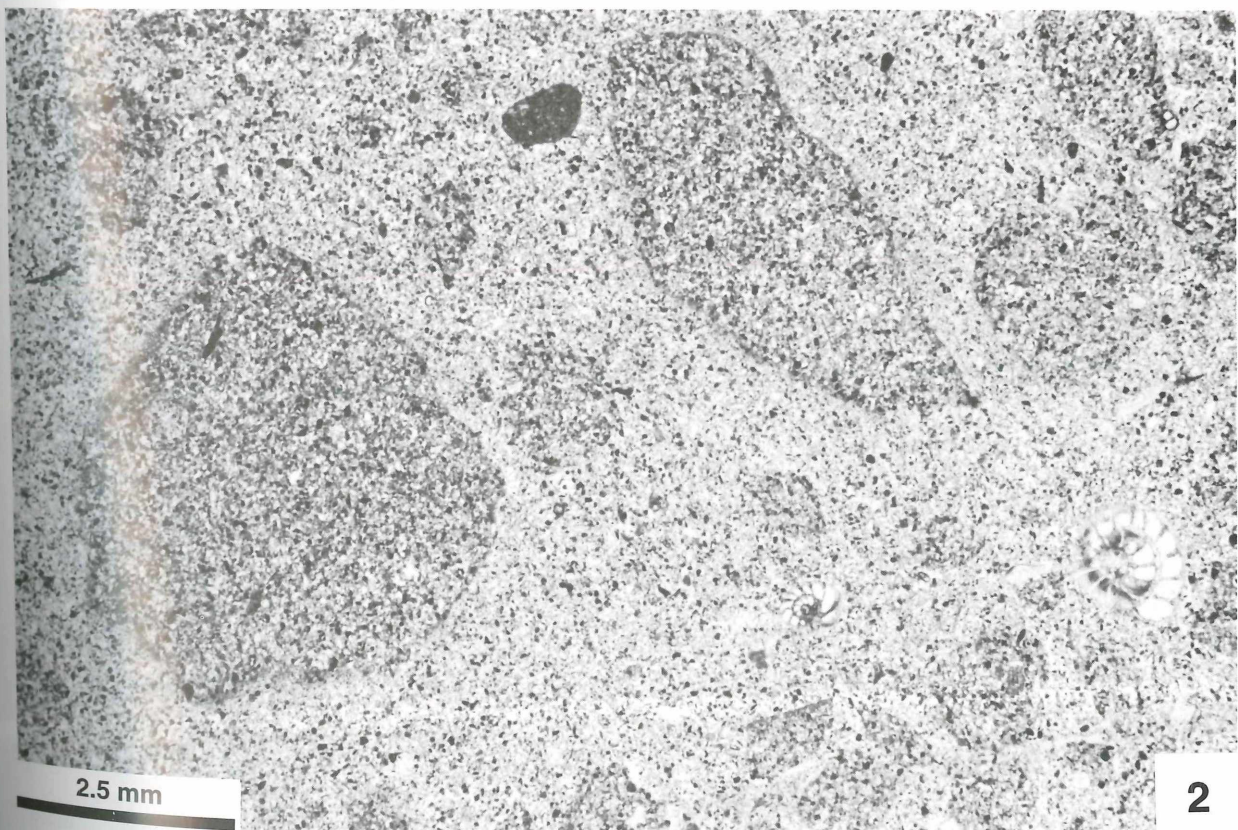
Fig. 1. *Operculina* facies. The abundant occurrence of the larger hyaline foraminifer *Operculina* (= *Assilina*) embedded in a fine grained sediment (unidentified grains and mud) characterizes this facies. This thin section is a good example for the differentiation between natural mud aggregates and loosely bound artificial aggregates. The two dark particles are mud aggregates, showing also typical incrustations by foraminifers (right upper corner), whereas the lighter multicomponent particles are artificial compound grains. – Sample B 34.

Fig. 2. Mud facies. The sediment is dominated by unidentified grains and mud (binding the artificial aggregates), pellets of the small type c are also present. The few larger particles are pellets and foraminifera. – Sample B 70.

PLATE 16



1



2

PLATE 17

Fig. 1. Terrigenous facies. Typical example of coarser grained, well rounded, relatively good sorted sediment dominated by non-carbonate particles. Carbonate particles are molluscs and compound grains. – Sample A 7.

Fig. 2. Terrigenous facies. This thin section is an example of a fine grained, well rounded sediment. Besides non-carbonate particles cryptocrystalline grains, ooids and rare foraminifera are present. – Sample D 1.

PLATE 17

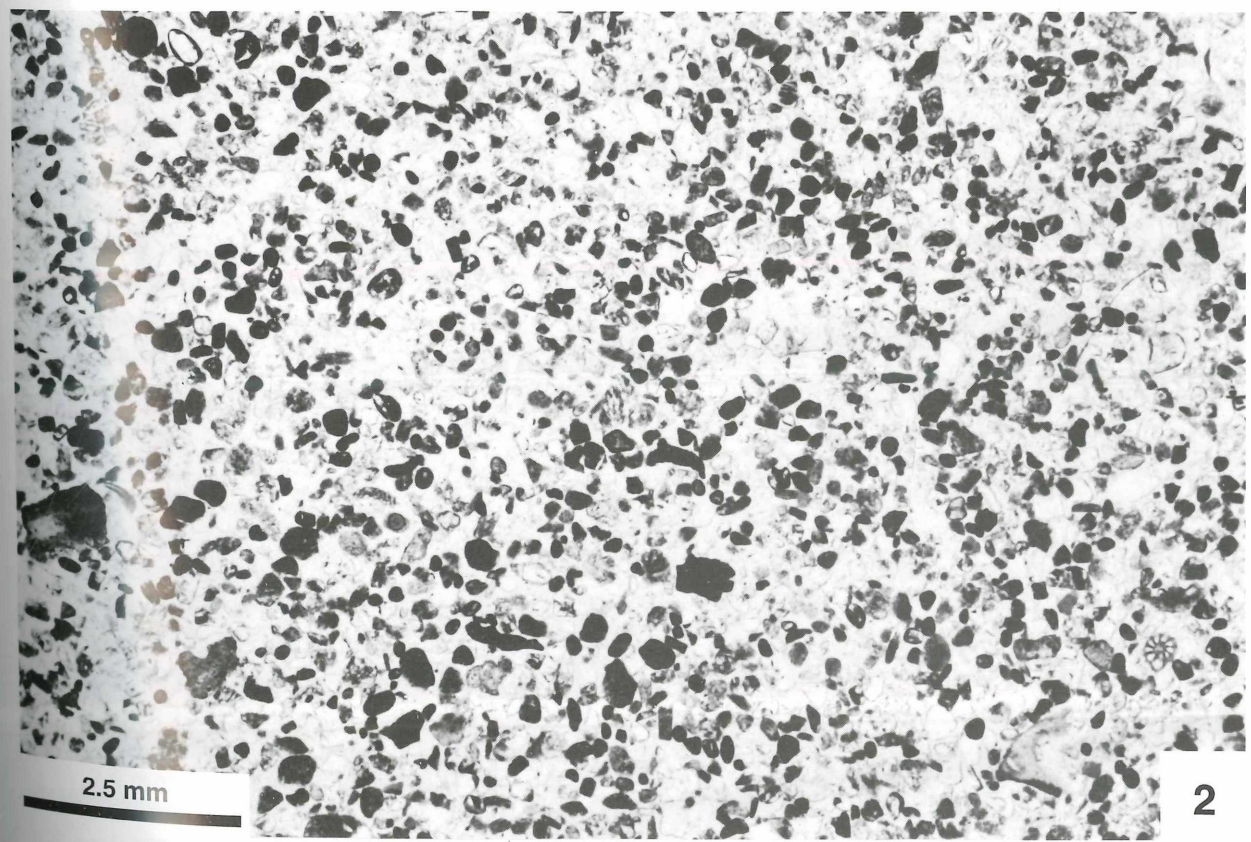
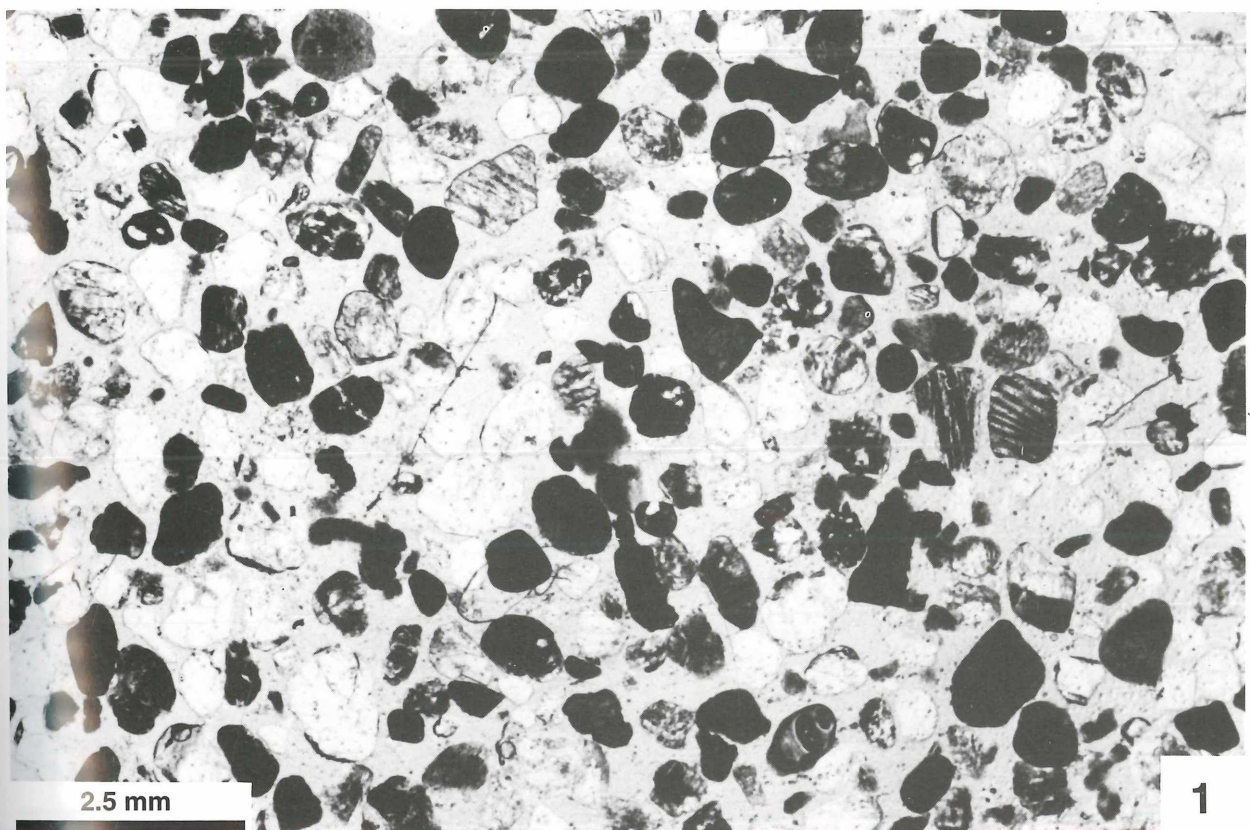


PLATE 18

Fig. 1. Terrigenous facies. This is an example of a very badly sorted, angular sediment dominated by non-carbonate particles (quartz and crystalline rock fragments). Carbonate particles are frequently micritized and belong to molluscs, porcellaneous foraminifera, and rare compound grains. – Sample A 10.

Fig. 2. Terrigenous facies. Fine grained, badly rounded and sorted example of this facies with relatively high amount of small porcellaneous foraminifers (mainly peneroplids and quinqueloculine types). – Sample A 9.

PLATE 18

